

Laser-Scope: The Affordable Confocal Scanning Laser Microscope for Surface Topography

Group 7

Collin Barber	Photonics Science Engineering
Luc Therrien	Photonics Science Engineering
Omar Castro	Computer Engineering
Karol Josef Woodhouse Thomae	Electrical Engineering

Reviewer Committee

Prof. Mark Llewellyn	Senior Lecturer, ECE
Dr. Yannick Salamin	Associate Professor, PSE
Dr. Wei Sun	Associate Professor, ECE
Prof. Mark Maddox	Instructor, ECE

Mentors:

Dr. Chung Yong Chan
Dr. Aravinda Kar



1. Executive Summary	1
2. Project Description.....	2
2.1 Motivation and Background	2
2.2 Prior Related Works.....	2
2.3 Project Goals.....	3
2.4 Project Objectives	4
2.5 Description of Features and Functionality	5
2.5.1 Illustrations	5
2.5.2 Overall Functionality	6
2.5.3 Stage Functionality	6
2.5.4 Microscope Head Functionality	6
2.5.5 Image Generation Functionality.....	7
2.6 Engineering and Marketing Requirements	7
2.7 House of Quality	10
2.8 Hardware Block Diagram	11
2.9 Software	11
2.9.1 GUI	12
2.9.2 Motor Control	12
2.9.3 Data Collection	12
2.10 Software Block Diagram.....	13
3. Research and Investigation	13
3.1 Technology Comparison and Selection	13
3.1.1 Lasers	13
3.1.2 Laser Current Controller	17
3.1.3 Beam Expanders	19
3.1.4 Beam Splitters.....	23
3.1.5 Microscope Objectives.....	26
3.1.6 Focusing Lenses.....	29
3.1.7 Apertures.....	30
3.1.8 Sensors	31
3.1.9 Amplifiers	34
3.1.10 MCU	39
3.1.11 Microscope Stages	41
3.1.12 Stage Motors	43
3.1.13 Stage Motor Controllers.....	46

3.1.14 Power Supply	48
3.1.15 Regulators	51
3.1.16 Communication Protocols.....	54
3.1.17 Software Packages for UI	56
3.1.18 MCU Development Languages.....	60
3.1.19 Integrated Development Environment (IDE).....	62
4. Standards & Design Constraints	64
4.1 Standards.....	64
4.1.1 Optics Standards	64
4.1.2 Electronics Standards.....	66
4.1.3 Communication Protocol Standards.....	68
4.1.4 GUI Communication Standards.....	69
4.2 Practical Constraints	70
4.2.1 Economic	70
4.2.2 Time	71
4.2.3 Environmental/Space	72
4.2.4 Manufacturability.....	73
5. Applications of Artificial Intelligence	74
5.1 AI Limitations, Pros, and Cons.....	74
5.1.1 Case Study 1	74
5.1.2 Case Study 2	75
5.1.3 Case Study 3	76
5.1.4 Case Study 4	77
6. Hardware Design	78
6.1 Power Delivery	78
6.1.1 Power Delivery System Schematic.....	78
6.2 Transimpedance Amplifier	79
6.2.1 Low Level Block Diagram.....	79
6.2.2 Transimpedance Amplifier Schematic.....	80
6.3 Motor Controllers.....	80
6.3.1 Low Level Block Diagram.....	80
6.3.2 Motor Controller Schematic.....	80
6.4 UART-USB Converter.....	82
6.5 MCU Schematic & Laser Current Controller	83
6.6 Overall Schematic Design.....	85

6.6.1 Low Level System Block Diagram	85
6.6.2 System Schematic	86
7. Software Design	86
7.1 MCU Programming	87
7.1.1 Delta Stage Movement.....	87
7.1.2 ADC Data Gathering.....	88
7.2 Computer Side	89
7.2.1 Data Collection	89
7.2.2 Graphical User Interface (GUI)	90
7.3 Diagrams	91
7.3.1 Flowchart	91
7.3.2 UI Mockup Drawing	93
7.3.3 UI Navigation Flow	102
7.3.4 Use Case Diagram.....	103
8. System Fabrication.....	106
8.1 PCB Layout.....	106
8.1.1 5V and 3.3V Regulators.....	106
8.1.2 Motor Controller	108
8.1.3 CLSM Main Board	110
8.1.4 UART-USB Converter.....	111
8.2 Stage.....	112
8.3 Microscope Head Design	113
8.4 System Stabilization.....	114
9. System Testing and Evaluation.....	114
9.1 Hardware Testing.....	115
9.1.1 Power Supply Testing	115
9.1.2 ESP32 Testing.....	116
9.1.3 Motor Controller Testing	117
9.1.4 Stage Testing.....	118
9.2 Software Testing	119
9.2.1 GUI	119
9.2.2 ESP32.....	120
9.3 Optical Layout Testing	121
9.4 Optoelectronics Feasibility Study	122
9.4.1 Photodiode	122

9.4.2 Transimpedance Amplifier	123
9.5 Senior Design II Test Plan	124
9.5.1 Power Supply Testing	124
9.5.2 Optics	124
9.5.3 Stage Control	124
9.5.4 UI System.....	125
9.6 Senior Design II Developments, Changes, and Implementations.....	125
9.6.1 Optics	126
9.6.2 Electronics.....	126
9.6.3 Software	127
10. Administrative Content.....	127
10.1 Budgeting and Financing	127
10.2 Bills of Materials.....	128
10.3 Project Milestones.....	130
10.4 Table of Work Distribution.....	130
11. Conclusion	131
Appendix A – References	i
Appendix B – Copyright Permissions.....	iv
Appendix C – Datasheets.....	v
Appendix D – Software Code	vi
Appendix E – AI Prompts & Results.....	vi

Table of Contents

List of Figures

Figure 1: Initial Design	5
Figure 2: Optical Layout.....	5
Figure 3: House of Quality (HOQ)	10
Figure 4: Hardware Block Diagram.....	11
Figure 5: Software Block Diagram	13
Figure 6: Simple Keplerian Beam Expander Design.....	20
Figure 7: Simple Galilean Beam Expander Design	21
Figure 8: 5V and 3.3V Regulators Schematics	79
Figure 9: Transimpedance Amplifier Schematic	80
Figure 10: Single Motor controller unit schematic	81
Figure 11: 3 Motor controller units as per project scope	82
Figure 12: UART-USB Converter Schematic	83
Figure 13: MCU Schematic	84
Figure 14: Laser Controller Connections.....	84
Figure 15: Low Level System Block Diagram	85
Figure 16: System Schematic.....	86
Figure 17: Object Scanning Process	88
Figure 18: CSV Data Tabulation	90
Figure 19: Flowchart Diagram.....	93
Figure 20: First Iteration Idea	95
Figure 21: Home and Scanning Screen Mockup Second Iteration	96
Figure 22: Home Page	97
Figure 23: How to Use page	98
Figure 24: Configuration Page.....	99
Figure 25: Debugging Scan Page.....	100
Figure 26: Scanning Page	101
Figure 27: UI Navigation Flow	103
Figure 28: Use Case Diagram	105
Figure 29: Class Diagram	106
Figure 30: 5V Regulator	107
Figure 31: 3.3V Regulator	108
Figure 32: Motor Controller.....	109
Figure 33: CLSM Main Board.....	111
Figure 34: UART-USB Converter.....	112
Figure 35: OpenFlexure Delta Stage.....	113
Figure 36: AC-DC Converter Setup	115
Figure 37: Motor Controller Prototype	118
Figure 38: Optical Test Layout (left image is in focus, right image is out of focus).....	121
Figure 39: Amplified Detector Circuit by Thorlabs Inc.	123

List of Tables

Table 2.1: Marketing Specifications	7
Table 2.2: Engineering Specifications	8
Table 3.1: Laser Comparison.....	15
Table 3.2: Laser Diode Selection.....	16
Table 3.3: Laser Current Controller Technology Selection.....	18
Table 3.4: Laser Current Controller Technology Selection.....	19
Table 3.5: Beam Expander Comparisons.....	21
Table 3.6: Lens Selection for Beam Expander	23
Table 3.7: Beam Splitter Comparison.....	25
Table 3.8: Beamsplitter selection.....	26
Table 3.9: Microscope Objective Comparison	28
Table 3.10: Microscope Objective Selection	29
Table 3.11: Focusing Lens Selection.....	30
Table 3.12: Aperture Selection	31
Table 3.13: Photodiode vs. Phototransistor comparison.....	33
Table 3.14: Photodiode Selection	34
Table 3.15: Amplifier Comparisons	36
Table 3.16: TIA Selection.....	38
Table 3.17: MCU Selection	40
Table 3.18: Microscope Stage Comparison	42
Table 3.19: Stage Motor Comparison.....	45
Table 3.20: Motor Selection	46
Table 3.21: Motor Controllers Comparison.....	47
Table 3.22: Motor Controller Selection	48
Table 3.23: System Power Requirements	48
Table 3.24: Power Supply Selection.....	49
Table 3.25: AC-DC Converter Selection.....	50
Table 3.26: Voltage Regulator Comparisons.....	52
Table 3.27: Regulator Selection.....	53
Table 3.28: UART-USB Converter Selection	56
Table 3.29: Software Packages Comparison	59
Table 3.20: Programming Language Comparison	61
Table 3.31: MCU and Programing Language Compatibilities	62
Table 9.1: Power Supply Test Results	116
Table 9.1: Photodiode Test Results	122
Table 9.2: TIA Test Results	123
Table 10.1: Budget and Finances.....	128
Table 10.2: Bill of Materials.....	128
Table 10.3: Senior Design 1 Documentation Dates.....	130
Table 10.4: Senior Design 1 Design Dates	130

Table 10.4: Senior Design 2 Design Dates	130
Table 10.5: Senior Design Work Distributions.....	131

1. Executive Summary

High-resolution microscopy plays a crucial role in advancing research across fields such as biology, photonics, material science and many others. Among the most powerful imaging techniques is Confocal Laser Scanning Microscopy (CLSM), which enables 3D imaging by eliminating out of focus light and isolating precise optical sections of a sample. However, CLSM systems have a high barrier of entry – cost. The cost of these systems can prevent students, educators and researcher institutions operating under tight budgets from acquiring such a system. To address this limitation, the Laser-Scope project was conceived and developed by a team of undergraduate engineering students at the University of Central Florida. Its aim is to deliver an accessible, low-cost CLSM system that retains key functionality of commercial alternatives while remaining open-source, compact and modular.

The Laser-Scope project is composed of three integrated subsystems: photonics, electrical and software. The photonics subsystem will govern the optical pathway – it will be responsible for directing, focusing and collecting light from the sample. The electrical subsystem will enable precise control of power, signal conditioning, stage actuation and serve as the bridge between subsystems, ensuring reliable data collection. The software subsystem will act as the interface between the system and the user, managing the scanning process and image reconstruction from raw data. The three systems will form a complete and functional platform capable of generating clear, micron-level images without relying on expensive commercial hardware.

The Laser-Scope project sets itself apart from other CLSM systems in that rather than relying on traditional galvanometer-based scanning or immersion-based objectives, the design focuses on mechanical simplicity and digital adaptability. With an emphasis on affordability, repeatability and ease of use, the Laser-Scope project aims to make CLSM technology more approachable for educational demonstrations, small lab experimentation, or as a foundational tool for development. The project also seeks to give a user a product that can be easily customized or extended, taking a modular approach with its components.

The following document will be a complete record of the Laser-Scope project from inception to implementation. The basic context behind CLSM microscopy will be explained, followed by research, motivation, and engineering requirements and constraints. The document will then look at subsystem design, technology and component selection, standards used, and contributions of artificial intelligence. The document will demonstrate hardware schematics and software design followed by fabrication methods and testing of components and software. The report will conclude with a development timeline, budgets and an overall reflection on system performance and potential areas for improvement. Finally, appendixes containing any references, datasheets, copyright permissions, AI prompts and results, and code will be presented.

2. Project Description

2.1 Motivation and Background

Laser scanning microscopy (LSM), or confocal laser scanning microscopy (CLSM), is the backbone of many sciences. Confocal imaging is the idea of using point illumination and a pinhole in front of an optical detector to eliminate the out-of-focus reflections (or transmissions) of light on a sample. Furthermore, using a beam of laser light, that is scanned point-by-point across a sample in this microscope setup allows for a cleaner and less invasive imaging process compared to other forms of microscopy.

The basic concept of confocal microscopy was originally patented in 1957 by Marvin Minsky, a then-postdoctoral student at Harvard University.³ However, due to the lack of intense light sources (lasers), confocal microscopy did not take off until the patent had expired. During the 70's and 80's not only was confocal microscopy built upon but rather improved with the use of lasers. After these improved designs showed promise the first commercial SLM was presented in 1987 by Carl Zeiss, 30 years after the initial concept of confocal microscopy.⁴

From in-vivo biological research to topological imaging of certain materials, CLSM has played a major role in contributing to high-resolution imaging systems in the digital age. One major problem of CLSM, however, is the affordability for many different research groups. Without the ability to afford such high-resolution imaging systems, the need for a cheaper and just as accurate alternative is present.

In the market for microscopy instruments, there are plenty of different microscopes to choose from. For most biological research, the use of fluorescence microscopy is used to achieve a better depth of field of an organism by exciting the fluorescent liquid and reading the excited light through a photodiode.⁵ Most CLSM use this method of excited fluorescent light, usually at the cost of an increased price tag on said microscopes. There is a type of CLSM that does not need to use excited fluorescent light but rather, uses reflection of a focused laser beam on a sample without the need for a thicker medium such as fluorescent liquids or even water. In material science research, the use of reflection CLSM is seen as the standard for characterization of surface texture or roughness of material surfaces.⁶ This type of reflection-based CLSM is the motivation for the proceeding project in this paper.

2.2 Prior Related Works

There are several examples of technologies that share functional and conceptual similarities with our proposed project. The laser based non-contact; high resolution surface analysis has been used as tools for quite some time.

Fluorescence microscopy as previously mentioned, as devices that utilize fluorescence liquids that are then excited by light incident on the sample area. These microscopes are typically wide-field meaning the entire sample is shone with light. While this allows for faster and still very accurate results, in comparison to CLSM, the results of the imaging

system allow for more blurry, hard-to-decipher images. This is due to a fluorescent microscope's inability to record thin optical slices of a sample, leading to normal use in biology and in-vivo research and struggling to compete with other 3D imaging and surface profiling methods, such as can be seen in comparison to CLSM

Laser profilometers are devices that also use laser beams for non-contact, high resolution surface analysis. The laser would scan across a surface and measure reflected intensity to map surface profiles calculating the surface metrology and providing a roughness evaluation. However, the one capability a laser profilometer doesn't share is CLSM's capability of optical sectioning.

Do it yourself (DIY) and open-source microscopy platforms also tackle the same problem this project is trying to solve. Lowering the cost of these high-end tools while preserving the best imaging capabilities. The OpenFlexure Microscope stage leans on 3-D printing to reduce cost and includes a module for driving stage element with motors to move objects. The flexibility of DIY allows for adding additional components like lasers to act in a similar nature to the profilometers but with the capabilities of CLSM and can create bitmaps up to 3D if configured accordingly.⁷

2.3 Project Goals

When designing and working on a project of any kind, keeping three levels of goals, from basic, advanced, and stretch goals help organize the workload. This project aims to maintain the essential imaging capabilities of commercial CLSMs while reducing overall cost. The overall goals of the CLSM are as follows.

- Create a fully functional CLSM under \$1000
- Develop a CLSM with all essential capabilities of commercial CLSMs

Shown below are the three levels of project goals for creating and designing this CLSM

Basic Goals:

1. Maintain total cost under \$1000 using off-the-shelf (not obsolete) components from known vendors
2. 3D printed housing for all optical components to reduce cost and increase customizability
3. Achieve sub-micron movement from the OpenFlexure 3D printed microscope stage
4. Detect reflection of the laser on the object-under-illumination (OUI) into the photodiode
5. Create 2D greyscale images of surface topography based on the information from the photodiode

Advanced Goals

1. Make the 3D printed Microscope head adjustable for ease of use and alignment purposes

2. Enable auto XYZ calibration of the microscope stage
3. Achieve processed images within 5 minutes of scanning
4. Implementation of custom PCBs for laser control, motor control, photodiode power, transimpedance amplifier power, and MCU power.
5. Maintain consistent laser spot size of $\sim 1 \mu m$

Stretch Goals

1. Creation of 3D surface reconstructions of samples for higher quality images
2. Achieve a resolution of $< 1 \mu m$ for higher quality images
3. Optimize lens systems to account for aberrations
4. Let the user interface run in real time with the scanning for data visualization

2.4 Project Objectives

In order for this project to succeed in the completion of the goals listed previously, some objectives must be met first. In the microscope head, the design will need to include the use of only a 405nm laser beam with a very low power as the source for the microscope. The microscope head design will also need to account for out-of-focus light by utilizing a pin-hole rejection system with adjustable diameters. The CLSM must be able to be calibrated to ensure accurate pixel-to-pixel position while having very minor distortion of the reflected light. The CLSM will be powered by a wall outlet, only needing 12V to power the whole system. Implementation of a photodiode with a sufficient signal-to-noise ratio and can detect very weak signals will be needed to make sure processing of the data goes smoothly.

Use of open-sourced 3D printable parts will help not only the cost of the overall system but customizability for the microscope head, where all the optical components will be held. This microscope head should have the capability to adjust all optical components to ensure the most accurate signal is received. By utilizing 3D printed parts, the CLSM can also be ensured to fit inside of a 1m x 1m x 1m cubic area to help with ease of assembly and use in other research laboratories or for other demonstrations.

Processing the data in a reasonable time is the biggest concern with this CLSM. By utilizing a transimpedance amplifier (TIA) to amplify the signal from the photodiode, we can get a more accurate measurement of the position and height of the object under illumination (OUI). Prolonged exposure of the object to the laser beam can cause photobleaching (comparable to oversaturation in a common camera system). To reduce the influence of photobleaching, the need for a quicker way to process the data and then move to the next pixel is a must. This program will use the characterization of the systems lateral and axial resolutions to make fast and accurate movements of the motors so that the OUI is not under direct illumination for too long.

Design and fabrication of PCBs will need to be implemented for laser power, motor control and power, MCU power, and photodiode power. PCB implementation will also allow the CLSM to have a more compact layout, better for a more modular system, to allow for ease-of-access for repairs, modifications, and adjustments of optical components.

2.5 Description of Features and Functionality

2.5.1 Illustrations

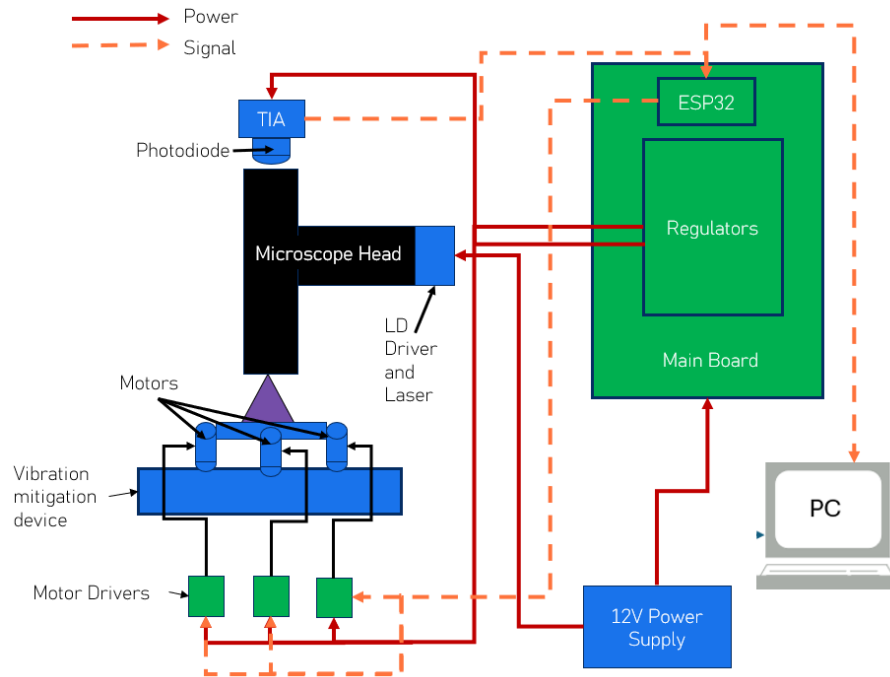


Figure 1: Initial Design

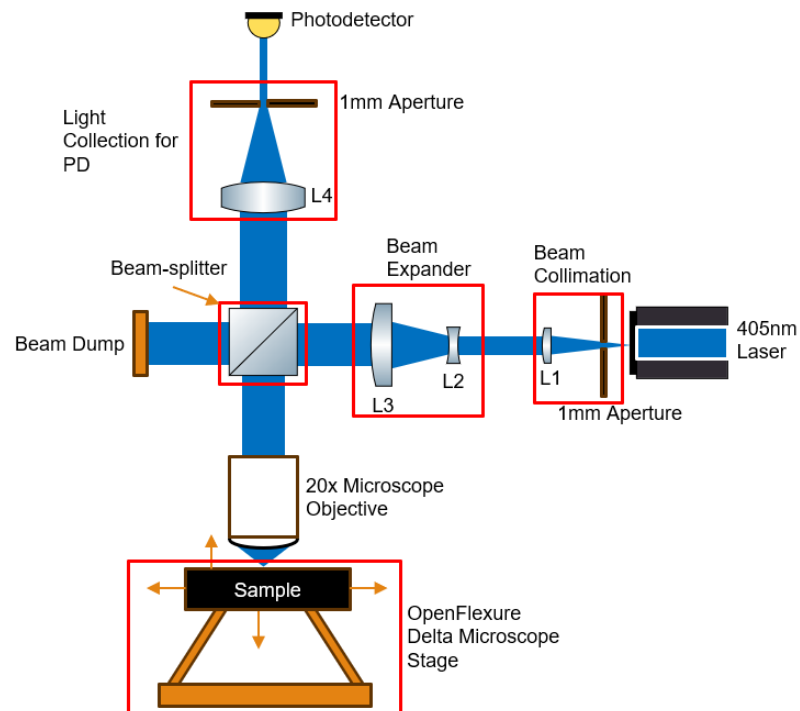


Figure 2: Optical Layout

2.5.2 Overall Functionality

The overall functionality of the project is to create a fully functional scanning laser microscope as described above. In essence, this microscope should be easily recreated by any individual or institution with minimal difficulty. The primary objective is to deliver a platform from which users can create micron-sized images while maintaining a budget of under \$1000. The system will do so through a custom optical design, a precision motorized stage, and a laser scanning mechanism. The collected data will be processed through a custom-made program to generate the image within a 5–15-minute interval for a 1mm x 1mm area. By eliminating commonly used yet expensive components such as galvanometers and creating an open-source platform, the project will balance performance and accessibility, making it available to a wide range of audiences.

2.5.3 Stage Functionality

The stage of the system is responsible for moving the sample precisely beneath the head of the microscope. This retains the ease of assembly for the user as it requires easily available stepper motors and an open-source mechanical platform by OpenFlexure to achieve controlled linear motion with high resolution. The precision of the motors should be around 0.88 to allow for micron movements. Because the scanning process will rely on the synchronized movement of the stage with the laser position, having such a system will allow for the sample to be scanned on either a point-by-point or line-by-line basis. Additionally, this stage is designed to create reliability, ensuring consistency between each individual scan.

2.5.4 Microscope Head Functionality

The microscope head will house the optical elements in the system; the beam expander, focusing lenses, beam-splitting elements, and photodiode. The beam, originating from the laser diode, will be transmitted through the beam expander before being redirected through the beamsplitter into the microscope objective. The microscope objective will focus the beam onto the sample in a spot on the order of $\sim 15\mu\text{m}$, from which it will be reflected back through the microscope objective, transmitted through the beamsplitter, and then focused by a lens through an aperture and onto the active area of the photodiode. The photocurrent generated by the photodiode will be amplified through a transimpedance amplifier and processed to obtain a depth measurement for each pixel. As the microscope stage moves the sample beneath the microscope objective, it will take measurements of each pixel on the order of $15\mu\text{m}$ across a 64×64 grid, resulting in a $1\text{mm} \times 1\text{mm}$ image with a resolution of $15\mu\text{m}$.

The airy disk of the spot size should be $\sim 1\mu\text{m}$ and should reflect about 1% of the overall light transmitted into the system. The incident light on the photodiode should be greater than $1\mu\text{W}$, as this would allow the system to produce a photocurrent out that is greater than 1 pA, this being the bare minimum to achieve a good signal.

Unlike a conventional laser scanning microscope, this design will not use galvanometers for scanning, instead, it will keep a fixed path for the laser, making the stage handle all movement, allowing this design to be more accessible to individuals as it will eliminate the heavy costs associated with galvanometers.

2.5.5 Image Generation Functionality

The data acquisition for image generation is achieved through the systems listed above. The signal that comes from the transimpedance amplifier will be digitized to be processed into a 2D image. This method will allow for real-time image construction with micron resolution. By avoiding other methods of microscopy like fluorescence-based imaging, this system will also remove the need for any special dyes or media, which will in turn enable faster scans and create ease of use as the sample will require less preparation.

The microscope's scanning area will be covering an area of 1mm by 1mm. OpenFlexure Delta stage has the capabilities to adjust the stage in the X, Y, and Z axis allowing for the laser to get a pixel of information at one point. As the stage translates across the object we will get more pixels of information. The resolution of the object will be 64 pixels by 64 pixels. The way we are getting the information for a pixel of laser is through a transimpedance amplifier. The amplifier will provide a voltage value and produce a minimum signal delta of 130 milli volts. The culmination of all these processes should have a target scanning processing time for approximately ~10 minutes.

2.6 Engineering and Marketing Requirements

Listed below are the engineering and marketing requirements for the CLSM:

Table 2.1: Marketing Specifications

Marketing Requirement	Specification
Affordability	Maintains a budget under \$1000, making it accessible to individuals and educators
Ease of Use	Minimizes sample preparation time, easy to assemble, open-source software and printable parts
Product Efficiency	Product consumes a reasonable amount of power, and image repeatability is feasible when little change is introduced
Reliability	Built in tolerance for varying conditions such as differences in external light conditions, electrical noise, etc.
High Image Quality	Achieves micron resolution with high contrast images

Scanning Speed	Achieves full data acquisition and processing within 5-15 minutes based on sample size
Footprint	Fits within a reasonable area, no more than 1m x 1m x 1m

- Engineering Requirements:

1. TIA Bandwidth at least 100 kHz of bandwidth to ensure fast and accurate detection of the current provided by the photodiode
2. TIA Gain: The amplifier must have a gain of 1×10^6 V/A to ensure fast and accurate detection of the current provided by the photodiode
3. Data Processing Time: Real-time image rendering with a total generation time of 5-15 minutes, with 5 minutes roughly being a 1mm x 1mm scanned area and 15 minutes roughly equating to a 1cm x 1cm scanned area
4. Stepper Motor Precision: Achieve low level micron precision in scan positioning with a step angle of 0.088° , which allows for a single step to move about $0.1 \mu\text{m}$
5. Scanning Area: Utilize the maximum area provided by the OpenFlexure platform while maintaining optimal scanning speeds. 1 mm x 1mm minimum size, 1 cm x 1 cm maximum size
6. Reading Accuracy: Maximize signal to noise to ensure reliable signal transmission and image quality $\sim 40\text{-}56\text{dB}$
7. Laser spot size: having a spot size of $\sim 1\mu\text{m}$ will allow for more pixels to be taken, making some longer images have a higher quality
8. Photodiode Responsivity: Select a photodiode that will allow for efficient light-to-current conversion such that it is compatible with the TIA, the responsivity must be greater than 0.3 A/W to achieve a readable signal
9. Laser Focus Accuracy: Ensures consistent airy-disk size of about $0.5 \mu\text{m}$ of the laser, allowing for consistent resolution and contrast and letting the CLSM achieve low level micron image quality.
10. Power Consumption: must be less than 5W to allow for the CLSM to utilize wall outlets for power

Table 2.2: Engineering Specifications

Marketing Requirements	Engineering Requirements	Specification
<i>Reliability, High Image Quality</i>	TIA Bandwidth	1 kHz of bandwidth
<i>Reliability, High Image Quality</i>	TIA Gain	1×10^6 V/A
<i>Ease of Use, Product Efficiency, Reliability, High Image Quality, Scanning Speed</i>	Data Processing Time	5-15 minutes

<i>Affordability, Ease of Use, Product Efficiency, Reliability, High Image Quality, Scanning Speed</i>	Stepper Motor Precision	Step Angle = 0.088°
<i>Ease of Use, Product Efficiency, Reliability, High Image Quality, Scanning Speed, Footprint</i>	Scanning Speed	1mm x 1mm, 64x64 pixel scan in ~15 min
<i>Affordability, Ease of Use, Product Efficiency, Reliability, High Image Quality, Scanning Speed</i>	Reading Accuracy	TIA signal-to-noise ratio ~30 – 40 dB
<i>Ease of Use, Product Efficiency, Reliability, High Image Quality, Scanning Speed, Footprint</i>	Laser spot size	~ 10 μm
<i>Affordability, Ease of Use, Product Efficiency, Reliability, High Image Quality, Scanning Speed</i>	Photodiode Responsivity	~ 0.6 A/W
<i>Ease of Use, Product Efficiency, Reliability, High Image Quality, Scanning Speed</i>	Laser Focus Accuracy	Laser Spot size $\pm 0.5 \mu\text{m}$
<i>Affordability, Product Efficiency, Reliability</i>	Power Consumption	< 5W
<i>Affordability</i>	Cost	< \$1000

2.7 House of Quality

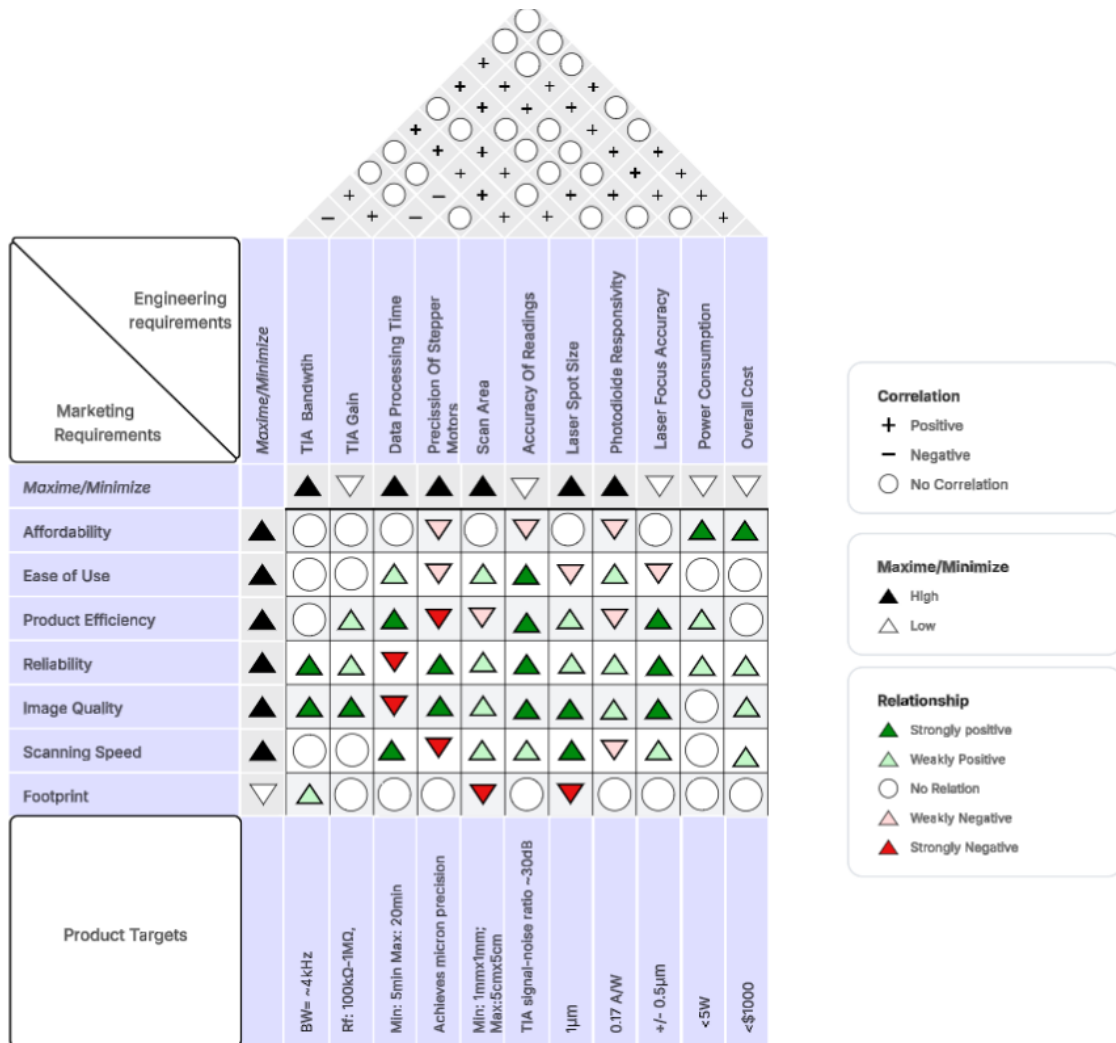


Figure 3: House of Quality (HOQ)

2.8 Hardware Block Diagram

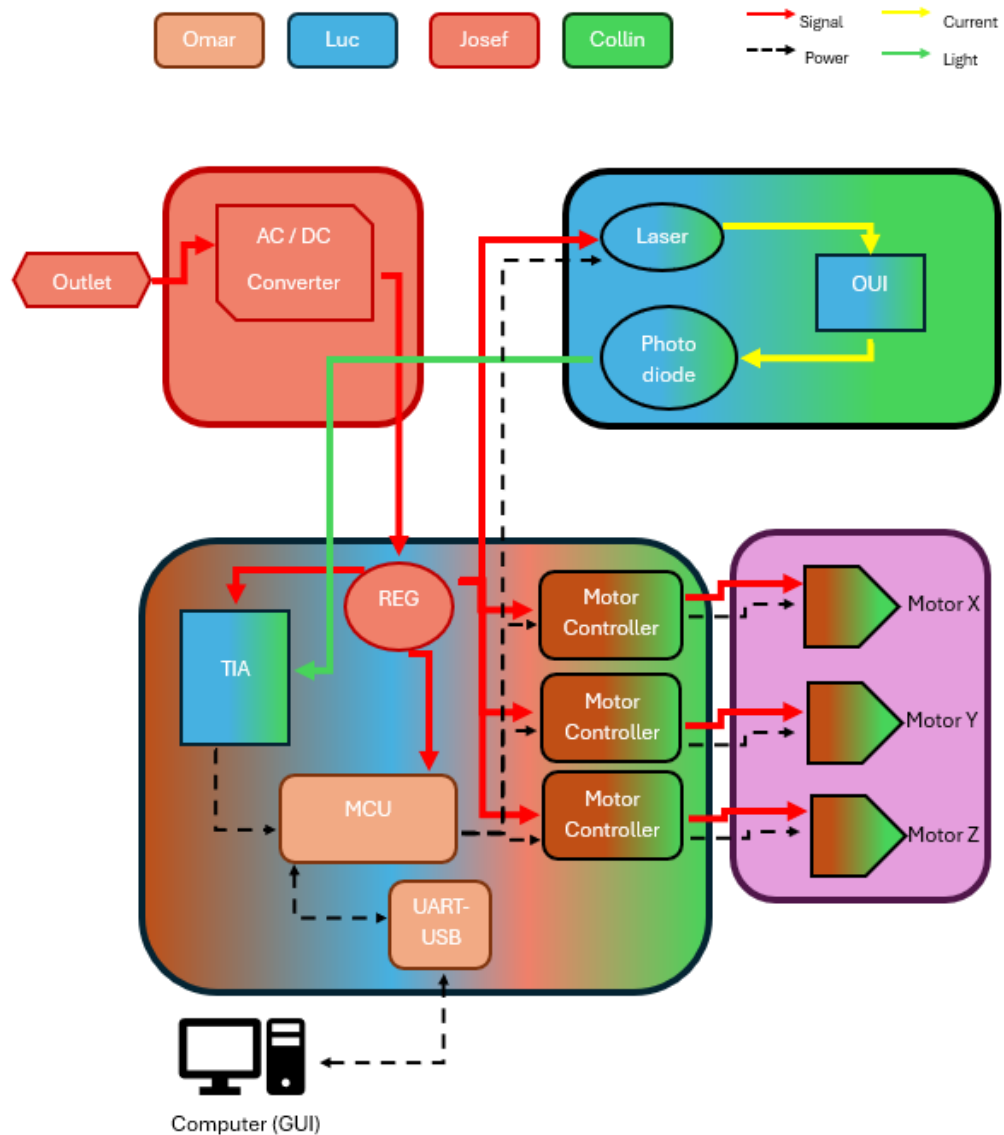


Figure 4: Hardware Block Diagram

2.9 Software

The software elements of this project are divided into 3 sections. The GUI element, motor control, and Transimpedance Amplifier data collection. These three elements would coalesce into a fully integrated system that would scan an object in our Laser Microscope.

2.9.1 GUI

The graphical user interface (GUI) is the window for the user to interact with our microscope. This feature would provide controllable settings to all the connecting peripherals in our system, such as calibrating our microscope stage and ensuring that the object is within our workable dimensions.

2.9.2 Motor Control

Controlling the motor of our system is an integral part of our project; it allows us to move our object to a reliable working distance. Once the stage is calibrated to the objective's working distance, we would begin scanning the object by moving the stage in a coordinated fashion across the x, y, and z axis. The precision of the motor control is also significant, delicate movements of this platform allow for a better resolution of data that the MCU would collect and the computer to process.

2.9.3 Data Collection

The stream of data comes from the transimpedance amplifier; the type of information in this stream is current values. When a stable stream of data comes through the system, it signifies that our object is within working distance. However, if the data tends to fluctuate this indicates that our object is out of our working distance and that we need to calibrate the stage in the z axis to be in our working distance range. The shifts in the x, y, and z axis would be noted with these current values and would be sent to our computer where the pooling of all this data would present a 2D bitmap.

2.10 Software Block Diagram

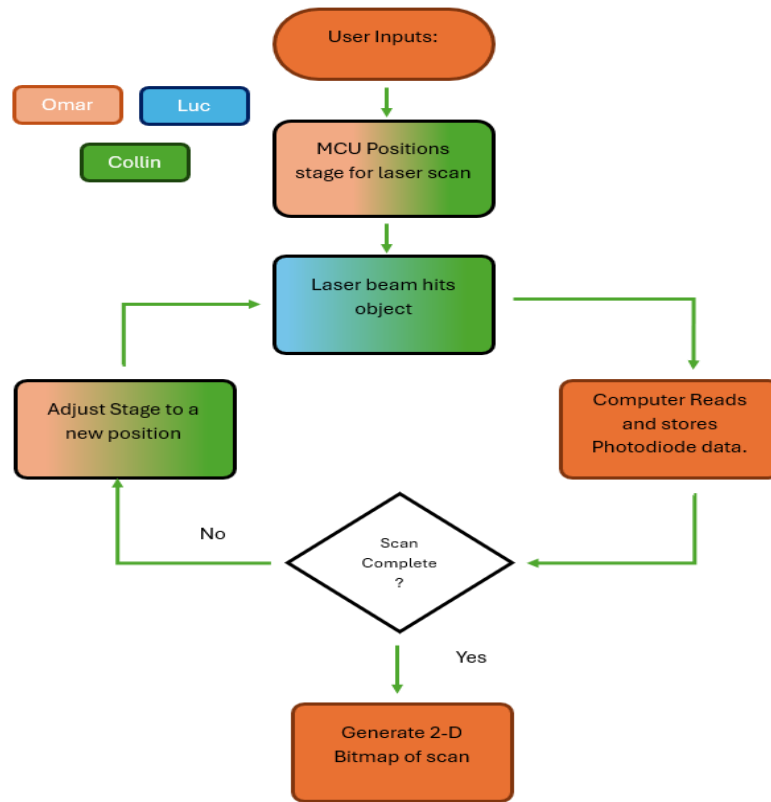


Figure 5: Software Block Diagram

3. Research and Investigation

3.1 Technology Comparison and Selection

3.1.1 Lasers

One of the most important components in CLSM is the laser. Different kinds of lasers have a massive impact on performance based on illumination, wavelength of light, output power, beam quality (M^2), thermal stability, modulation, and cost. Specifically in the case of beam quality, it is evaluated as the M^2 factor. The M^2 factor explains how “Gaussian” a laser beam is by comparing it to that of an ideal Gaussian Beam, the closer the M^2 factor gets to 1.0, the better the beam quality is.

Moreover, lasers provide monochromatic coherent beams of light, which means the light output by the laser is a constant phase (coherent) as well as only being a single wavelength (monochromatic). The output beam also has a divergence angle, or angle of spread over a certain distance, which can affect the way the beam expander/collimator is positioned. The wavelength of a laser is also very important since resolution is inversely proportional to the wavelength, shown in (5), which limits the total resolution able to be achieved when processing the data. The wavelength of lasers used in CLSM usually is

lower wavelength visible light for easier alignment, as well as still allowing for precise and accurate images for processing. With CLSM, lasers are the ideal choice for precisely illuminated points needed for scanning over a sample.

$$R = \frac{1.22 \times \lambda}{2 \times NA} \quad (5)$$

3.1.1.1 Diode Lasers

One of the more compact and common place lasers are diode lasers. Diode lasers are electrically efficient semiconductors that are pumped electrically, allowing for very fast turn on and off times. These lasers are also easy to set up and use and usually have a very long lifetime. The beam quality of diode lasers is usually lower, typically having an M^2 between 1.2 to 2.5, while having higher divergences of the beam when compared to other types of lasers. The output beam will tend to be very divergent or even elliptical based on the construction of the semiconductor. However, depending on the optical setup after the diode, the beam can be tuned to have a better quality and become more precise.

With a linewidth, the range of wavelengths or frequencies present in an outputted beam, roughly between 1 – 10 nm, diode lasers are the broadest but still allow for precision around the specified wavelength. These lasers allow for use in compact systems, usually without the need for any thermal management systems in place. Typical uses of a diode laser reside in systems with a strict budget or through optical fibers to guide the beam.

3.1.1.2 Diode-Pumped Solid-State Lasers

DPSS lasers have a crystal medium, primarily either Nd:YAG (Neodymium-doped Yttrium Aluminum Garnet) or Nd:YVO₄ (Neodymium-doped Yttrium Orthovanadate), that are optically pumped by a diode laser. This allows for high quality beams (M^2 factor is usually between 1.1 – 1.3), very low noise, and narrow linewidths. DPSS lasers usually require a cooling system to allow for the aforementioned benefits, which can make the laser bulky and if not actively cooled will allow the beam to lose quality and gain a large amount of noise.

The optical power of DPSS lasers is higher than typical lasers due to the higher power needed to pump the crystal from the diode, usually between 100 – 1000 mW. Modulation of DPSS lasers is external with the need for either an acoustic-optic modulator (AOM) or an electro-optic modulator (EOM), both of which are not direct modulations meaning modulation times are typically longer than other laser types. DPSS laser uses are usually found in fluorescent microscope systems as a core excitation source for fluorescent mediums.

3.1.1.3 Gas Lasers

Gas Lasers operate through electrical excitation of a gaseous medium. Once the gas is excited enough it will produce a highly coherent, low noise, and low divergence beam. The power required to turn on and run gas lasers is typically very high, which allows these lasers to have very stable beams. The beam uniformity gives way for very little aberrations of the output beam with a M^2 roughly being 1.0, while also having a very

small linewidth. While these benefits usually require gas lasers to be larger in size when compared to other laser types, gas lasers are one of the best lasers to use as reference beams in systems when consistent beams are necessary such as alignment or instrument calibrations. The cost of a gas laser is also typically high when compared to newer laser options available.

3.1.1.4 Femtosecond/Pulsed Lasers

While the most expensive and complex laser systems to integrate, Femtosecond lasers have some of the most benefits when it relates to output power, thermal management, and very clean beams (M^2 factor is roughly 1.0). However, femtosecond lasers are not only one of the single most expensive types of lasers but also have a plethora of challenges that follow. From having a large footprint, very sensitive alignment, requiring specialized safety systems due to high powers needed to properly control the beam, and having the cheapest femtosecond system commercially being about \$30,000. While the benefits and quality of the laser beam of a femtosecond laser is the best, in a situation where it would need to be implemented into CLSM using femtosecond lasers does not seem like the best choice.

Table 3.1: Laser Comparison

	Diode Lasers	Solid-State Lasers (DPSS)	Gas Lasers	Femtosecond / Pulsed Lasers
Wavelength (nm)	375 – 2000	355, 532, 1064	543, 594, 633, 1060	700 – 2000
Power Consumption	Low (<5 W)	High (10 – 50 W)	Moderate to High (5 – 100 W)	High to Very High (50 – 300 W)
Output Power	1 – 100 mW	100 – 1000 mW	0.5 – 50 mW	~ 100 mW
Beam Quality (M^2)	1.2 - 2.5, Typically elliptical or very divergent	1.1 – 1.3, Gaussian and circular	~ 1.0 Ideal Gaussian	~ 1.0 Ideal Gaussian
Size	Very Compact	Compact (depending on the size of the TEC)	Large	Large
Thermal Regulation Required	No	Yes	No	Yes

Cost	\$10 - \$1000	\$400 - \$15,000	\$500 - \$10,000	\$30,000 - \$150,000
Technology Selection	✓			

The laser source is one of the main components in CLSM. In almost all scanning laser microscopes the need for the lowest power, but most reliable and consistent source is key. The decision was made to utilize a laser diode instead of gas, DPSS, or femtosecond lasers, due to certain factors such as compact form factors, minimal power usage, direct modulation, and the overall price of laser diodes. The use of laser diodes is necessary due to the need for a low cost, widely available option that can be repeatably used without needing maintenance or thermal regulation.

Another major piece of criteria was the need to be able to lase at 405 nm (or similar) as lower wavelengths can increase the resolution of the system compared to wavelengths higher on the visible spectrum. While there are options to be able to lase lower than 405 nm, the ability to see the laser beam would be critical in alignment and tuning of the system.

Table 3.2: Laser Diode Selection

Model	Laser-makers B0788D62ML	Lights88 B072JB71G8	Thorlabs LP405P20
Cost	\$12.89 (for 10 diodes)	\$13.65	\$62.28
Output Power	5 mW	5 mW	20 mW
Size	5.6 mm (TO-18 Package)	Cylindrical (14.5 mm x 45 mm)	5.6 mm (TO-18 Package)
Input Voltage	3 – 5 V	3 – 5 V	4.8 V
Modulation	No	No	Analog/TTL Compatible
Part Selection			✓

For prototyping and alignment, the Laser-Makers B0788D62ML and Lights88 B072JB71G8 are both great options due to the price point and ease of access to these diodes. However, for final system integration, the Thorlabs LP405P20 was selected due to the quality, precise manufacturing, and high consistency when operated for long periods of time. The performance of the LP405P20 is needed for consistency and higher quality images when compared to the other options presented. The LP405P20 is also capable of being modulated, with an option for thermal management to ensure the system runs smoother and more accurately.

3.1.2 Laser Current Controller

Precise control of current into the laser diode is essential to ensure both optimal performance and long-term reliability. Laser diodes are highly sensitive components—exceeding their current ratings even briefly can lead to immediate damage or degraded output over time. To address this, a dedicated current driver circuit will be employed to limit the maximum current to a safe threshold, providing stable operation and protecting against power supply fluctuations or electrical noise. This regulation is critical for maintaining consistent laser intensity, which directly impacts the accuracy and resolution of the CLSM.

3.1.2.1 Current Control Modules

Current control modules are electronic circuits specifically designed to deliver a stable, regulated current to components that are sensitive to fluctuations, such as laser diodes. Unlike voltage regulators, which maintain a constant voltage, these modules focus on keeping the current consistent regardless of changes in load or supply voltage. This is crucial for preventing thermal runaway, maintaining consistent light output, and protecting the diode from damage. They often incorporate feedback mechanisms to actively monitor and adjust current levels, ensuring precise control. Current control modules are commonly used in systems where precision and safety are priorities, offering a reliable and efficient solution for driving current-sensitive devices.

3.1.2.2 Passive Voltage-Resistor Conversion

Passive voltage-resistor conversion is a simple method of limiting current to a laser diode by placing a series resistor between the power supply and the diode. The idea is that the resistor drops voltage proportionally to the current, based on Ohm's Law, thereby restricting how much current flows. While this approach is easy to implement and inexpensive, it lacks precision and stability. The current can vary significantly with changes in supply voltage or diode forward voltage, making it unreliable for sensitive components like laser diodes. Additionally, this method offers no active feedback or protection, increasing the risk of overcurrent and thermal damage. As a result, passive current limiting is generally considered inadequate for applications requiring consistent and safe diode operation.

3.1.2.3 Linear Constant Current Regulator

Linear Constant Current Regulator can be implemented using a linear voltage regulator configured with a current-setting resistor or an op-amp-based constant current source. This approach delivers a steady, regulated current and is quieter (low ripple) compared to switching regulators, which is beneficial for sensitive optical systems. Unlike passive resistors, it actively maintains a set current regardless of voltage fluctuations or diode characteristics. However, it dissipates excess voltage as heat, making it less efficient and often requires heat sinking, especially when the voltage drop across the regulator is significant.

Table 3.3: Laser Current Controller Technology Selection

Criteria	Current Control Modules	Passive V-R Conversion	Linear Constant Current Regulator
Cost	Moderate	Low	Low
Output Power	Low-High (Adjustable)	Low	Low
Integration Complexity	Low	Low	Moderate
Input Voltage	0-48V depending on application	Supply Dependent	0-48V depending on application
Technology Selection			✓

3.1.2.4 Micro FlexDrive V5

The Micro FlexDrive V5 is a dedicated laser diode driver that offers precise current regulation with built-in protection features, making it ideal for safely powering sensitive components. Its compact size and ease of integration make it a strong choice for projects that require reliability and consistent performance. However, it can be more expensive than other options and may require some tuning or configuration based on the diode used.

3.1.2.5 FlexMod P3

The FlexMod P3 is a more advanced constant-current driver from the same company that makes the Micro FlexDrive. It supports a much wider current range—up to 4 A—and is fully linear, allowing for analog modulation with low noise and high stability. It includes features such as soft-start, enable/disable control, TTL and analog modulation, and comprehensive fault protection including over-temperature and short-circuit protection. Because of its linear topology, it's particularly well-suited for sensitive optical applications where current ripple needs to be minimized. The main drawback is that it can run hot at higher currents and voltages due to power dissipation, so proper heat sinking is often necessary. It's also frequently out of stock due to high demand, making procurement a potential bottleneck in time-sensitive projects.

3.1.2.6 Super X-Drive (Bucking Laser Driver)

The Super X-Drive is a high-efficiency buck-mode laser diode driver designed for high-power applications. Unlike linear drivers, it uses a switching regulator topology, allowing it to convert higher voltages to lower, regulated currents without excessive heat dissipation. This makes it ideal for scenarios where the supply voltage is significantly above the diode's forward voltage or when running high-current diodes without a large heat sink. It supports TTL and analog modulation, thermal shutdown, and current

trimming, offering a good balance of efficiency and control. However, as with all switching drivers, it introduces some switching noise, which may not be acceptable in ultra-sensitive analog or optical systems. Additionally, the physical size and need for external components like inductors or capacitors may complicate integration compared to the FlexDrive.

Table 3.4: Laser Current Controller Technology Selection

Criteria	Micro FlexDrive V5	FlexMod P3	Super X-Drive (Bucking Laser Driver)
Cost	\$19.99	\$35.99	\$32
Output Power	Low	Moderate	High
Output Current Range	~35mA – 500mA	~100mA~4A	Up to 5A
Input Voltage	~2.5-6V	~4.5V-12V	5V-30V
Reliability	High	Very High	High
Part Selection	✓		

3.1.3 Beam Expanders

One of the main factors in how the laser beam will travel through each of the optical sub-systems can be seen through design and implementation of collimation and expansion of the laser beam. Beam expander systems play a crucial role in allowing for long distance propagation, alignment, and consistent beam quality. In a system such as a microscope the need for high precision with minimized diffraction of the beam is required. There are typically two types of beam expanders utilized in microscope design: Keplerian and Galilean. A beam expander with low overall optical aberrations, low cost, compact structure, and lowest loss of optical power are all key factors in the context of designing a CLSM.

3.1.3.1 Keplerian Expander

The Keplerian beam expander uses two positive focal length lenses which results in a focal point where the focal lengths of both lenses meet. While this design is great for most low-power laser systems, not only is it simple to build but also allows for higher magnification (shown in (3)) of the incident laser light.

$$M = \frac{f_1}{f_2} \quad (3)$$

However, the constraints of a Keplerian expander can be seen with usually higher optical aberrations as well as a less compact structure needed to support the lens distances as shown in (4). While most optical aberrations that are present in these designs can be cleaned up through the use of an aperture at the internal foci, this can still allow for some spherical aberrations to be present which may affect the image quality of the system.

$$t = f_1 + f_2 \quad (4)$$

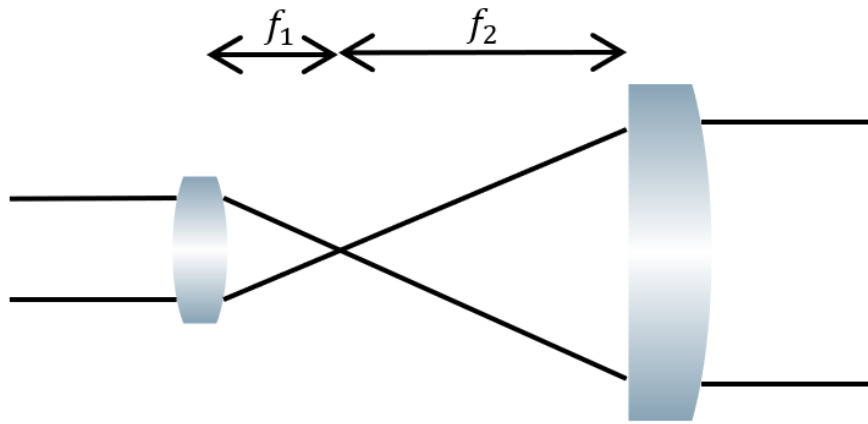


Figure 6: Simple Keplerian Beam Expander Design

3.1.3.2 Galilean Expander

Galilean beam expanders typically use one negative and one positive focal length lenses which result in a focal point behind the first lens (the objective lens) and do not allow for any internal foci. Another advantage of the Galilean design can be seen in not only lower cost, but also in a more compact size (as shown in (4)) with lower overall aberrations. This design does not need any internal apertures or pinholes to clean up the beam as well, leading to higher transmitted power through the expander with very low optical aberrations.

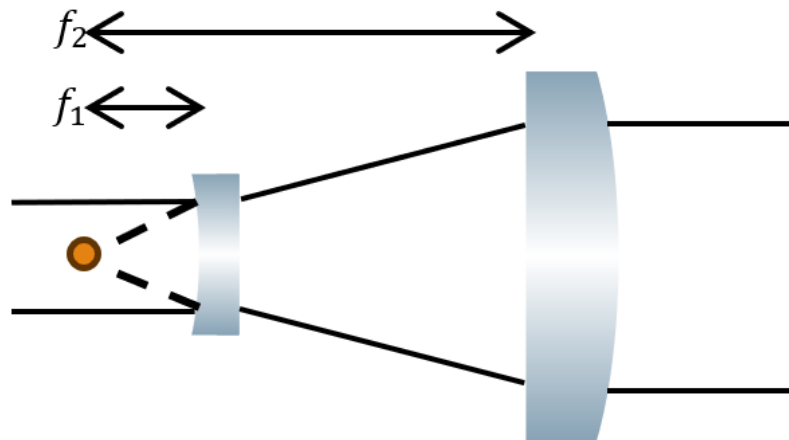


Figure 7: Simple Galilean Beam Expander Design

Table 3.5: Beam Expander Comparisons

	Keplerian	Galilean
Optical Aberrations	Moderate	Low
Cost	Low	Low
Size (t) (~5x Mag., $f_1 = 20\text{mm}$, $f_2 = 100\text{mm}$)	~120 mm	~80 mm
Optical Losses	Low (Moderate with aperture)	Low
Technology Selection		✓

To achieve the 5x magnification of the beam needed to have the beam fill the entrance pupil of the microscope objective, while also considering the total size the expander will take up in the system, the Galilean beam expander will be the best option for this. However, the optics used in the expander must also be specifically defined as the difference in size of the optics can play a crucial role in how the beam interacts with the beam expander.

Now that the Galilean beam expander has been chosen as the expander type, the focus then shifts to properly deciding a selection of lenses that can fit the criteria needed for the system. The requirements for the selection of the lens must include a 5x magnification of the beam, while still allowing for the beam to be collimated, having a length that does not contribute to problems with mechanical stability or total size of the microscope head, offering good transmissivity of the beam, and minimized optical aberrations. All presented lens pairings are N-BK7 glass due to the affordability and commonality of this type of glass. N-BK7 is often used in systems with a need for high-quality optics at a

fraction of the price compared to less common alternatives such as UV fused silica or N-SF11 glass.

3.1.3.3 LF1822-A Negative Meniscus and LB1869-A Bi-Convex Lens

The Thorlabs LF1822-A negative meniscus lens offers a focal length of -100 mm, while the LB1869-A bi-convex lens offers a +500 mm focal length. Both lenses are 25.7 mm in diameter, which could be an issue due to the size of the negative meniscus lens being much larger in diameter than the input laser beam. While these lenses still offer a 5x magnification, the total length of the expander will be about 400 mm long. The significant length of this system must be taken into consideration when integrating into the microscope head as having a longer layout can create problems with vibrations and mechanical stability. This selection of lenses is ideal for minimized chromatic and spherical aberrations as well as having a higher combined transmissivity than other typical Galilean expander designs at roughly ~99% transmissivity at 405 nm due to Thorlabs -A broadband coating (AR coating from 350 - 700 nm).

3.1.3.4 LD2060-A Bi-Concave and LA1608-A Plano-Convex Lens

The Thorlabs LD2060-A bi-concave and LA1608-A plano-convex lenses offer focal lengths of -15 mm and 74.8 mm respectively. Both lenses are also coated in Thorlabs -A broadband coating, allowing for ~99% transmissivity at 405 nm. The total length of this lens system is about 60 mm, while having a 4.99x magnification of the beam. This size not only minimizes the problem with mechanical stability, but the magnification is also very close to the magnification specification needed for the system.

The LD2060-A lens is smaller than the previously mentioned LF1822-A negative meniscus lens, which allows for more beam coverage of the input beam in the system, with the LD2060-A lens having a 12.7 mm diameter and LA1608-A having a 25.4 mm diameter. The smaller diameter not only allows for a more compact design but also can reduce the stray light and vignetting of the optical design.

3.1.3.5 LC1054 Plano-Concave and LA1986 Plano-Convex Lens

The Thorlabs LC1054 plano-concave and LA1986 plano-convex lenses offer a slightly cheaper alternative to the previously mentioned beam expander lens designs due to not having an AR coating on the lenses. While the LC1054 lens has a focal length of -24.9 mm, the LA1986 lens has a focal length of 124.6 mm. The total length of the system is about 100 mm, while still offering a magnification of 5x. The LC1054 lens is also 12.7 mm in diameter while the LA1986 lens is 25.4 mm in diameter.

One of the major problems this lens pairing presents is not having Thorlabs -A coating designed for the 405 nm wavelength used in this system. This will allow for less transmissivity of the beam throughout the beam expander, with a loss of roughly 8% through both lenses, and increased internal reflections which could affect the overall image quality once processed.

Table 3.6: Lens Selection for Beam Expander

Criteria	LF1822-A / LB1869-A	LD2060-A / LA1608-A	LC1054 / LA1986
Total Cost of Lens Pair	\$82.30	\$87.88	\$46.09
Length of Optical System	400 mm	60 mm	100 mm
Magnification	5x	4.99x	5x
Transmission %	~99%	~99%	~92%
Diameters of Lenses	25.4 mm, 25.4 mm	12.7 mm, 25.4 mm	12.7 mm, 25.4 mm
Amount of Optical Aberrations	Low	Low	Moderate
Part Selection		✓	

3.1.4 Beam Splitters

An optical beamsplitter is a passive optical device that divides a single beam of light into two or more separate beams. It involves both partial reflection and transmission, using either a thin, semi-reflective coating or a carefully engineered optical interface between materials of different refractive indices. Beamsplitters typically come in the form of flat plates, cubes, or fiber-based components, depending on the application. The most common configuration is a 50/50 beamsplitter, which ideally reflects 50% of the incoming light and transmits the remaining 50%, but there are applications for many other reflection-transmission ratios.

The behavior of a beamsplitter depends on factors such as wavelength, polarization, and angle of incidence, so it must be carefully chosen to fit the design of a system. Specialized types of beamsplitters include dichroic beamsplitters, which separate light based on wavelength (often used in fluorescence microscopy), and polarizing beamsplitters, which split light based on its constituent polarized components.

Beamsplitters are critical in many complex optical system designs, but they can introduce unwanted effects such as losses, ghost reflections, or interference, and therefore must be appropriately considered during design.

3.1.4.1 Plate Beam Splitter

A plate beamsplitter is a flat, thin piece of transparent material with a partially reflective thin film coating on one surface. This coating allows the plate to reflect a portion of the incident light while transmitting the rest, thereby dividing the beam into two paths. Plate beamsplitters are typically positioned at a 45-degree angle to the incident beam so that one portion is reflected at 90 degrees while the rest continues straight. The reflectance-to-

transmittance ratio is a function of the coating design and can be customized for different wavelengths or polarizations.

One advantage of plate beamsplitters is that they introduce less optical path distortion and wavefront error compared to other styles of beamsplitters, especially for high-precision applications. This is because the beam passes through only a single layer of glass, and there is reduced absorption and chromatic dispersion. Additionally, unwanted internal reflections can be mitigated by anti-reflective coatings on the back surface of the plate or by tilting the plate slightly to steer ghost beams away from other components.

3.1.4.2 Cube Beam Splitter

A cube beamsplitter splits incoming light beams using a compact, robust structure. It is comprised of two right-angle prisms cemented together along their hypotenuse faces, with a partially reflective dielectric coating at the internal interface. This coating divides the light so that a portion is reflected at 90 degrees, while the remainder is transmitted straight through the cube. Cube beamsplitters are typically designed for use at a 45-degree angle of incidence to the incident beam.

One big advantage of cube beamsplitters is their mechanical stability and alignment precision. Because the optical elements are fixed within a rigid, monolithic structure, cube beamsplitters are less sensitive to vibrations or misalignment compared to plate beamsplitters. They also have lower beam displacement, as the transmitted beam exits the cube along the same line as the incoming beam.

Cube beamsplitters have some limitations, however. Their cemented interface introduces material absorption, and they can introduce interference effects or multiple reflections if not properly coated. Additionally, like plate beamsplitters, cube beamsplitters can exhibit polarization sensitivity, especially if not specifically designed to be non-polarizing.

3.1.4.3 Polarizing Beam Splitter

A polarizing beamsplitter separates light based on polarization state rather than by intensity. The most common form is a polarizing beamsplitter cube, which consists of two right-angle prisms joined at the hypotenuse, with a multilayer dielectric coating at the interface. This coating allows transmission of light of one linear polarization while reflecting the orthogonal polarization at 90 degrees.

Because a PBS cleanly separates polarizations, it enables high extinction ratios, meaning the unwanted polarization is effectively blocked from being transmitted. However, polarizing beam splitters do have some limitations. Their performance is highly dependent on the angle of incidence, so they are typically optimized for a fixed incident angle. Additionally, non-polarized or elliptically polarized light will be split unevenly, so unless a signal has been carefully polarized, it can introduce high loss and affect the quality of a signal.

Table 3.7: Beam Splitter Comparison

Criteria	Plate	Cube	Polarizing
Chromatic Dispersion, other aberration	Low	Moderate	Moderate
Transmittance	High	Moderate	High; selects for chosen polarization
Extinction Ratio	High	High	High
Cost	Moderate	High	High
Technology Selection	✓		

The design considerations involved in choosing an appropriate beamsplitter involved their transmittance/reflection ratio, wavelength selection, price point, thickness, and physical size relative to the beam. The three best choices are described and compared below.

3.1.4.4 Thorlabs BST04

This beamsplitter is a 70:30 device with a coating tuned to be effective in the 400-700nm wavelength range. It has a 0.5in diameter which is sufficient to pass the entirety of the beam and has a thickness of 3mm. It comes at a price of \$98.18. This is a reasonable price for this type of component, and because it is designed to achieve 70% transmission at the wavelength selected for the operation of this microscope (405nm), it is a top contender for incorporation into this optical design.

3.1.4.5 Thorlabs BSW10R

This beamsplitter is a 50:50 device that is tuned to work in the 400-700nm range. It is a circular, 25mm diameter plate which means it is more than large enough to encompass the entire beam and has a thickness of 3mm. It is the most expensive of the three final choices at \$108.38, however because of its 50% transmission at the target wavelength, it made it into the final selection for this optical design.

3.1.4.6 Thorlabs EBS1

This beamsplitter is a 50:50 device that is tuned to operate between 400-650nm. It is circular with a 25.4mm diameter, making it large enough to fit the entire beam, and comes in at the cheapest of the three options at \$41.00.

The EBS1 beamsplitter is the most economical decision and satisfies all the base level optical requirements under consideration for this design. However, because it is marketed as an ‘economy’ product and has no mention for any tolerance for variation within the system, it may not be robust to minor adjustments that may be necessary after

construction of the system permits testing. Both BST04 and BSW10R have high quality coating and have a slight tolerance for variation in the incident angle of the optical beam. This is an important consideration as preparations are being made to test for possible negative effects on back reflection through the system, because minor adjustments to the incident angle of the beam may be necessary to mitigate this.

Concerns about saturation and possible photobleaching of the photodiode make it necessary to introduce losses into the system to limit the optical intensity of the signal reaching the photodiode. While this can be accomplished through the incorporation of several different components, it is advantageous to refrain from introducing another filter or aperture that may cause aberration in the signal. With this consideration in mind, the BSW10R beamsplitter was chosen for this design. Though it is the most expensive option of the three, it is a worthy investment and important to the functionality of this microscope.

Table 3.8: Beamsplitter selection

Criteria	Thorlabs BST04	Thorlabs BSW10R	Thorlabs EBS1
Transmission	70:30	50:50	50:50
Wavelength of Operation	400-700nm	400-700nm	400-650nm
Diameter	12.7mm	25mm	25.4mm
Part Selection		✓	

3.1.5 Microscope Objectives

Infinity plan objectives allow for the output of collimated light, where light exists as parallel rays out of the objective. These parallel rays allow for the rest of the optical system to have more flexibility as to what can be put between the sensor and the exit pupil of the objective. Another advantage of having parallel rays passing through the objective is that it allows for a wider range of movement of the objective, without creating image shifting or changing an internal point of focus.³⁴

In the case of creating a CLSM, the choice of a microscope objective lens with a specific magnification, numerical aperture (NA), working distance, as well as the type of immersion the objective has are the major deciding factors that determine which magnification to choose. Magnification of an objective lens describes the size ratio of an image to the original sample. A few relevant objective types will be discussed further below.

3.1.5.1 10X Objective

10x objective lenses allow for a wide field of view and much longer working distances compared to that of higher magnification objectives. Where 10x objectives support easier

alignment and a more ideal choice for surveying samples, it falters with a lower NA that limits the total resolution of the microscope as well as limited uses in cases with the need for high-resolution images.

3.1.5.2 20X Objective

20x objectives offer a balance between magnification and field of view. While struggling to achieve high-resolution for sub-micron imaging it does allow for a working distance that allows for a good amount of range of movement of the sample before losing focus. Another beneficial factor of 20x objectives is having a middle point NA between lower and higher magnification objectives. This NA point still allows for higher resolutions than the 10x objectives but still lies short in the resolution capabilities of 40x objectives and higher. The use case of 20x objectives would lie in general purpose imaging systems with a good level of resolution for samples greater than sub-micron sizes.

3.1.5.3 40X Objective

The 40x objectives are a common choice for needing a balance between super high resolution while still having a reasonable working distance to the sample. These objectives are able to be used for micron level imaging but do not accommodate for ease of use and alignment, usually needing finer care in implementing into microscope systems. However, the field of view on 40x objectives starts to fall off heavily when compared to that of lower magnifications which can become a problem depending on the size of the sample under the objective.

The immersion types of 40x objectives are also not limited to dry objectives. 40x objectives allow for the use of water as an immersion type depending on how the sample is viewed. This can give way for a wider range of uses in certain cases where biological samples may need to be viewed while in a viewing glass having water or other liquids as the medium.

3.1.5.4 60X Objective

While 60x objectives allow for the highest magnification and resolution when compared to the objectives above, it has many limiting factors. Some of the main limiting factors of 60x objectives are the tiny field of view and very shallow working distance. These limitations alone do not allow for 60x objectives to be used in other cases except for subcellular imaging. The optical slices of the sample are also very small, not allowing for very deep measurements into the sample.

60x objectives have high NA values, sometimes up to 1.4 depending on the immersion type. These objectives will almost always be immersed in some sort of liquid, that being water or oil.

Table 3.9: Microscope Objective Comparison

	10x Objective	20x Objective	40x Objective	60x Objective
NA	0.25 - 0.30	0.40 - 0.50	0.65 - 0.75	0.95 – 1.40
Working Distance	~7 – 15 mm	~1 – 5 mm	~0.2 – 0.7 mm	~0.1 – 0.3 mm
Immersion Type	Dry	Dry	Dry, Water	Water, Oil
Field of View	Wide	Moderate - Wide	Moderate - Narrow	Very Narrow
Resolution	Low	Moderate - High	High	Very High
Technology Selection		✓		

Of the previously mentioned infinity plan microscope objectives, the 20x objective type was selected as the most appropriate for the microscope design. The 20x objective was selected not only due to the magnification but also the working distance, NA, field-of-view, resolution, and immersion type. 20x objectives offer a good compromise between performance and cost. It allows for sufficient clearance to the sample, allowing for easy alignment, while also having a good resolution to create clear images without the need for any extra optical components after it. This is needed due to the nature of confocal microscope systems that require frequent sample changes and adjustments of focus.

One of the major concerns with choosing the right 20x microscope objective for this system is the price. Many companies offer their own 20x objectives, and the prices can vary from \$50 to almost \$1000. Three great options of infinity corrected 20x objectives include AmScope PA20X-INF objective, Olympus PLN 20X objective, and Newport LIO-20X objective.

The main difference between the presented microscope objectives is that of price and working distance. All three objectives have a NA of 0.40, include 405 nm in the range of working wavelengths, and do not utilize any immersion liquids. However, the working distance of the AmScope PA20X-INF and Olympus PLN 20X objectives is 1.2 mm while for the Newport LIO-20X objective it is 1.5 mm. The differences in the working distances of these microscope objectives are not a problem since most sample heights will be much thinner than 1 mm, as well as the chosen microscope stage allows for another 4 mm of movement in the z-axis.

The microscope objective that will be used will be the AmScope PA20X-INF objective due to the price being under \$100, the Olympus PLN 20X and Newport LIO-20X are

\$476 and \$146 respectively. This price difference is enough to be the deciding factor when it comes to which microscope objective will fit best with this system.

Table 3.10: Microscope Objective Selection

Criteria	AmScope PA20X-INF objective	Olympus PLN 20X objective	Newport LIO-20X objective
Numerical Aperture	0.4	0.4	0.4
Working Distance	1.2 mm	1.2 mm	1.5 mm
Immersion Type	Air	Air	Air
Price	\$100	\$476	\$146
Part Selection	✓		

3.1.6 Focusing Lenses

After transmission through the beam expander, both directions through the beam splitter and microscope objective, and after reflection off the object under illumination, the final step in the handling of the microscope optical signal will be to focus it onto the photodetector. This is accomplished by two optics, the first of which is a focusing lens. The parameters of this lens can be considered to have more flexible design constraints than most of the other parts of the optical assembly for this design, as its function is very simple in comparison.

The optical signal must be focused from a beam of the same diameter as it is when emerging from the microscope objective down onto the active region of the photodetector. Besides practical constraints –it would not make sense for the focusing distance to be the largest part of this microscope design- it does not require the same precision the other calibrations for the optical components require.

With this in mind, it is important for the focusing lens to have a diameter marginally greater than that of the collimated beam exiting the microscope objective and transmitting back through the beamsplitter in order to fill its numerical aperture and focus the signal into a spot that can sufficiently fill the active region of the chosen photodetector. It is important that the beam cover as close to the full area of the photodetector's active region to ensure the most accurate measurement and strongest output signal.

3.1.6.1 Thorlabs LB1761

This is a spherical biconvex lens with a 25.4mm diameter and a 25.4mm focal length. It is made of NBK7 glass.

3.1.6.2 Thorlabs LB1569

This is a spherical biconvex lens with a 25.4mm diameter and a 60mm focal length. It is made of NBK7 glass.

3.1.6.3 Thorlabs LA1255

This is a spherical plano-convex lens with a 25mm diameter and a 50.1mm focal length. It is made of NBK7 glass.

Table 3.11: Focusing Lens Selection

	LB1761	LB1569	LA1255
Shape	Biconvex	Biconvex	Plano-convex
Focal Length	25.4mm	60mm	50.1mm
Diameter	25.4mm	25.4mm	25mm
Material	NBK7	NBK7	NBK7
Part Selection		✓	

When choosing the focusing lens, it is important to consider how it will be incorporated into the larger system. With an incident beam diameter of approximately 20mm, each of these lenses is large enough to fill the majority of its numerical aperture before the beam is focused through the pinhole onto the photodiode. Because the pinhole aperture must be placed along the path of the beam and adjusted to filter out the edges of the beam, it is advantageous to have a beam with a longer focal length/smaller numerical aperture. A beam that diverges at a slower rate makes adjusting the pinhole easier, as lateral displacement will not have as extreme an effect on the diameter of the beam.

It is also advantageous to use a biconvex lens instead of a planoconvex lens, as adjustments made through a lens where there is refraction on both surfaces instead of one larger refraction at the convex surface of a plano-convex lens will be more suited to making micro adjustments by hand to the system in order to focus the beam onto the active area of the photodiode.

3.1.7 Apertures

The second optic involved in focusing the optical signal onto the photodetector is a pinhole aperture, which is a critical component in confocal microscopy. The aperture is the last optical component through which the signal will pass before being incident on the photodetector, and its function is important to achieving a high-quality signal and ensuring a high enough resolution. Because only light that has been focused through the pinhole aperture will be incident onto the photodetector, a significant amount of out-of-focus light will be blocked from the detector. Not only will this directly mitigate the negative effects of any residual aberrations in the system, it is also important in improving the depth resolution in imaging systems and increasing the clarity and contrast.

One design consideration when incorporating a pinhole aperture for confocal microscope systems is the tradeoff between signal strength and resolution when determining the size of the pinhole. A smaller pinhole increases resolution and overall ‘cleanness’ of the signal at the cost of signal strength. In a signal such as this microscope where too much optical power loss can prevent the photodetector from taking significant measurements, it

is important to have enough transmission through the pinhole aperture to ensure proper function of the photodetector.

3.1.7.1 Thorlabs ID12

This aperture is an iris diaphragm that is adjustable between 1-12mm. It has 8 leaves and comes in at \$62.39.

3.1.7.2 Thorlabs ID15

This aperture is another iris diaphragm very similar to the first, though it is adjustable between 1.2mm and 15mm. It has 10 leaves and costs \$62.39

3.1.7.3 Thorlabs 2000MB

This aperture is a true pinhole with a fixed diameter of 2mm for a price of \$144.02.

Table 3.12: Aperture Selection

	ID12	ID15	2000MB
Diameter	1-12mm	1.2-15mm	2mm
Fixed/Adjustable	Adjustable	Adjustable	Fixed
Price	\$62.39	\$62.39	\$144.02
Part Selection		✓	

The 2000MB pinhole is truly a pinhole. It has an exact circular shape, whereas the adjustable iris diaphragms will have slight variations due to the leaves of the iris joining together at slight angles. Also, because it has a fixed diameter, it is more robust to factors such as vibrations and accidental contact like bumping or shaking that might cause the adjustable irises to vary slightly from their adjusted values. However, because its diameter is fixed, it would have to be placed very precisely at a point along the focusing beam that matches that diameter. For this reason, it is advantageous to use an adjustable iris, as it can be made to fit the diameter of the beam at any point along its path.

Between the ID12 and ID15, both irises have acceptable ranges that include diameter that can fit the focused beam through and can be adjusted accordingly. At the same price point, their functionality is almost identical for the purposes they will serve. However, the main difference is that the ID15 has 10 leaves whereas the ID12 has 8. This makes the ID15 ever so slightly more ideal, as any aberration introduced by the angular joints where the leaves meet each other will be less than the ID12. Realistically, the precision of this system will not likely be affected by this and any aberration introduced will be negligible, but in order to be thorough, the ID15 is the better choice.

3.1.8 Sensors

This laser scanning microscope design relies on the use of a photodetector for the collection and measurement of its signal. A photodetector is an electrical device that captures photons from an optical signal and converts them into a usable electrical one, usually in the form of voltage or current. These devices are useful in a variety of

applications and are the foundation for technologies like digital cameras, optical communications, solar cells, and more. They enable the measurement of optical intensity, depth, temperature, wavelength, and other characteristics of optical signals.

For the purposes of this design, the function of the photodetector will be to measure the optical intensity of the signal being transmitted through the microscope and convert it into an electrical signal that can be used to compute a measurement of depth for each pixel of what will result in a final image that is a two-dimensional depth map of an object of interest. There are several different photodetector devices that can complete this function by different methods; the photodiode, phototransistor, and photoconductor are all viable options, and a detailed description and comparison of these devices is available below.

3.1.8.1 Photodiodes

A photodiode is a semiconductor device designed to convert an optical signal into current or voltage. Specifically, it is a PN-junction device, meaning that it is comprised of a positive-charged ‘p-type’ semiconductor on one side and a negative-charged ‘n-type’ semiconductor on the other. At the boundary or “junction” of these two semiconductors is a region, known as the depletion region, whose default state is to be empty of any free charge carriers.

Through different configurations of positive or negative voltages applied at the terminals of a PN-junction diode, it can be operated in different settings or “modes” that affect its inherent electrical properties and behaviors as part of a circuit. The standard mode of operation for a photodiode is reverse bias, in which the positive terminal of the voltage source is connected to the n-type semiconductor, and the negative terminal to the p-type semiconductor. This induces conditions in the junction where the size of the depletion region increases and only a very small current leaks across the junction. In the absence of light, this small leakage of current, referred to as ‘dark current,’ is the minimum signal transmitted by a photodiode and is an important design consideration when implementing this device.

When photons are incident on the active region of a photodiode, they can energize electrons and cause them to break free from the atoms in the semiconductors to generate an electron-hole pair within the depletion region. The reverse biasing voltage applied across the device pulls the negative-charged electron towards the n-side and positive-charged holes towards the p-side, creating a photocurrent. The strength of this photocurrent is dependent on the intensity of the incident optical power on the device, so measurable differences in the electrical output of a photodiode can correspond to measurable values, such as depth measurements in the context of this microscope.¹⁸

Photodiodes are characterized by their responsivity, a measure of how much current they will produce relative to input optical power. The responsivity in combination with the physical size of the active region of the device are the determining factors for the magnitude of the signal it produces and must be considered during the design process.

Other important considerations are the reverse-biasing voltage necessary for the operation of the device, the dark current inherent to its function, and the speed at which its measurements can be made. It is also necessary to take preventative measures against photobleaching, a phenomenon in which the photodiode receives a relatively high level of incident optical power that causes it to output a maximum photocurrent, above which there is no linear relationship between input optical power and output current, and the device loses its ability to make accurate measurements.

3.1.8.2 Phototransistors

A phototransistor is a device that converts light into an electrical signal. It is a semiconductor that is similar to a standard NPN bipolar junction transistor, but instead of an electrical signal applied to the base terminal, light incident on the device acts as the input stimulus. The phototransistor is composed of three semiconductor layers—an emitter, base, and collector—with the base region made photosensitive to incoming photons. In its default state, with no incident light, only a very small leakage current flows through the device.

When photons are incident on the active base region, they excite electrons and generate electron-hole pairs, much like in a photodiode. These photo-generated carriers effectively act as a base current, and the transistor becomes conductive. Because of the internal gain or inherent current amplification property of BJTs, even a small amount of light-induced base current results in a significantly larger collector-emitter current. This amplification makes phototransistors sensitive to lower light levels than photodiodes without requiring external amplification circuitry.

Phototransistors are typically operated with the base terminal left unconnected, allowing light to fully control conduction. While phototransistors are more sensitive, they have slower response times than photodiodes due to charge storage and have limited bandwidth. As a result, they are favored for applications such as light detection, object sensing, and simple optoelectronic switches, where speed is not as essential as sensitivity.

Table 3.13: Photodiode vs. Phototransistor comparison

	Photodiode	Phototransistor
Sensitivity	Moderate	High
Amplification (by external amplifier)	Necessary	Unnecessary
Response Time	Low (Fast)	High (Slow)
Risk of Saturation/ Photobleaching	Moderate	High
Operating Voltage	Low	Moderate

Technology Selection	✓	
----------------------	---	--

3.1.8.3 Thorlabs FD11A

This photodiode is rated for 320-1100nm, with a projected responsivity of 0.17A/W at 405nm, the chosen operating wavelength for this microscope. It has an active area of 1.21mm² and the lowest dark current of the three options listed at 2pA.

3.1.8.4 Thorlabs FDS010

This photodiode is rated for 200-1100nm, with a projected responsivity of 0.14A/W at 405nm. It has an active area of 0.8mm² and a dark current between 0.3nA under normal operation.

3.1.8.5 Thorlabs FDS015

This photodiode is rated for 400-1100nm with a projected responsivity of 0.19 A/W at 405nm. It has an active area of 150μm² and a dark current of 0.5nA.

Table 3.14: Photodiode Selection

	FD11A	FDS010	FDS015
Wavelength	320-1100nm	200-1100nm	400-1100nm
Responsivity at Chosen Wavelength	0.17A/W	0.14 A/W	0.19A/W
Active Area	1.21mm ²	0.8mm ²	150μm ²
Dark Current	2pA	0.3nA	0.5nA
Part Selection	✓		

Each of these photodiodes cost less than \$10, meaning that price was not a main consideration in the selection between these three options. The photodiode with the highest responsivity (and assumedly the most accurate response to input optical power) is the FDS015. However, it also has the largest dark current value, and a very small active area which would make it difficult to align the system with enough precision to properly fill the active area with the focused beam. Comparison of FD11A and FDS010 show that they have very similar specs, including very close values for responsivity at 405nm, although the dark current for the FDS010 is larger by a factor of 100. FD11A also has the advantage of having a larger active region by 0.41mm², and the combination of these advantages is the reason that FD11A was the final component selection for this design.

3.1.9 Amplifiers

An amplifier will be required for this project due to the small photocurrent provided by a photodiode, this current cannot be directly passed through an analog-to-digital converter and as such must be passed through an amplifier such that a measurable voltage can be read.¹⁷

3.1.9.1 Transimpedance Amplifier

The transimpedance amplifier (TIA) circuit in the Scanning Laser Microscope is the bridge between the photodiode and data collection systems. The TIA would be necessary in order to convert the photocurrent generated by the photodiode into a voltage signal such that the output can be constructed into an image through the data processing system. This is because the photodiode output current is in the μA range; data gathered in this range would be inaccurate as it is difficult to accurately measure current in the μA range – leading to noise and therefore lower image quality. The TIA mitigates this as it will provide the necessary gain to convert these small currents into an easily measurable voltage, allowing for a reduction in noise and therefore higher image quality.¹⁸

Additionally, the TIA provides a fast response time and high bandwidth, making it suitable for a scanning system where rapid signal changes occur as the laser moves across the sample. However, the use of a TIA comes with design challenges. Depending on photodiode responsivity, the feedback resistor in this circuit could reach the $\text{M}\Omega$ range, making it such that the bandwidth is reduced significantly due to parasitic capacitances. Additionally, TIA circuits can be sensitive to board layout and stray capacitance, which must be addressed directly to avoid instability.

Another consideration of a TIA is its power consumption. While on the low end, it is higher than a passive approach, meaning low noise op-amps must be selected to maintain signal integrity while keeping power consumption at its lowest.

3.1.9.2 Photomultiplier Tube

A photomultiplier tube (PMT) is a light detection device that utilizes the photoelectric effect followed by electron multiplication to produce a measurable signal. PMTs can detect extremely low levels of light which can then be converted to a small signal which is then amplified through secondary emission across dynodes (often achieving a factor up to 10^6), making a PMT suitable for applications such as low-light imaging or fluorescence microscopy.²⁹ However, while a PMT excels in low-light detection, its utilization comes with several constraints; PMTs require high voltage power supplies $\sim 1\text{kV}$, introducing safety considerations as well as being the technology with the highest power consumption. Also, PMTs are large and fragile, making their integration more challenging for a user seeking to build an affordable scanning laser microscope and increase the device's area. Lastly, PMTs are significantly more expensive than taking an approach where a photodiode current is amplified through an external device/circuit.

3.1.9.3 Logarithmic Amplifier

A logarithmic amplifier is an analog signal processing component capable of outputting a voltage proportional to the logarithm of an input current. This creates a nonlinear relationship that can be utilized for systems with a wide range of signals, creating a smaller range and a more manageable voltage range. This makes a logarithmic amplifier theoretically suitable for the scanning laser microscope as it can help preserve detail where there might be brighter/darker regions. However, the use of a logarithmic amplifier

presents multiple complications. First, the microscope requires a more linear relationship between signal and scanned data such that an image can be accurately constructed based on light intensity. A logarithmic amplifier distorts this relationship as its output is a relationship of the natural log of its input current and reference current.

$$V_{out} = -\frac{kT}{q} \cdot \ln\left(\frac{I_{in}}{I_{ref}}\right) \quad (1)$$

Another design challenge introduced by the utilization of a logarithmic amplifier is the fact that they introduce higher noise than other technologies presented, meaning further signal calibration would be required to make this a suitable choice.

3.1.9.4 Passive Current-Voltage Conversion

Passive current-voltage (I-V) conversion is the simplest method for obtaining a measurable voltage from a photodiode. This method is achieved by utilizing a resistor across the photodiode terminals. The photodiode current that would then flow through the resistor would generate a corresponding voltage based on Ohm's law.

$$V = IR \quad (2)$$

As this method is achieved with passive components, it requires the least amount of costs and power and is good for an open-source project as all parts are easy to access. However, the use of this method introduces several complications for a scanning laser microscope application. First, a large resistor must be used (KΩ to MΩ). This combined with any capacitance introduced will create a large τ (RC constant) that will limit bandwidth and create a slower system response, making it difficult to achieve a low image processing time. Additionally, due to the lack of an active component, noise and drift become much more prominent and require further signal processing, which could lead to signal degradation.

Note: A checkmark (✓) indicates the most suitable technology for that criterion among those compared. Multiple technologies may be marked if they are suitable for use.

Table 3.15: Amplifier Comparisons

Criteria	TIA	PMT	Logarithmic Amplifier	Passive I-V Conversion
Cost	✓			✓
Bandwidth & Gain	✓	✓		
Power Consumption	✓		✓	✓

Linearity	✓			
Noise Performance	✓			
Integration Complexity				✓
Technology Selection	✓			

3.1.9.5 OPA380/2380

The OPA380 (2380 is the same device but dual channel) from Texas Instruments is part of a family of transimpedance amplifier (TIA) op-amps that provide a 90 MHz Gain Bandwidth Product (GBW), low 1/f noise, and rail-to-rail output, making it ideal for high-speed photodiode applications. It features an input offset voltage of 25 μV , offset drift of 0.1 $\mu\text{V}/^\circ\text{C}$, and an input bias current of 50 pA. The OPA2380 is a dual-channel version of the OPA380, offering identical electrical performance with a compact layout that may simplify routing in dual-channel systems. Both devices support user-defined feedback resistor and capacitor configurations, enabling custom transimpedance gain settings to match the input current range. The OPA380 is suitable for the CLSM due to its ability to measure and amplify signals ranging from 1 nA up to 100 μA , providing enough flexibility and sensitivity for sub-microwatt photodiode signals.

3.1.9.6 OPA381

The OPA381 is a dedicated transimpedance amplifier optimized for low-current photodiode applications, delivering high precision and extremely low input noise. It features a reduced GBW of 18 MHz compared to the OPA380, but with improved input bias current of 3 pA, making it well-suited for higher-sensitivity setups. The OPA381 maintains an offset voltage of 25 μV and offset drift of 0.1 $\mu\text{V}/^\circ\text{C}$, and its performance surpasses that of conventional JFET-input op-amps in terms of noise and stability. The lower GBW is offset by better performance in ultra-low current detection, making it more suitable for 10 nA to 1 mA signal ranges. However, it may be less suitable for high-speed scanning where higher bandwidth is required.

3.1.9.7 ADA4530-1

The ADA4530-1 from Analog Devices is a femtoamp-level electrometer-grade op-amp designed specifically for applications requiring ultra-low input bias currents, such as ion detection, charge sensing, and low-light photodiode measurements. It boasts an input bias current of less than 20 fA, making it ideal for measuring currents in the picoampere or even sub-picoampere range. It offers a GBW of 2 MHz, which is sufficient for slowly

varying signals but not ideal for high-speed scanning applications like CLSM. However, for low-light detection scenarios or integration-based systems where temporal resolution is not critical, the ADA4530-1 provides unmatched sensitivity. It also includes a guard ring driver to further reduce leakage currents on the PCB, which can otherwise dominate in femtoamp-level designs.

3.1.9.8 LTC6268

The LTC6268 from Analog Devices (formerly Linear Technology) is an ultra-low bias current, high-speed op-amp designed for photodiode TIA applications. It features a gain bandwidth product of 500 MHz, input bias current of less than 3 fA, and voltage noise of 4.3 nV/ $\sqrt{\text{Hz}}$, making it suitable for high-speed, low-light optical applications. It is especially valuable in fast-scanning or modulated light systems where both temporal resolution and signal integrity are crucial. Like the OPA380, the LTC6268 allows the user to select external feedback components, enabling high transimpedance gains with careful design. It is ideal for situations where both high fidelity and extreme sensitivity are required.

Table 3.16: TIA Selection

Criteria	OPA380	OPA2380	OPA381	ADA4530 -1	LTC6268
Channels	1	2	1	1	1
Input Bias Current	50 pA	50 pA	3 pA	< 20 fA	< 3 fA
Input Offset Voltage	25 μV	25 μV	25 μV	50 μV	625 μV
Output Swing	Rail-to-Rail	Rail-to-Rail	Rail-to-Rail	Rail-to-Rail	Rail-to-Rail
Cost	\$4.11	\$4.50	\$4.38	\$6.00	\$5.50
Min Detectable Current	$\sim 1\text{nA}$	$\sim 1\text{nA}$	$\sim 10\text{nA}$	<1 pA	<1 pA
Gain Bandwidth (GBW)	90 MHz	90 MHz	18 MHz	2 MHz	500 MHz
Use Case	Moderate Speed, low photocurrent	Moderate Speed, low photocurrent	High Precision, low photocurrent	Ultra-low photocurrent signals	High-Speed Ultra-low photocurrent

Part Selection	✓				
----------------	---	--	--	--	--

3.1.10 MCU

The microcontroller is one of the most important pieces of hardware equipment needed for this project to work. This microcontroller will serve two important functions for the microscope. First would be to control the stage in which the object is placed upon; the microcontroller would be sending signals to 3 different stepper motors to orient and shift the stage into the proper alignment. Second would be to receive data inputs from the photodiode and send them to a computer to process and develop the data to create a 2D bitmap. Understanding the significance and purpose of the microcontroller, we can narrow our selection of microcontrollers to the following.

3.1.10.1 ESP32

The ESP32 is introduced to be one of the more common types of MCU's on the market created by Espressif Systems and has been shown to have a wide array of applications. The major highlights that this microcontroller has is that it has Bluetooth and Wi-Fi capabilities. The CPU and the internal Memory of the device have been supported with 448 KB of ROM, 520 KB of SRAM. Additionally, this MCU has dual-core hardware which allows for multithreading capabilities.

This Microcontroller has 38 pins and approximately 30 of these pins are GPIO pins that can serve any purpose. There are 16 PWM outputs that are configurable to any of the mentioned GPIO pins. The max current in each pin is about 40 mA and the input voltage is about 3.3V

For the microcontroller, there is an ADC resolution of 12 bits supporting 18 ADC1 / ADC2 channels. These channels need to be calibrated due to nonlinear behavior. The sampling rate is approximately 6-18 kHz. ESP32 has 4 hardware timers with a 64-bit high precision along with an RTC timer for low-power applications. The interrupt mechanism in the MCU houses 32 interrupt sources and can allow for pin-change and timer-based interrupts. The amount of power that this MCU consumes varies depending on what mode it is in. It needs to have a supply voltage of 3-3.3V. While active can consume about 160~260mA compared to the idle being 20-40mA. In deep sleep it consumes about 10 μ A.¹⁰

The ESP32 MCU has chemistry with stepper motors due to it being able to generate very precise step pulses (can work by using timers). For the photodiode, the 12-bit ADC is adequate for receiving the measurements produced by it. The MCU can use either I2C or SPI communication protocols to send serial information. Additionally, due to the dual core feature, one core can be responsible for controlling the motors and the other for collecting data from the photodiode.

3.1.10.2 Raspberry Pi Pico

Raspberry Pi Pico is another MCU in the market that takes an angle of a low-cost development platform and brings a myriad of features. The microcontroller chip in the Raspberry Pi Pico is a Raspberry Pi RP2040. This MCU has a total of 40 pins, of which 26 of them are for multi-function GPIO pins that include (ADC, PWM, I2C, SPI, and UART). As for the PWM there are 16 channels. The ADC resolution of the MCU is 12-bits long but has only 3 ADC channels and are supported in pins GPIO 26,27 & 28.

The Raspberry Pi Pico has 4 hardware timers and an alarm interrupt that can be worked into scheduling tasks. The power consumption of this device while active is about 90-100 mA however during sleep mode it is about 1.3mA. The voltage supply needed ranges from 1.8V - 5.5V

The MCU can perform the functions needed for this project. The wide array of GPIO pins can control the stepper motors. For the photodiode, the 12-bit ADC is sufficient for capturing the needed data and sending it to the computer to process it.

3.1.10.3 Arduino Mega

The Arduino Mega 2560 Rev3 is a development board that houses the ATmega2560 microcontroller and boasts of helping with applications and projects that need many inputs and output pins along with high processing power. This board does come along with compatibility with Wi-Fi; the processor has a throughput of 16 MHz along with 54 Digital and 16 Analog IO pins. The CPU of this device is an 8-bit AVR that has a speed of 16MHz.

The Arduino Mega has about 86 pins, 54 of which are digital I/O pins. 15 of the pins support the PWM output and 16 of the pins support analog input with a resolution of 10 bits. The timer and interrupts of this device support 6 timers and can allow for 6 external interruptions on certain pins. This MCU doesn't have advanced scheduling but can support motor functions. When the Arduino Mega is running it can consume 70-90 mA compared to the 5-10mA it consumes during sleep mode. It also needs the support of a 5V supply to run.

Due to the wide array of digital pins, this can support a large number of devices that connect to it. The built-in ADC supports basic photodiode measurements with a 10-bit resolution.

Table 3.17: MCU Selection

MCU Selection			
Features	ESP32	Raspberry Pi Pico	Arduino Mega 2560
Core / Clock Speed	Dual Core / 240 MHz	Dual Core / 133 MHz	Single Core / 16 MHz
RAM / Flash Storage	520 KB / 16 MB	264 KB / 2 MB	8 KB / 256KMB

ADC	12-bit / 18 Channels	12-bit / 3 Channels	10-bit / 16 Channels
Digital Pins	34 / 16 PWM Channels	26 / 16 PWM Channels	54 / 15 PWM Channels
Timers / Interrupts	4 / Pin, Timer, External	4 / Pin, Timer	6 / Pin, External
Power Consumption	3.0V - 3.3V 160mA - 260mA	1.8V - 5.5V 90mA - 100mA	7V - 12V 70mA - 90mA
Form Factor	25.5 x 18 mm	51 x 21 mm	101.5 x 53.4 mm
Programming Languages	Arduino, C, MicroPython	C/C++, MicroPython	Arduino C++
Cost	\$4-10	\$4-6	\$10-45
Part Selection	✓		

3.1.11 Microscope Stages

With the need to have very accurate lateral and axial movements of the sample, the microscope stage of the system then becomes one of the most important parts of any CLSM. The stage not only creates axial and lateral movements that can affect the image but can also affect sample stability, system performance, and scanning precision. The movement of the stage needs to be able to produce micron and submicron levels of precision in movement, while still allowing for complete control of the axial distance to the sample without having too small of Z-range. Operating power is another major factor that will need to be considered as depending on the overall power sourced for the entire system, only a dedicated amount of power will be given to the stage subsystem. Lastly the cost of the stage and the equipment required to run the stage will need to be taken into consideration as well, as this can majorly affect the quality of the stage overall.

3.1.11.1 Manual Stage

Usually the simplest, most cost-effective stages are manual stages. Having no need for electrical interfaces, as manual stages do not use motors, makes it an ideal choice for quick and easy setups or prototypes. The mechanical simplicity of manual stages is another attractive point as there would be no need to program or calibrate stage heights and movements. Not relying on electrical components also allows manual stages to usually have higher load capacities compared to stages with reliance on multiple gear reduction systems.

However, manual stages have many problems. While being great for use in coarse and less fine adjustments, manual stages struggle to achieve very fine adjustments needed in CLSM. Even with less fine movements, many manual stages cannot achieve the repeatability needed in CLSM either. These manual adjustments are almost always based on mechanical movements of the operator to adjust screw pitch, which only allows for about 10 – 50 μm of movement. Another critical failure of manual stages is not having the speed given to the use of motors and computer programs to guide them. Furthermore, manual stages can achieve their best use in simple alignment and single point imaging systems.

3.1.11.2 Motorized Linear Stage

Motorized linear stages are typically found in CLSM systems. These stages allow for precise movements of x-y-z directions, while still allowing for accurate repeatability for consistent results. Widely used for raster scanning and image stitching, motorized stages can be programmed for many different use cases. The benefits of a motorized stage usually include fully programmable movement, compatibility with widely available motion controllers and open-source content, low costs, and x-y-z travel ranges that are usually not limiting where and how the sample can be placed.

However, motorized linear stages don't come without challenges. From needing a motion controller, correctly and consistently sourced power, and needing isolation, motorized stages have limitations that restrict the range of uses available to it. Mechanical isolation is one of the most prominent problems with motorized stages as if not properly isolated imaging systems will create blurry and inaccurate media of the sample. Another major problem of motorized stages is that the drift is some stepper-based stages. While this may not be an initial problem, the more the stage gets used the more the drift becomes noticeable, thus meaning more calibration and alignment is required. Still, the use of motorized linear stages does find consistent use in CLSM systems due to the nature of speedy and accurate layer control.

3.1.11.3 Piezoelectric Z-Stage

Piezoelectric Z-stages can allow for ultra precise ($< 10 \text{ nm}$) and high-speed motion in the Z-axis. While piezoelectric Z-stages have a large footprint, as well as an increased cost due to the sheer amount of expensive components and controllers needed, they do not usually encounter many problems that cheaper motorized stages may have. Some of these problems piezoelectric Z-stages may not have can range from mechanical isolation problems to motor drift. While this type of stage has many benefits when compared to previous stage types, the limited travel of the Z-axis as well as being very sensitive to load distributions, can be a massive deciding factor in choosing a piezoelectric Z-stage for use in a CLSM.

Table 3.18: Microscope Stage Comparison

	Manual Stage	Motorized Linear Stage	Piezoelectric Z-Stage
--	--------------	------------------------	-----------------------

Moveable Axes	X, Y	X, Y, Z	Z only
Resolution	$> 10 \mu m$	$5 - 0.01 \mu m$	$< 10 \text{ nm}$
Travel Range	10 – 50 mm	10 – 100 mm (X, Y), 5 – 25 mm (Z)	100 – 400 μm
Repeatability	Low	Moderate - High	High
Speed	Slow (manual movements)	1 – 20 mm/s (depending on motor controller)	$< 1 \text{ mm/s}$
Power Consumption	N/A	10 – 50 W	$< 5 \text{ W}$
Cost	Very Low	Low – Moderate	High
Technology Selection		✓	

In selecting a microscope stage to be used in the system, the motorized linear stage was determined to be the most viable option. While there are many motorized linear stages on the market, there were a few constraints that had to be considered in this decision. The biggest constraint that was encountered was keeping the cost as low as possible while still being able to maintain high levels of reproducibility.

The best option of a motorized linear stage that was found was the OpexFlexure delta microscope stage. The OpenFlexure delta stage is an open-source 3D printable microscope stage with sub-micron precision in Z-axis movements. With capabilities to not only be motorized with simple stepper motors, the OpenFlexure delta stage also allows it to have very fine adjustments when compared to manual stages.

Another major factor in selecting the OpenFlexure delta stage was reproducibility of stage movements, since the mechanical design relies on flexure deformation rather than the movement of gears or rails. This mechanical design negates the major axis drift over long periods of time. This stage also supports Z-stacks as well as automation of the axis movements. The X and Y axes support ~12 mm of movement while the Z-axis supports ~4 mm of movement. This range of movement also allows for a wider range of microscope objectives to be used in the system.

3.1.12 Stage Motors

In order to ensure accurate image reconstruction, precise stage movements are critical. The technology used to move the stage in X, Y and Z axes must be capable of ensuring reliable control, speed and torque while balancing resolution and cost for the CLSM. Integration with the MCU must also be considered due to different motor controller technologies. It is worth noting that the technologies discussed must be capable of achieving micron resolution as well as submicron given the project's current and stretch goals. Finally, power consumption must be considered as this is a large subsystem within the CLSM.

3.1.12.1 Stepper Motors

Stepper motors are electromechanical devices that convert an electrical pulse into mechanical movements where each pulse moves a shaft at a fixed angle. This allows for precise open-loop control and makes them suitable for the CLSM. Stepper motors have high precision and ease of interfacing as they do not require any feedback for basic operation, which reduces integration complexity. However, stepper motors can lose torque at high speeds and can miss steps under excessive load, which can compromise position accuracy and cause lower quality images or misreadings. Additionally, stepper motors can suffer from thermal performance if the system is active for prolonged periods of time. Power consumption is moderate in this case and not a big concern.¹⁶

3.1.12.2 Closed-Loop Stepper Motors

Closed-loop stepper motors integrate with an encoder to provide real-time feedback. This enables a controller to correct any missed steps and maintain precise positioning, essentially negating one of the main issues of regular stepper motors. Closed-loop stepper motors are suitable for the CLSM due to their high reliability and repeatability, especially in high precision conditions. However, closed-loop stepper motors require higher integration complexity and tend to have higher associated costs. Additionally, power consumption is higher than an open-loop system and can create thermal issues depending on operating conditions.²⁴

3.1.12.3 Brushless Servo Motors

Brushless servo motors are high performance actuators that use closed-control loop control to achieve precise positioning. They utilize encoders and operate with PID controllers to ensure smooth and accurate motion, making them suitable for the CLSM. Brushless servo motors have high torque and fast response times, allowing for high precision and responsiveness even at higher speeds. Additionally, these motors have excellent reliability and repeatability, making them ideal for a motorized stage. However, brushless servo motors are typically used in industrial-grade systems and as such have high costs. Furthermore, they require much higher power consumption due to the active control systems they use, which in turn can create substantial heat which must be taken into consideration when designing the stage itself.

3.1.12.4 Piezoelectric Actuators

Piezoelectric actuators use the deformation of piezoelectric materials to produce ultra-fine movements. These devices are capable of nanometer-scale resolution and are highly suitable for precision optics such as the CLSM. Piezoelectric actuators excel in Z-axis focusing and have high reliability and repeatability. However, they have high costs and although the actuators themselves do not require much power, they require high-voltage drivers, drastically increasing power consumption. Heat generation in these devices is minimal but must still be considered due to their use within the system. Finally, although piezoelectric actuators can allow for high resolution imaging it is worth noting that they

cannot do so at high speeds as they have limited travel range (<1mm) and as such scanning time will be higher.

Table 3.19: Stage Motor Comparison

Criteria	Open-Loop Stepper Motors	Closed-Loop Stepper Motors	Brushless Servo Motors	Piezoelectric Actuators
Cost	Low	Moderate	High	Very High
Torque	Moderate	High	High	Low
Low	Moderate	Moderate	High	Low
Repeatability/Reliability	Moderate	High	Very High	Extremely High
Required Voltage	5-12V	12-24V	24V+	100V+
Integration Complexity	Low	Moderate	High	High
Power Consumption	Moderate	High	High	Low (drivers not considered)
Travel Range	~50-300mm	~50-300mm	~100mm	~10 μ m - 1mm
Technology Selection	✓			

3.1.12.5 28BYJ-48

The 28BYJ-48 is a 5-wire unipolar stepper motor with an internal reduction gearbox, widely used in low-cost precision positioning systems. It has a step angle of 5.625° before gearing, and ~0.088° per step after the internal 64:1 gearbox, making it ideal for fine control in compact mechanisms. It operates at 5 V and draws roughly 240 mA per phase. The motor is lightweight, inexpensive, and easily driven by ULN2003 driver boards, making it well-suited for low-load micro-positioning stages.

3.1.12.6 NEMA 8 20BYGH

The NEMA 8 stepper is a small bipolar stepper motor with a 20 mm faceplate size and direct drive operation. The 20BYGH model has a 1.8° step angle and supports current ratings around 300 mA per phase at 5–6 V. These motors provide holding torque (up to ~12 mN·m) and fast response times compared to gear-reduced steppers at the cost of reduced microstepping resolution. Their compact form factor makes them a viable option for precise stages.

3.1.12.7 15BY25 Unipolar Micro Stepper

The 15BY25 is a miniature unipolar stepper motor with low power consumption. It has a step angle of 18° (20 steps/rev), it is often paired with external gearing systems to achieve higher positioning resolution. These motors operate in the 3–5 V range and draw currents under 100 mA, making them well-suited for compact precision systems.

Table 3.20: Motor Selection

Criteria	28BYJ-48	NEMA 8 20BYGH	15BY25
Step Angle	0.088°	1.8°	18°
Torque	$\sim 34 \text{ mN}\cdot\text{m}$	$\sim 12 \text{ mN}\cdot\text{m}$	$\sim 3\text{-}5 \text{ mN}\cdot\text{m}$
Microstepping Resolution	Up to 4096 Steps/revolution	200 Steps/Revolution	20 Steps/Revolution
Voltage/Current Draw	5V/ $\sim 240\text{mA}$	$\sim 5\text{-}6\text{V}/\sim 300\text{mA}$	3-5V/ $<100\text{mA}$
Cost	\$1-2	\$10-\$15	\$4-\$6
Part Selection	✓		

3.1.13 Stage Motor Controllers

Given the selection of open-loop stepper motors, the way in which they are controlled is another consideration that must be considered. For open-loop stepper motors there are three main technologies that can be taken into consideration, direction drivers, integrated modules, and MCU-based control. Precise control over the stepper motors is necessary in order to achieve micron resolution.

3.1.13.1 Step-Direction Drivers with External MCU

Direction drivers are the most common method of driving stepper motors. These controllers receive a step and direction signals from an MCU to command motors movement. Each pulse on the step line will cause the motor to move by one step while the direction line determines the direction of the rotation. These drivers are suitable for controlling the stepper motors as they are inexpensive and support micro stepping which will allow for higher resolution for the CLSM. Additionally, the integration complexity of these drivers is quite low and does not require much voltage (5-12V) and current to operate. However, these drivers require precise timing signals from the MCU and do not have any stall detection or feedback sensors. Furthermore, heat dissipation must be considered due to the constant output of current, especially in a stage application.

3.1.13.2 Integrated Stepper Controller Modules

Integrated stepper controller modules combine a stepper driver, MCU, and interface onto a single board. These modules then control everything about the motor including position, running scripts, and do not require a separate MCU. These modules are suitable for the CLSM as they have equal capabilities to direction drivers with the added benefit

of having low to no integration complexity. However, these modules are more expensive and may require further consideration in terms of heat dissipation as current ratings are usually between 1-3A per phase. Furthermore, these modules may introduce limitations in motion profile due to a lack of customization.

Note:

Values represent typical ranges for commonly used drivers and modules in open-loop stepper motor control systems. “Microstepping Capability” reflects the maximum supported resolution.

Table 3.21: Motor Controllers Comparison

	Step-Direction Drivers w/ External MCU	Integrated Stepper Controller Modules
Cost	~\$2-5 (MCU not considered)	~\$20-45 Per module (3 needed)
Current Rating	1-2.2A/phase	1-3A/Phase
Voltage Range	5-12V	9-30V
Micro Stepping Capability	Up to 1/16-1/256	Up to 1/256
Integration Complexity	Moderate	Low
Technology Selection	✓	

3.1.13.3 ULN2003 Driver

The ULN2003 is a basic transistor array module used with unipolar stepper motors and comes included with most 28BYJ-48 kits. It includes seven Darlington pairs with built-in flyback diodes for inductive load protection. Operating at logic-level signals, it can source up to 500 mA per channel. These driver boards are very cost-effective, making them suitable for the CLSM. However, due to limited microstepping capabilities and fixed step timing, it offers less flexibility than dedicated step-direction drivers.

3.1.13.4 A4988 Stepper Driver

The A4988 is a stepper motor driver capable of driving bipolar stepper motors in full, half, quarter, eighth, and sixteenth step modes. It supports adjustable current limiting, over-temperature protection, and operates from 8 V to 35 V. While the 28BYJ-48 is unipolar by default, it can be rewired as bipolar to be compatible with the A4988. This allows the use of step-direction control via an external microcontroller, enabling smoother, more precise motion profiles for the CLSM.

3.1.13.5 DRV8825 Stepper Driver

The DRV8825 is a stepper driver capable of delivering up to 2.2 A per coil with adequate cooling, and operates in a voltage range of 8.2 V to 45 V. It supports six microstepping modes, including up to 1/32 step resolution, making it ideal for applications requiring precision control. Like the A4988, it is designed for bipolar stepper motors and can be used with a rewired 28BYJ-48 for improved stepping precision. The DRV8825 includes protection features such as overcurrent, thermal shutdown, undervoltage lockout, and

crossover-current protection. The DRV8825 is suitable for CLSM implementations where higher resolution and more robust thermal handling are desired.

Table 3.22: Motor Controller Selection

Criteria	ULN2003	A4988	DRV8825
Driver Type	Darlington Transistor Array (Unipolar)	Chopper Stepper Driver (Bipolar)	Chopper Stepper Driver (Bipolar)
Cost	\$1-2 (May come with selected motors)	\$2-4	\$3-6
Input Type	4-step sequence	Step/Direction	Step/Direction
Max Current per Phase	500mA	1A	1.5A
Voltage Range	5-12V	8-35V	8.2-45V
Protection	Basic Flyback Protection	Thermal Shutdown, Overcurrent & Undervoltage	Thermal Shutdown, Overcurrent, Undervoltage, Crossover
Part Selection	✓		

3.1.14 Power Supply

Stable power delivery is critical to ensure proper operation of all CLSM subsystems, including the MCU, stage motors, analog circuitry, and laser components. The two technologies best suited for application in the CLSM are an AC-DC converter, which takes power from a wall outlet and converts AC current into DC, and a battery bank, which provides portable, regulated power. Other technologies, such as solar cells or inductive power systems, are not viable due to limited power output and incompatibility with laboratory environments.

3.1.14.1 Power Requirements

Table 3.23: System Power Requirements

Part	Supply Voltage (V)	Current Drawn (A)	Power Consumed (W)
Laser Diode (LP405P20)	5V	~38 mA	0.19
Laser Current Controller (Micro Flexdrive V5)	5V	65-100mA	0.5
Photodiode (FD11A)	N/A	N/A	N/A
TIA (OPA380)	3.3-5V	0.76 mA	38mW
3x Motors (28BYJ-48)	5-12V	720 mA (240 mA each at stall)	8.64

3x Motor Controllers (ULN2003)	5-12V	~4.2 to 6 mA (total)	0.7
MCU (ESP32)	3.3V	~20–60 mA (300mA peak)	.2
UART-USB (CP2102)	5V	~30-40mA	.2
Buck Converter (MP1584EN)	12V (From AC-DC converter)	0.7–0.93A	11.16
LDO Regulator (LM1085-3.3)	5V	~85mA	0.42
Total Power			~22W

To provide margin and long-term thermal reliability, a converter rated for at least 3 A at 12 V (36 W) will be considered ideal.

3.1.14.2 AC-DC Converter

AC-DC power supplies convert 120–240VAC into a regulated DC voltage, typically 12V or 24V. This makes them ideal for the CLSM due to their stability, high output capacity, and low integration complexity. Additionally, regulators within the system can distribute the supplied voltage to all components based on their requirements.

This power supply method is especially suitable for a laboratory setting, where extended operation is expected, and continuous scanning of multiple samples is required. Efficiency typically ranges from 85–95%, and most commercial units include built-in heatsinks or active cooling for thermal management.

3.1.14.3 Battery Bank

Using battery power would involve integrating rechargeable cells, such as Li-ion or LiPo packs, to supply the system. This could reduce the system footprint and offer portability — a clear advantage over AC-DC supplies in field or mobile applications.

While theoretically suitable for the CLSM, battery power introduces several constraints. First, the system would be limited by battery capacity and would require regular recharging, making it less ideal for prolonged operation. Additionally, proper voltage regulation, overcurrent protection, and battery monitoring circuits must be included, increasing system complexity.

At higher current draws (e.g., powering stepper motors and analog loads simultaneously), system efficiency may drop due to the demands on DC-DC regulators and internal battery resistance. Heat generation within the battery is minimal under moderate loads, but high-discharge scenarios require thermal consideration.

Table 3.24: Power Supply Selection

Criteria	AC-DC Converter	Battery Bank
Cost	~\$10-25	~\$20-50
Integration Complexity	Low	Moderate
Rated Current	3-10A	2-5A
Efficiency	85-95%	~70-90% (Depending on load conditions)
Heat output	Moderate	Low
Voltage Range	12-24VDC	7.4-12.6V
Technology Selection	✓	

3.1.14.4 Mean Well LRS-50-12

The LRS-50-12 is an enclosed AC-to-DC converter that supplies 12 V at up to 4.2 A (50 W). It supports a wide input range of 85–264 VAC, with a typical efficiency of ~88% under full load. The unit has integrated protections against short circuit, overload, and overvoltage, and is capable of continuous operation in ambient temperatures up to 70 °C with appropriate derating. The LRS-50-12 is best suited for systems with motor and laser subsystems operating concurrently. Its additional headroom increases reliability and reduces the risk of voltage sagging under load.

3.1.14.5 Mean Well LRS-75-12

The LRS-75-12 is a higher-capacity version of Mean Well’s LRS series, providing 12 V at up to 6.2 A (75 W). It accepts 85–264 VAC input, includes standard protections (overload, overvoltage, short-circuit), and achieves ~89% efficiency. With its large power margin, it is suitable for the CLSM as it can power multiple high-current subsystems—such as stepper motors, laser modules, and voltage regulators simultaneously, without approaching thermal or current limits.

3.1.14.6 RECOM RAC60-12K/OF

The RAC60-12 from RECOM is a high-efficiency enclosed power supply capable of delivering 12 V at up to 5 A (60 W). It operates from an input range of 90–264 VAC and delivers up to 89% efficiency. The unit includes robust protections such as short-circuit, over-temperature, and overvoltage shutdown. Its low no-load power consumption makes it ideal for sensitive lab systems requiring tightly regulated 12 V power with minimal ripple. This supply is particularly well-suited for CLSM configurations with higher current demands and precision analog circuitry that may be sensitive to noise.

Table 3.25: AC-DC Converter Selection

Criteria	Mean Well LRS-50-12	RECOM RAC60-12K/OF	Mean Well LRS-75-12
----------	---------------------	--------------------	---------------------

Output Voltage	12 V	12 V	12 V
Max. Current Output	4.2 A	5A	6.2A
Power Rating	50W	60W	75W
Efficiency	~88%	~89%	~89%
Protections	Short Circuit, Overload, Overvoltage	Short Circuit, Over-temperature, Overvoltage	Short Circuit, Overload, Overvoltage
Cost	\$11-13	\$25-30	\$15-18
Part Selection	✓		

The Mean Well LRS-50-12 AC-DC converter was selected to meet the CLSM requirements.

3.1.15 Regulators

Voltage regulation is required for the scanning laser microscope due to the varied voltage requirements of each subsystem. The primary input of the system consists of 12VDC supplied from an AC-DC converter (3.1.3.13). However, components such as the MCU, TIA, and optics circuits require regulated voltages for proper operation. The two main types of voltage regulators are linear and switching regulators; linear regulators are easier to design, cost-effective, and reliable. However, linear regulators are less efficient and have larger heat dissipation needs than switching regulators. In either case, these systems must be capable of responding to changes in load and supply the voltage needed.

3.1.15.1 Linear Regulator

Linear regulators are devices that maintain a constant output voltage by dissipating excess input voltage as heat. Their operation results in continuous, low-noise output, which makes them a suitable choice for analog circuitry such as the TIA where low noise is critical. Additionally, linear regulators are usually low-cost, which is ideal for the microscope.²⁰

Linear regulators, however, can only step down voltage, and as such all excess voltage is dissipated as heat, which largely reduces the efficiency of the regulator. As an example, in a 200mA load on a 5V rail 1.4W would be dissipated as heat ($P = (12V - 5V) \times 0.2A$). This would likely necessitate further thermal management, which would increase this subsystem's size and costs. Additionally, it is worth noting that linear regulators cannot step-up voltage and are unable to create negative voltage supplies unless a more complex circuit is introduced, placing limitations on their usage within the project.

3.1.15.2 Switching Regulators

Switching regulators are devices that rapidly switch the input voltage on and off, adjusting duty cycle to regulate the output at a specified voltage. This signal is then passed through inductors and capacitors to filter the ripple voltage created by the switching. The resulting DC voltage can then be used to power the load. There are several types of switching regulators such as Buck, Boost, and Buck-Boost converters. Switching regulators are suitable for this project as they are highly efficient and can handle higher current demand with minimal heat generation.

Buck converters – a type of step-down converter, ideal for high input voltages to lower output voltages. Buck converters are highly efficient and well suited as a medium to deliver voltage to digital components from the 12VDC coming from the power supply.

Boost converters – a type of step-up converter, ideal for stepping up a lower voltage input to a higher output voltage. The use of a boost converter would be suitable for the stepper motors, but their application has limited applicability within the scope of the project.

Buck-Boost converters – a type of converter that has the functionality of both a buck and boost converter, making it ideal for a variable input system where negative voltages are required. However, a buck-boost converter introduces additional complexity in terms of integration due to its higher output ripple voltage.

Note: Technology Selection (✓) reflects components selected based on voltage needs, noise requirements, and efficiency considerations.

Table 3.26: Voltage Regulator Comparisons

Criteria	Linear Regulators	Switching Regulators		
		Buck	Boost	Buck-Boost
Regulator Category (step-up/down)	Step-Down	Step-Down	Step-Up	Both Step-up and Down
Efficiency	Moderate	High	High	High
Output Ripple Voltage	Low	Low	Moderate	High
Cost	Low	Low	High	Low
Heat Dissipation	Moderate	Low	Low	Low
Integration Complexity	Low	Moderate	Moderate	High
Technology Selection	✓	✓		

Linear Regulators

3.1.15.3 LM1085IT-3.3

The LM1085IT-3.3 is a fixed 5V low dropout linear regulator capable of supplying up to 3A of output current. It has a dropout voltage of ~1.3V at full load and has moderate efficiency (but is extremely robust) when input voltage is kept close to the output. It has high line and load regulation of ~0.015% and ~0.1% respectively, low quiescent current ~5mA and thermal protection, making it suitable for the CLSM.

3.1.15.4 L7805CV

The L7805CV is a fixed 5V linear regulator capable of delivering up to 1.5A. It is highly reliable and requires a minimum input voltage of 7V due to a ~2V dropout voltage. It lacks efficiency under high voltage differentials but is extremely rugged and robust with high thermal overload protection, making it suitable for the CLSM.

Buck Converters

3.1.15.5 LM2596

The LM2596 is a buck regulator capable of delivering up to 3A of output current with high efficiency (up to 92%) under optimal conditions. It operates at a frequency of 150kHz and can be purchased at a fixed 3.3, 5, and 12V or adjustable output versions. The application of the LM2596 would be utilized where power dissipation from a linear regulator would be excessive.

3.1.15.6 MP1584EN

The MP1584EN is a high-efficiency, step-down (buck) switching regulator capable of converting a wide input voltage (up to 28 V) to a lower, adjustable output voltage, typically used to supply 5 V or 3.3 V rails. It supports output currents up to 3 A, making it suitable for powering microcontrollers, motor drivers, or other moderate-load devices. Its compact size, integrated high-side switch, and thermal protection features make it ideal for space-constrained embedded applications where efficiency and reliability are important.

Table 3.27: Regulator Selection

Criteria	LM1085IT-3.3	L7805CV	LM2596	MP1584EN
Type	Linear (LDO)	Linear	Buck	Buck
Output Voltage	3.3V	5V	3.3-12V (adjustable)	0.9-5.5V
Output Current	3A	1.5A	3A	Up to 3A
Dropout/Switching Frequency	~1.3 Dropout	~2V dropout	150kHz	800kHz
Efficiency	~60-70%	~55-65%	Up to 92%	~90%
Cost	\$1.84	\$0.49	\$2.83	\$2.84
Technology Selection	✓		✓	

3.1.16 Communication Protocols

3.1.16.1 UART

UART is a simple, asynchronous serial communication protocol used for point-to-point communication between two devices. It transmits data one bit at a time over a pair of lines—one for transmitting (TX) and one for receiving (RX). UART does not require a clock line, relying instead on pre-agreed baud rates to synchronize data transfer between devices.

Advantages:

- Minimal wiring (only two data lines required).
- Easy to implement and widely supported on microcontrollers.
- Ideal for simple communication between a microcontroller and a computer.

Limitations:

- Only supports communication between two devices (point-to-point).
- Limited speed compared to SPI or I2C.
- Lacks built-in addressing for multiple devices.

3.1.16.2 SPI

SPI is a high-speed, synchronous serial communication protocol commonly used for short-distance communication between microcontrollers and sensors or memory devices. SPI uses four main lines: Master Out Slave In (MOSI), Master In Slave Out (MISO), Serial Clock (SCLK), and Chip Select (CS). SPI operates in a master-slave configuration, where one master device controls communication with one or more slave devices.

Advantages:

- Very fast data transfer rates (much faster than UART and I2C).
- Simple protocol structure with low latency.
- Supports multiple slave devices via individual chip select lines.

Limitations:

- Requires more wiring (at least four lines).
- No built-in device addressing; each device needs a separate CS line.
- Less suitable for long-distance communication.

3.1.16.3 I2C

I2C is a synchronous, multi-master communication protocol designed for short-distance communication between a master and multiple slave devices. It uses only two lines: Serial Data (SDA) and Serial Clock (SCL), making it efficient for connecting multiple devices on a shared bus. Each connected device has a unique address, allowing the master to communicate with multiple peripherals without additional chip select lines.

Advantages:

- Only two wires required, regardless of the number of devices.
- Supports multiple devices with built-in addressing.
- Well-suited for low-speed peripheral communication (e.g., sensors).

Limitations:

- Slower than SPI, typically limited to 100 kbps to 1 Mbps.
- Susceptible to noise over long distances due to shared lines.
- Not suitable for high-speed data streaming.

Due to the simplicity of integration and the benefits discussed above the UART communication protocol was selected. The ESP32 does not have a native UART-USB converter as such one must be constructed for the project. Suitable options for a UART to USB converter will be discussed in the following sections.

3.1.16.4 CP2102

The CP2102 is a very common and inexpensive USB-to-UART bridge. It supports full speed USB 2.0 and works with baud rates up to 1Mbps. It integrates all necessary USB transceivers and requires minimal external components. Additionally, it is available in a variety of packaging and is therefore a suitable choice for the CLSM.

3.1.16.5 FT232RL

The FT232RL is a robust and reliable USB-UART converter, it has strong driver support and wide adoption in industry and development tools. It supports flexible baud rates and includes additional GPIO pins, EEPROM, and even bit-bang I/O modes. Though more expensive than alternatives, its reliability and FTDI's detailed documentation make it a go-to for professional applications. It comes in SSOP-28 and QFN-32 packages.

3.1.16.6 CH30G

The CH340G is a cost-effective USB-to-serial converter that's popular in budget electronics and Arduino clones. It supports standard baud rates up to 115200 or higher with tuning and is has low integration complexity. It requires a crystal oscillator and a few passive components, but it's easy to use and readily available in SOP-16 and DIP-16 packages.

3.1.16.7 PL2303HX

The PL2303HX is another USB-to-UART bridge. It supports a wide range of baud rates and is compatible with many operating systems, though recent Windows updates have blacklisted some versions, leading to driver issues. It has internal USB transceivers and

supports 3.3V and 5V logic levels. The chip comes in SSOP and QFN packages and is best suited use where strict reliability isn't a must.

Table 3.28: UART-USB Converter Selection

Criteria	CP2102	FT232RL	CH30G	PL2303HX
Baud Rate	~1Mbps	>3Mbps	115200-2Mbps	~1Mbps
Pin Package	QFN-28	QFN-32	DIP-16	SSOP-28
Integration Complexity	Low	Medium	Low	Low
Driver Support	Excellent	Excellent	Decent	Some devices unsupported
Available Documentation	Good	Extensive	Basic	Limited
Cost	\$5.25	\$4.88	\$0.48	\$0.821
Part Selection	✓			

3.1.17 Software Packages for UI

3.1.17.1 Java Packets

SPI

SPI is a high-speed, synchronous serial communication protocol commonly used for short-distance communication between microcontrollers and sensors or memory devices. SPI uses four main lines: Master Out Slave In (MOSI), Master In Slave Out (MISO), Serial Clock (SCLK), and Chip Select (CS). SPI operates in a master-slave configuration, where one master device controls communication with one or more slave devices.

Advantages:

- Very fast data transfer rates (much faster than UART and I2C).
- Simple protocol structure with low latency.
- Supports multiple slave devices via individual chip select lines.

Limitations:

- Requires more wiring (at least four lines).
- No built-in device addressing; each device needs a separate CS line.
- Less suitable for long-distance communication.

I2C

I2C is a synchronous, multi-master communication protocol designed for short-distance communication between a master and multiple slave devices. It uses only two lines:

Serial Data (SDA) and Serial Clock (SCL), making it efficient for connecting multiple devices on a shared bus. Each connected device has a unique address, allowing the master to communicate with multiple peripherals without additional chip select lines.

Advantages:

- Only two wires required, regardless of the number of devices.
- Supports multiple devices with built-in addressing.
- Well-suited for low-speed peripheral communication (e.g., sensors).

Limitations:

- Slower than SPI, typically limited to 100 kbps to 1 Mbps.
- Susceptible to noise over long distances due to shared lines.
- Not suitable for high-speed data streaming.

Java Packages

Java offers a variety of mature and versatile software packages for graphical user interface (GUI) development. These packages are widely used in both academic and industry settings due to their platform independence, robust feature sets, and broad community support. Among the most commonly utilized packages are Swing, JavaFX, and JFreeChart, each serving distinct purposes depending on the application's design and functionality requirements.

The Swing framework is one of the most established GUI toolkits within the Java ecosystem. It provides a comprehensive collection of components such as buttons, panels, sliders, and menus, which allow developers to construct complete desktop applications. Swing is known for its simplicity, stability, and ease of use, making it an ideal choice for applications where rapid development and cross-platform compatibility are priorities. Despite its strengths, Swing's graphical appearance is considered outdated by modern design standards, and it lacks built-in support for advanced graphics or animations without the use of external libraries.

For more modern and visually appealing interfaces, Java developers often turn to JavaFX. JavaFX is a successor to Swing and introduces a more flexible and contemporary approach to GUI design, incorporating features such as hardware-accelerated graphics, built-in animations, and styling through CSS. JavaFX allows for the development of dynamic, rich-client applications with responsive user interfaces. It also supports a scene graph architecture, which simplifies the creation of complex graphical layouts and interactive elements. While JavaFX provides a significant improvement in visual design, it involves a steeper learning curve compared to Swing, especially when dealing with advanced features or integrating multimedia elements.

When it comes to integrating data visualization within Java applications, JFreeChart is a widely used open-source library that complements both Swing and JavaFX. JFreeChart enables the creation of professional-quality charts, including line charts, bar charts, pie charts, and more advanced scientific plots. It is particularly useful in applications where real-time data monitoring, statistical analysis, or graphical representation of numerical

data is required. JFreeChart integrates smoothly with Swing and JavaFX environments, although it is traditionally used alongside Swing. While JFreeChart excels in data visualization, it is not intended for building complete GUIs, meaning it is typically used in combination with other GUI frameworks.

3.1.17.2 Python Packets

Python offers a diverse range of software packages for graphical user interface (GUI) development, each designed to address different levels of complexity and functionality. One of the most commonly used packages is **Tkinter**, which is included in Python's standard library. Tkinter is favored for its simplicity and ease of use, making it suitable for basic applications that require straightforward interfaces such as buttons, sliders, and simple data displays. While Tkinter is limited in terms of modern styling and advanced visualization capabilities, it remains a dependable choice for lightweight GUI applications with minimal setup requirements.

For more advanced and professional applications, PyQt and PySide are widely used GUI frameworks in the Python ecosystem. Both of these packages are Python bindings for the Qt framework, providing access to a broad set of widgets, tools, and graphical capabilities. PyQt and PySide enable the development of modern, feature-rich applications with polished user interfaces. They offer extensive flexibility, including multi-window management, dynamic data display, and responsive design features. PyQt requires a commercial license for closed-source projects, whereas PySide offers a more permissive licensing model, making it attractive for academic and open-source projects.

Another Python option is Kivy, a cross-platform framework designed for building applications that work seamlessly on desktops and mobile devices. Kivy is particularly well-suited for touch-screen interfaces and interactive applications, offering a flexible design approach through its kv language. This package excels in environments where multi-touch support or mobile deployment is necessary. However, Kivy's design philosophy focuses on flexible interaction rather than traditional desktop interfaces, which may make it less suitable for conventional control panel applications.

For scientific visualization and dashboard applications, DearPyGui provides a fast and efficient solution. DearPyGui is a GPU-accelerated framework built for real-time data display and interactive dashboards. It offers a minimal learning curve, enabling rapid development of responsive graphical interfaces. While DearPyGui is not intended for complex multi-window applications, it performs exceptionally well in cases where graphical performance and simplicity are prioritized, such as in data acquisition or monitoring systems.

3.1.17.3 C# and C++ Packets

The C# programming language, primarily used within the Windows operating system environment, provides robust support for GUI development through the Windows Forms (WinForms) package. Windows Forms is a long-standing GUI framework known for its straightforward, drag-and-drop interface design capabilities. It is highly accessible to

developers of all skill levels and is particularly useful for creating basic desktop applications with minimal development time. While Windows Forms remains popular for simple use cases, it lacks modern styling and advanced graphical features found in newer frameworks.

For more advanced and visually dynamic applications, C# offers Windows Presentation Foundation (WPF). WPF is a more modern alternative to Windows Forms, utilizing XAML markup language to separate design from application logic. It supports advanced styling, data binding, and graphical effects, allowing developers to create visually rich, interactive applications. WPF is especially advantageous for applications requiring responsive layouts, animations, and complex user interactions. Despite its advantages, WPF remains a Windows-only solution, limiting its use in cross-platform projects.

In the C++ ecosystem, Qt is the most prominent GUI framework, renowned for its cross-platform capabilities and professional-grade interface design. Qt provides a comprehensive suite of tools for creating high-performance desktop applications that can operate on Windows, Linux, and macOS. It supports a wide range of widgets, graphics handling, and multi-language support. Qt is particularly well-suited for applications that demand high reliability, responsive performance, and modern graphical interfaces. However, Qt's complexity and licensing structure, which requires commercial licensing for proprietary software, can be limiting factors in some projects.⁸

Another C++ option is wxWidgets, a cross-platform GUI library designed to provide native look-and-feel on different operating systems. wxWidgets simplifies application development by abstracting away platform-specific details while maintaining performance and native appearance. It is an open-source package suitable for projects that prioritize cross-platform compatibility and straightforward GUI requirements. Compared to Qt, wxWidgets offers a simpler set of features but may lack the modern styling and flexibility required for highly customized user interfaces.

Table 3.29: Software Packages Comparison

Programming Language	Software Package	Key Features	Strengths
Python	Tkinter	Built-in GUI toolkit, basic widgets	Simple, easy to learn, no extra setup
	PyQt / PySide	Qt framework binding, advanced widgets	Modern design, professional interfaces, cross-platform
	Kivy	Cross-platform, touch support, kv language	Mobile-friendly, flexible layouts, Android/iOS support
	DearPyGui	GPU-accelerated, fast plotting, easy setup	Rapid development of dashboards, high rendering speed
C# (.NET)	Windows Forms (WinForms)	Classic drag-and-drop designer	Fast development, easy for beginners

	WPF (Windows Presentation Foundation)	XAML-based, advanced graphics, animations	Modern visuals, data binding, responsive layouts
C++	Qt	Cross-platform, extensive widget set, advanced graphics	High performance, native look, scalable
	wxWidgets	Native-looking GUI, minimal dependencies	Simple cross-platform GUIs, open-source
Java (Selected ✓)	Swing	Classic Java GUI toolkit, basic widgets	Stable, easy to integrate, cross-platform
	JavaFX	Modern UI with CSS styling, animations	Polished visuals, hardware acceleration
	JFreeChart	Charting library for data visualization	Professional-quality charts, easy integration

3.1.18 MCU Development Languages

3.1.18.1 C / C++

C is the most widely used language in embedded systems programming. Designed in the early 1970s, it provides direct access to memory, hardware registers, and system-level resources, making it highly suitable for low-level development. It is procedural, efficient, and deterministic — critical qualities for systems where timing, memory size, and processor speed are constrained. In microcontrollers, C enables developers to write firmware that interacts with sensors, controls GPIO pins, manages memory buffers, and configures hardware peripherals like timers, ADCs, and UART modules. It is also commonly used in development environments such as AVR-GCC, MPLAB XC8/XC32, and ESP-IDF (Espressif's framework for ESP32).⁸

3.1.18.2 Python Languages

Python

Python is a high-level interpreted language known for its simplicity, readability, and vast ecosystem of libraries. It is widely used in scientific computing, automation, machine learning, and web development. While standard Python is not designed for low-level hardware interaction, it has become increasingly popular in embedded systems thanks to more powerful platforms like the Raspberry Pi, which runs a full Linux OS. On such systems, Python can interact with hardware through libraries like RPi.GPIO, gpiozero, and pySerial, enabling developers to write hardware-interfacing code without needing to compile or manage memory manually.

Python excels in rapid prototyping, data processing, and GUI development. It is ideal for systems where the MCU interacts with sensors or controls and sends the data to a host application for visualization and decision-making.

MicroPython

MicroPython is a lightweight version of Python 3, designed to run directly on microcontrollers with limited resources. It provides a compact runtime and a REPL (Read-Eval-Print Loop) interface over serial, allowing developers to write and test code interactively. MicroPython exposes low-level hardware functionality through modules like machine, pin, ADC, and UART, enabling access to peripherals much like in C, but with easier syntax and dynamic typing.

It is supported on various MCUs, including the ESP32, ESP8266, and RP2040. While not as fast as C/C++, MicroPython is suitable for sensor polling, simple control loops, and educational use, particularly where real-time constraints are minimal.

Circuit Python

CircuitPython, a fork of MicroPython developed by Adafruit, aims to be even more beginner-friendly. It emphasizes plug-and-play development: when connected to a computer, a CircuitPython-compatible device appears as a USB drive, and code can be edited directly using a .py file. It is tightly integrated with Adafruit’s hardware ecosystem and simplifies access to sensors and displays using busio, digitalio, and other libraries. CircuitPython trades performance and flexibility for simplicity and accessibility, making it ideal for education, quick prototyping, and wearables.

3.1.18.3 JavaScript

JavaScript, primarily known as the language of the web, has seen some adoption in embedded systems through Espruino, a JavaScript interpreter designed to run on microcontrollers. Espruino enables developers to write JavaScript directly on boards like the Espruino Pico or ESP32 (with custom firmware). The language is event-driven and non-blocking by nature, which aligns well with asynchronous operations often needed in embedded programming, such as button presses, sensor inputs, or timers.

JavaScript in this context is not meant for high-performance control loops or low-level memory operations. However, its familiar syntax and ease of use make it attractive for web developers entering embedded hardware. It’s particularly well-suited to IoT devices, where an MCU might send data to a web server or act as a local HTTP endpoint.

In more powerful embedded Linux systems like the Raspberry Pi, Node.js — a runtime for executing JavaScript server-side — can be used to build complete IoT hubs, web-based GUIs, or data logging systems. Node.js leverages the full Linux environment and connects easily with GPIO through packages like onoff or johnny-five.

Table 3.20: Programming Language Comparison

Language	Performance	Ease of Use	Memory Efficiency	Real-Time Suitability
C	Very High	Moderate	Very High	Excellent
C++	High	Good	High	Very Good

Python	Low	Very High	Low	Poor
MicroPython	Moderate	High	Moderate	Limited
Circuit Python	Low	Very High	Low	Poor
JavaScript	Moderate	High	Moderate	Limited

Table 3.31: MCU and Programing Language Compatibilities

Language	ESP32	Raspberry PI	Arduino Mega
C	Supported	Supported	Supported
C++	Supported	Supported	Supported
Python	Not Supported	Supported	Not Supported
MicroPython	Supported	Not Supported	Not Supported
Circuit Python	Supported	Not Supported	Not Supported
JavaScript	Not Supported	Supported	Not Supported

3.1.19 Integrated Development Environment (IDE)

Having a proper Integrated Development Environment is important to the development and workflow of the project. Factors like debugging and code organization are important and each IDE is specialized for different uses. Since there is a considerable amount of programming in this project, we will be utilizing different IDEs to perform specific uses for creating a GUI, image construction, and MCU programming. Understanding each

IDE's limitations and constraints can be essential for picking the best one for each facet of the project.

3.1.19.1 Arduino IDE

The Arduino Integrated Development Environment (IDE) is a cross-platform application written in Java, designed primarily to simplify C and C++ programming for microcontrollers. Initially created for use with Arduino boards, the IDE has grown into a universal tool that supports many hardware platforms through "board definitions," including the ESP32 and Arduino Mega. The IDE offers a lightweight interface, built-in serial monitor, and extensive community-contributed libraries for peripherals such as UART communication, analog-to-digital conversion (ADC), and stepper motor control. Arduino's language is based on simplified C++, making it beginner-friendly while maintaining low-level access to hardware.

In this project, the Arduino IDE serves as the primary environment for writing and uploading firmware to the ESP32 microcontroller and the Arduino Mega (if used). The IDE is configured to support the ESP32 by installing the appropriate board definitions through the Boards Manager, and libraries such as AccelStepper, HardwareSerial, or analogRead() are used to implement motor control, data acquisition from the transimpedance amplifier (TIA), and UART-based communication with the computer. The firmware will include precise control logic for generating step sequences and managing ADC sampling routines. The built-in serial monitor can be used for testing raw output, and simple test scripts can be rapidly deployed for debugging hardware during development.⁹

3.1.19.2 VS Code

Visual Studio Code (VS Code) is a modern, open-source code editor developed by Microsoft that supports a wide range of programming languages and extensions. Its lightweight architecture, powerful IntelliSense engine, integrated terminal, and robust extension ecosystem make it ideal for Python, C++, and JavaScript development. For data processing tasks, VS Code can serve as a unified platform for writing, running, and debugging scripts that interface with microcontrollers via serial ports, manipulate data structures, and perform post-processing tasks such as filtering or visualization.

VS Code is used to develop Python-based scripts that run on the host computer and communicate with the MCU over USB-UART using the PySerial library. These scripts are responsible for reading streamed data from the ESP32, storing it in structured formats such as JSON or CSV, and possibly performing initial filtering, timestamping, or statistical analysis. Additionally, extensions like the Python extension pack, Jupyter Notebooks, and Pandas will be used to support data manipulation and exploratory analysis. This setup allows for flexible testing and validation of data integrity from the ADC and supports automated logging for experiment runs. The IDE's integrated Git support and code linting features ensure maintainable and traceable code development.

3.1.19.3 Eclipse

Eclipse is a robust, extensible integrated development environment commonly used for Java application development. Known for its plugin architecture and large user base, Eclipse supports full-scale application design with GUI components via frameworks like

Swing, JavaFX, and SWT. In embedded and instrumentation systems, Eclipse is often used to create cross-platform desktop applications that interface with external devices and provide real-time control, visualization, and configuration tools.

In this project, Eclipse will be used to design and implement a Java-based graphical user interface (GUI) that communicates with the ESP32 via the serial port. Using Java libraries such as jSerialComm or RXTX, the GUI will receive UART data from the microcontroller, decode it, and display meaningful metrics such as signal intensity, scanning progress, or system status. The interface may include elements like real-time plots, control buttons for initiating scans, dropdowns for selecting parameters, and status indicators. Eclipse's strong UI design support and modular structure will allow the GUI to evolve as the system grows — for example, to support multiple channels, additional sensors, or configuration profiles. The use of object-oriented principles ensures scalability and code reusability.

4. Standards & Design Constraints

4.1 Standards

4.1.1 Optics Standards

4.1.1.1 ANSI Z136.1-2022 Laser Safety

The ANSI Z136.1-2022, “Standard for Safe Use of Lasers”, defines the general safety recommendations needed for safe operation, as well as maximum permissible exposure (MPE), of lasers with wavelengths between 180 nm to 1000 μm in the United States. This standard includes both the environment where the laser is being used as well as around the laser beam. This is needed to control and minimize injuries such as burns or eye damage when using lasers.

The classifications of lasers are also under this standard, referred to by Class 1, Class 1M, Class 2, Class 2M, Class 3R, Class 3B, as well as Class 4. The lowest hazard lasers are those of Class 1 lasers with complete exemption from any kind of control, where class 4 is the highest hazard and requires PPE, engineering controls, administrative controls, and signage to operate.

In the CLSM, the operating power of the laser being used classifies it as Class 3B, which, according to the standard these lasers can produce a hazard if viewed directly, including from specular reflections of the laser beam. While the natural aversion of the eyes does not provide enough protection from this laser, PPE will have to be used. However, the laser is enclosed completely during use, including the reflection point on the sample. For anytime the enclosure of the CLSM must be removed or moved, PPE such as laser safety goggles should be used at any time for reasons such as for maintenance or alignment of the system. The type of goggles

Another part of the ANSI Z136.1-2022 standard that needs to be taken into consideration is the safety requirements for non-beam hazards as well. These non-beam hazards include fumes, compressed gases, cryogenic materials, noise in excess of 70 dB, electrical hazards, flammables, and explosives. In the case of this CLSM, the only non-beam

hazard that needs to be considered will be electrical hazards. Electrical hazards under this standard include shocks with power supplies or high voltages, discharging capacitors, or improper use of grounds for equipment.

According to the standard, most injuries while using Class 3B or 4 lasers happen during alignment. There is a common procedure that should be followed while aligning Class 3B or 4 lasers.³³

1. If possible lower the beam to its lowest power.
2. When possible, use a lower powered visible laser for path simulation vs higher powered invisible or visible lasers.
3. When aligning an invisible beam use IR cards or image converter tools to trace the invisible beam path.
4. Always wear the appropriate laser safety glasses.
5. Keep the laser beam inside the designated laser-controlled area LCA.
6. Exclude unnecessary personnel from the LCA during beam alignment
7. Keep the work environment free of reflective surfaces. Unused optics should be placed inside storage.

Overall, the ANSI Z136.1-2022 standard for the safe use and handling of lasers serves as a comprehensive guide on how to handle different classes of lasers and create a safe environment around the use of these lasers to mitigate the hazards mentioned previously. These standards will be upheld to ensure safe use in environments where lasers can ultimately cause undoable damage to the people around them.

4.1.1.2 ISO 11146-1,2

ISO standards 11146-1 and -2 describe standardized test methods for measuring laser beam characteristics such as beam width, divergence, and propagation ratio for Gaussian lasers. These are critical parameters for evaluating the quality and focus ability of lasers, particularly for research and industrial applications where beam shaping, alignment, and precision are required.

The first standard, ISO 11146-1, focuses on stigmatic and simple astigmatic beams, which are lasers with a beam whose cross-section and propagation characteristics can be described as generally geometrical and where the principal beam axes are perpendicular to the propagation axis, much like the laser produced by the laser diode in use for this system. It details measurement methods that are based on the second-moment definition of beam width, including mathematical procedures for calculating divergence and the propagation ratio of the beam. It is applicable to most lasers used in optical labs and equipment where beam alignment and focusing accuracy are important.

ISO 11146-2 extends these methods to include general astigmatic beams, or beams where the principal axes of the beam may be tilted relative to the direction of beam propagation.

In lasers with this definition, the beam waists on each axis can be found at different longitudinal positions. This part of the standard is much more applicable when working with more complex laser systems than the one in use for this system, where the beam profile is not uniform or symmetrical. Some examples of such instances are in advanced optical setups or in systems with high amounts of aberrations or poorly aligned components. However, it can still give insight into important considerations when dealing with lasers such as that produced by the laser diode used in this design.

Both standards are important for the characterization of laser beam parameters to be accurate and consistent. For applications like confocal laser scanning microscopy, proper beam characterization is crucial for optimizing the system's focus and producing minimal aberrations at the sample plane.

Following ISO 11146-1 and 11146-2 ensures that measurements of beam quality are standardized, meaning they have been recorded and can be reproduced and compared across different labs and systems. This becomes especially important in research or other collaborative environments where a standard for the documentation of laser behavior is required.

Together, ISO 11146-1 and ISO 11146-2 provide detailed procedures and definitions to help understand and measure how lasers propagate, how they spread over distance, and how they may deviate from the ideal Gaussian shape. These standards will be followed to ensure proper characterization and optimal performance of the laser being incorporated into this system, as precise beam delivery will be essential to the function of the microscope.

4.1.2 Electronics Standards

4.1.2.1 IEC 61010-1 Electrical Safety

The IEC 61010-1 standard defines general safety requirements for electrical equipment used in a laboratory, control, and measurement system. This standard is critical to ensure that systems like the CLSM, which have AC mains, DC regulation, laser components, stepper motors etc. Are protected against electrical shock, overheating, fire hazards and mechanical damage during regular and fault operation.

In the CLSM, power will be sourced from an external AC-DC converter operating at 12V. Based on the IEC 61010-1 standard, components interfacing with mains voltage (Like the LRS-75-12 regulator) must provide reinforced insulation between live AC inputs and low voltage DC outputs. This requirement can be satisfied through the use of isolated, enclosed power supplies with built-in overvoltage, overload, and short-circuit protections; these prevent excessive current from reaching other circuits and minimize the risk of thermal damage or component failure during a fault condition.

Additionally, IEC 61010-1 defines minimum creepage and clearance distance requirements between conductors to prevent arc-over at high voltages. Although the system may operate on 12VDC internally, maintaining safe spacing and using properly

rated components on the primary side ensures the system would not have shock hazards or arc flashing during modification.

For thermal safety, IEC 61010-1 defines proper derating of components based on ambient temperature. For example, the Mean Well LRS series are rated for continuous operation at 50-70°C with derating curves provided in the datasheet. Proper installation and ventilation must be incorporated to keep temperature within safe limits, especially around the PSU and motor drivers.

Overall, IEC 61010-1 includes sections for ensuring electrical safety based on several factors. It outlines inspection criteria and requirements that must be employed in order to verify the integrity and proper operation of electrical components.

4.1.2.2 IPC Standards PCB Design & Manufacturing

The printed circuit board (PCB) is the housing for all components in the CLSM electrical system. The PCB design must follow a combination of manufacturer specific constraints (i.e. JLCPCB) and general industry guidelines from the IPC-2221 standard.

JLC PCB imposes several fabrication constraints based on their standard 2-layer stackup which include:

- Copper weight: 1oz and 2oz supported
- Minimum via hole size: 0.3mm with a minimum pad diameter of 0.5mm
- Drill pad clearance: 0.5mm for holes of different nets.
- Trace width and spacing: 0.127mm minimum for both, with 0.3mm clearance from board edge.
- Pad-to-pad and pad-to-track spacing: 0.127mm and 0.2mm respectively

All of these specifications are in place to ensure that the PCB is physically manufacturable and does not suffer any issues.

In parallel to JLCPCB's standards, IPC-2221 provides a generalized framework for design rules based on the application. For the CLSM, which would fall under class 2 (dedicated service electronic products), the following guidelines are in place:

- Trace Width and Spacing: Trace widths are calculated using IPC-2152 charts based on current density, especially for 12V supply rails and motor current paths. Wider traces or polygon fills are used for the motor power and regulator output nets.
- Thermal Management: Heat-generating components like the LM1085 linear regulator and ESP32 are placed to allow airflow and/or heatsinking. If needed, thermal vias can be added to transfer heat to ground planes or the back side of the board.
- Signal Integrity: Analog paths, especially from the TIA output to the ADC or MCU, are routed with minimal length, low capacitance, and isolated from noisy

motor driver lines. This aligns with IPC-2221's recommendations for minimizing EMI and crosstalk.

- **Design for Manufacturability:** All components are selected in standard SMD packages (e.g., SOT-223 for the regulator), and silkscreen markings follow IPC guidelines for readability and assembly clarity.
- **Layer Planning:** For the 2-layer board, one side is prioritized for signals and microcontroller routing, while the other serves primarily as a ground plane, improving return paths and reducing EMI.

IPC-2221 encourages re-fabrication design reviews and post-fabrication inspections, which JLCPCB offers as standard services.

Overall, following the guidelines set out by IPC-2221 ensures reliable electrical performance and allows for lower fabrication costs as following the standard will reduce the chance of errors, leading to less revisions and errors during testing.

4.1.3 Communication Protocol Standards

4.1.3.1 Universal Asynchronous Receiver Transmitter (UART)

The Universal Asynchronous Receiver-Transmitter (UART) is a fundamental hardware communication protocol that enables asynchronous serial communication between digital devices. As a standard, UART defines how binary data is transmitted over a single data line, typically without a separate clock signal. This asynchronous nature requires both sender and receiver to operate at a predefined and matching baud rate. UART typically transmits data using a start bit, a configurable number of data bits (commonly 8), an optional parity bit, and one or more stop bits. This structure enables relatively simple and low-overhead communication for low-to-moderate speed applications.

While the electrical and mechanical aspects of UART were historically governed by the EIA/TIA-232-F standard (commonly referred to as RS-232), modern microcontrollers like the ESP32 use logic-level UART implementations that operate at lower voltages (e.g., 3.3V TTL levels). The RS-232 standard originally used $\pm 12\text{V}$ signaling, but modern UART interfaces adapted the protocol to work efficiently in embedded systems while maintaining logical framing, start/stop conventions, and voltage thresholds consistent with their voltage domains. UART has become a de facto communication method in embedded systems for debugging, inter-device communication, and connecting to external peripherals.¹³

In the Confocal Laser Scanning Microscope project, the UART protocol is implemented on the ESP32 microcontroller to handle serial communication between the MCU and the host computer. The ESP32 transmits diagnostic data, ADC readings, and position-related feedback using its built-in UART peripheral. This data is framed using the standard UART protocol and passed to a USB-to-UART bridge chip (e.g., CP2102), which then converts it into USB data for the PC. On the microcontroller side, this requires initializing the UART peripheral with parameters such as baud rate (e.g., 115200), 8 data bits, no parity, and one stop bit. Ensuring stable communication under this standard involves

managing UART buffer sizes, avoiding overflows during high-speed data transmission, and maintaining signal integrity across PCB traces. Following UART conventions enables reliable and consistent communication between the data acquisition subsystem and the user interface.

4.1.3.2 Sending Analog-to-Digital Signal (UART)

Analog-to-Digital Conversion (ADC) is the process by which continuous analog signals are translated into discrete digital values suitable for processing by digital systems. The IEEE 1241 standard provides a comprehensive framework for defining the terminology, testing methodologies, and performance evaluation criteria for ADCs. This standard is especially important in precision applications such as scientific instrumentation, where measurement accuracy, resolution, and repeatability directly impact system performance.

IEEE 1241 defines performance metrics such as resolution (the number of discrete steps), sampling rate, signal-to-noise ratio (SNR), integral nonlinearity (INL), differential nonlinearity (DNL), and effective number of bits (ENOB). These parameters characterize how well an ADC performs in real-world scenarios, particularly when digitizing signals with varying amplitude and frequency content. High-precision ADC systems must minimize sources of error such as quantization noise, thermal noise, voltage drift, and distortion introduced by the analog front-end circuitry.

In the Confocal Laser Scanning Microscope, the ESP32's built-in 12-bit SAR ADC is used to sample analog signals generated by a transimpedance amplifier connected to a photodetector. This signal corresponds to the intensity of reflected laser light and is used for image generation and real-time monitoring. While the ESP32's internal ADC is not fully compliant with high-performance specifications like those in IEEE 1241, the principles of the standard guide the system's design choices. For example, attention is paid to PCB layout to reduce ground loop noise, analog signal routing is kept short to minimize coupling, and software filtering techniques (e.g., moving average or oversampling) are used to compensate for the ESP32's known non-linearity. Additionally, calibration routines may be introduced to correct for ADC gain and offset errors. Following IEEE 1241's guidelines ensure that the analog measurement subsystem performs within acceptable accuracy limits, contributing to the overall fidelity of the CLSM imaging system.

4.1.4 GUI Communication Standards

4.1.4.1 Universal Serial Bus (USB)

The Universal Serial Bus (USB) is a widely adopted serial communication protocol designed to standardize data exchange between a host (e.g., a computer) and various peripheral devices. While USB supports a range of device classes — including mass storage, human interface devices, and video streaming — one of the most applicable to embedded systems is the Communications Device Class (CDC). The USB CDC standard allows embedded devices to emulate legacy serial ports over USB, enabling easy communication with terminal software or custom graphical user interfaces on a computer without requiring specialized USB drivers.

The CDC standard defines how data should be structured into packets and transmitted over the USB's endpoint architecture. Data transfer typically uses bulk transfer mode, which is optimized for reliably transmitting large amounts of data without guaranteed timing constraints. Devices implementing CDC appear as Virtual COM Ports on the host operating system, providing plug-and-play serial communication and backward compatibility with UART-based software. The standard also defines control requests that allow the host to configure the virtual serial interface's parameters (e.g., baud rate, parity), even though these settings are simulated and not strictly needed in a USB environment.¹¹

In this project, the ESP32 itself does not natively support USB peripheral functionality (except in select variants); instead, it communicates over UART with a USB-to-Serial bridge IC such as the CH340 or CP2102. These bridge chips implement the USB CDC standard and present the ESP32's UART output to the host computer as a virtual COM port. This allows the GUI on the host machine to interface with the microcontroller as if it were a traditional serial device. Adhering to USB CDC standards ensures that the system is compatible with a wide variety of operating systems and terminal applications. From an implementation perspective, proper data formatting, UART buffer management, and USB endpoint handling are crucial for avoiding data loss or communication bottlenecks during periods of high throughput, such as continuous data streaming from the ADC subsystem.

4.2 Practical Constraints

4.2.1 Economic

One of the main motivating factors for the undertaking of this design project was to produce a schematic for a working confocal laser scanning microscope (CLSM) that could be made available to researchers on an open-source database, achieved resolution and performance metrics comparable to similar, commercially available devices of the same kind, and could be constructed by a researcher for a price as close to \$1000. The objective is to make tools, such as this CLSM, available in labs and research areas with small budgets, at a fraction of the cost of the commercially available devices.

In order to achieve this goal, components are selected for their widespread availability and affordability, and costs are reduced through engineering creativity wherever possible. Some examples of this are the design choice of operating this device using a 405nm laser diode, which is one of the cheaper laser diodes that still operate within a range of wavelengths that enable resolution on the order of that which the specs require. Similarly, there are photodiodes available that are tuned precisely to have peak responsivity at or near the desired wavelength of 405nm, but these devices can cost hundreds of dollars on the cheap end. For the purpose of saving costs without sacrificing functionality, cheaper photodiodes whose peak responsivity may be located elsewhere on the spectrum but can still be purposed to function at the correct wavelengths were selected, and choices like using a higher-power laser diode and correctly choosing appropriate transimpedance amplifiers were made to accommodate for this decision.

Unfortunately, there are some economic constraints that even creative engineering cannot totally make up for. For example, selection of the microscope objective involved, careful consideration of the magnification, working distance, and numerical aperture. Objectives with higher magnification can theoretically increase the resolution of the system, but that change typically corresponds with a wider numerical aperture. For measurements of depth, the numerical aperture is a limiting factor, as the laser cannot scan to the bottom of a feature that is narrower than its numerical aperture. In order to accommodate for this limitation, it would be possible to purchase a microscope objective with a high magnification that also has a narrow numerical aperture; however, the price difference between a standard 40x objective and one that has been designed to have a narrow NA is significant enough to nullify any goal of making an affordable microscope.

Other economic constraints include the prices of a polarizing beamsplitter, which would theoretically enable more efficient transmission and mitigate loss of optical power through the system in comparison with the chosen plate beamsplitter. However, lower transmission and higher optical power loss are a necessary sacrifice in order to maintain affordability for these components.

Another factor is the current economic climate, particularly in regard to tariffs and international trade conditions; this may, in turn, lead to higher or lower costs for future users of the CLSM. For instance, the cost of PCB manufacturing can vary significantly depending on ongoing trade relations between the United States and China, where many fabrication services are based. Additionally, certain electronic or optical components may become difficult to source or more expensive due to import restrictions, export controls, or shifting trade agreements. These fluctuations introduce uncertainty in both the cost and availability of critical parts, potentially impacting the scalability and reproducibility of the CLSM design.

4.2.2 Time

The time required to complete a full scan of an object is one of the most important performance constraints in this project. Several factors affect how long a scan takes, including the resolution of the scan, the size of the object, the mechanical speed of the stage movement, and the rate at which the ESP32 collects and sends data. In high-resolution mode, where every point on the surface is sampled without skipping, the scan can take a significant amount of time, especially for larger objects or dense scan grids. This extended scan time may not always be practical, particularly in cases where quick feedback is desired.

One major factor that increases scan duration is the number of points to be collected. For example, scanning a 10 cm by 10 cm surface with a 1 mm resolution results in 10,000 data points. At even modest sampling delays (such as 50 milliseconds per point to allow for movement, reading, and communication), this results in a total scan time of over 8 minutes. In cases where mechanical movement is slower or communication is delayed, this duration can increase further.

Obstacles that may lengthen scan time include motor speed limitations, voltage measurement stability, and serial communication delays. If the stepper motor requires more time to settle between steps for accurate measurements, the system must wait before

taking each reading. Likewise, the analog voltage signal from the transimpedance amplifier may require a short delay to stabilize before it is accurately sampled. Communication bottlenecks between the ESP32 and the computer can also slow down the process, especially if large volumes of data are being transmitted without proper buffering.

To help manage these constraints, the system includes a fast scan mode, which reduces the total number of scanned points by intentionally skipping over intermediate positions. This significantly decreases scan time by reducing both the number of physical movements and the number of data transmissions. The system then uses interpolation techniques on the computer to estimate the missing values and still produce a continuous surface map. While this reduces detail, it allows for quicker scans when high resolution is not essential.

Another major consideration for any group looking to build this type of CLSM will be to consider how long it may take to build this system. Based off of shipping times and locations of each group, the time it takes can wildly vary. The difference in being able to build this system in a couple weeks versus a couple of months can be the deciding factor in if this is a feasible option for many groups.

In summary, scanning time is influenced by the object's size, the resolution settings, mechanical speed, and the responsiveness of the data collection process. The system is designed to provide a balance between accuracy and speed, allowing users to adjust scan settings based on the specific needs of the task.

4.2.3 Environmental/Space

The primary environmental constraint for this project is the laboratory-controlled setting in which the CLSM will operate. While our proof of concept is designed for academic or research use, future applications introduce challenges that this prototype is not yet equipped to handle.

A major environmental factor is temperature stability. Optical systems, especially those involving lasers and precision scanning mirrors, can be sensitive to temperature fluctuations which may affect alignment and accuracy. In a typical lab setting, the temperature is relatively stable, so this constraint is not critical during testing, but any future deployment in less controlled environments would require robust thermal management solutions.

Another space-related constraint is vibration and physical isolation. The CLSM relies on highly sensitive photodetectors and scanning mechanisms, which can be disrupted by mechanical vibrations or shock. For our prototype we intend to mitigate this by using concrete slabs to stabilize the project, but this may not be available or possible for other users. Moreover, utilizing connection points between the microscope stage and microscope head allows these two systems to theoretically function as one. Having both the concrete slabs as well as these connections can minimize the need for any other vibrational reductions that would be needed otherwise.

Additionally, the cleanliness of the environment also plays a critical role. The CLSM's optical path must remain free of dust and particulates to maintain image clarity and system reliability. While clean lab environments suffice for our testing, industrial environments would demand sealed optics or HEPA-filtered enclosures, which add cost and complexity. Lastly, ambient light interference is a notable constraint. Because the photodetector is sensitive to reflected laser signal, stray light can introduce noise. During our testing, we control this with an enclosed stage as well as testing in a room with no lights, but future iterations may need optical shielding or compensation algorithms. For the final prototype, the decision of using a 3D printed housing was agreed upon, not only for cost reduction but also for the ability to enclose all of the optical components to reduce any stray light that may be present outside of the system.

These constraints are manageable within our conditions, however, any expansion of the system outside controlled environments would require significant design adjustments to maintain performance and reliability. Our prototype remains functional proof of concept built with these limitations in mind.

4.2.4 Manufacturability

The manufacturability of the CLSM system presents several challenges that must be addressed both during the initial build and for any potential future replication. These challenges can be categorized into precision and alignment, sourcing and standardization, repeatability, and environmental stability.

One of the most critical factors in manufacturing a CLSM is the tight tolerance required across its mechanical and optical subsystems. Even minor misalignments in the laser optics, detector alignment, or motion stages can lead to a significant loss in image quality or system functionality. Although the OpenFlexure delta stage enables a high level of manufacturability through its 3D-printable design and modularity, the reliance on plastic parts introduces mechanical wear over time, especially in moving components. If such wear occurs, the system's performance may degrade, requiring replacements or recalibrations that are not always plug-and-play. Long-term solutions may include switching to metal-reinforced parts or using precision-ground linear rails, but these options would trade off ease of manufacturing for increased performance and cost.

The CLSM's manufacturing process also lacks full standardization. While elements like PCB design, electronics assembly, and the use of 3D printable STL files are repeatable in theory, in practice, there is often variation in printer quality, material shrinkage, and tolerance stacking that can lead to assembly issues. Inconsistent 3D print resolution or warped parts may misalign the optics or destabilize the stage. To improve reproducibility, STL files should be accompanied by detailed printing instructions including layer height, infill, print orientation, and recommended material (e.g., PLA vs. PETG). Furthermore, consideration should be given to designing parts that are more forgiving to slight dimensional inaccuracies or that can be easily shimmed or calibrated.

Environmental stability plays a huge role in the repeatability and usability of the CLSM. Given the sensitivity of the optical system to vibration and thermal expansion, the system is susceptible to minor disturbances from the environment such as wind, table vibrations, or slight shifts during operation. To combat this, the team will be constructing a concrete

platform that will serve as a heavy, level base for the OpenFlexure stage. This platform significantly increases the system's robustness by absorbing ambient vibrations and eliminating tilt due to surface irregularities. The concrete also reduces temperature fluctuations and drift, further enhancing the long-term stability and reliability of the microscope during scans.

Another manufacturability aspect includes the use of 3D printing for larger assemblies, like the microscope head. While this enables rapid prototyping and customization, these parts must be designed with printability in mind, avoiding overhangs, ensuring proper mechanical tolerances, and accounting for thermal shrinkage of material. Additionally, the parts should ideally be modular to allow quick replacement or upgrades of individual subsystems (e.g., swapping out an objective lens mount or photodiode module without reprinting the entire assembly).

Lastly, since the CLSM project is open-source and intended for replication by students, hobbyists, or labs worldwide, extra care must be taken in documentation. This includes not only providing Gerber files, 3D models, and software repositories, but also annotating which parts are critical to precision, which are interchangeable, and what tolerances are acceptable. Offering a bill of materials with multiple sourcing options, as well as detailed build guides, will lower the barrier to entry for others.

Managing manufacturability constraints in the CLSM project involves standardizing parts and interfaces, building with accessible and reproducible methods like 3D printing, and mitigating environmental noise with stabilization structures like a concrete base. By designing with modularity and repeatability in mind, the CLSM system can be more easily adopted, repaired, or improved by others in the future.

5. Applications of Artificial Intelligence

5.1 AI Limitations, Pros, and Cons

ChatGPT and other Large Language Models (LLMs) have improved rapidly in a matter of years, now capable of giving quick and quality results with minimal input. However, ChatGPT and other LLMs still struggle to take multiple considerations into account for part selection, which was demonstrated when utilizing LLMs for TIA research. As such, the need for information verification, manual calculation, and assessment of LLM part recommendations was critical in order to ensure proper part selection. Prompts utilized with their response can be found in appendix E.

5.1.1 Case Study 1

The following sections discuss the utilization of ChatGPT and Google Gemini to determine “what are some safety standards of lasers”. The question was asked to both of these LLMs and the LLMs responses are delved into below.

5.1.1.1 ChatGPT

ChatGPT gives a very good overview of some basic laser safety standards that need to be addressed when handling lasers. This is great for trying to get a basic understanding of how these standards work. However, when trying to understand these safety standards without the use of ChatGPT, safety standards usually go into detail of the hazards themselves so the user can get a full understanding of what they are using and why these standards exist. In this case from ChatGPT, it seems to have missed the more specific hazards when talking about laser safety such as electrical safety and less common hazards such as chemical or gaseous hazards.

Moreover, ChatGPT does recognize the laser classes and explains the power each laser class represents. This is a good point to mention when talking about very basic standards, especially when needing to know if extra PPE is required to handle certain lasers.

While this is a good overview of some optics standards, it would be more beneficial to go to ANSI's website and read up on these standards separately from the LLM.

5.1.1.2 Google Gemini

Initially Google Gemini seems very similar to ChatGPT in the responses. Gemini starts off by listing the laser classes and safety requirements for handling certain power lasers. However, unlike ChatGPT, Gemini lists other standards, such as international optics standards that lost certain requirements for how to handle all lasers, how to power lasers properly to reduce risk, and how to handle setting up other kinds of lasers.

While it seems much better than ChatGPT's response, it would be a better option to go to the standard producers' websites. This way it will still give a more detailed overview of each specific standard.

5.1.2 Case Study 2

5.1.2.1 ChatGPT

ChatGPT is a very useful tool for collecting information from a large number of sources, but this can prove to be as much a weakness as it is a strength.

In this case, it provided a very informative summary about important criteria when selecting the proper photodiode for an imaging system, and some of the unique ways of tailoring a scanning laser microscope to perform surface topography, however the information provided should serve only as a starting point. Research into the topics it discussed is important to verify their legitimacy, and because an in-depth understanding of those topics is important for anyone trying to put them to use. Even the most well-crafted prompts still won't be able to get a result that perfectly fits the system that someone is trying to create.

Though it provided a wide range of options and summarized their advantages and applications, it is up to the researcher to decide on their implementation and whether or not they fit in the scope of their design.

5.1.3 Case Study 3

For the following section ChatGPT and Claude were utilized and compared to ascertain good practices and part selection for the TIA, prior to the prompt both LLMs were informed about basic project details for applicable answers. This section will be an analysis of the answers output by both LLMs regarding their usefulness to the project.

5.1.3.1 ChatGPT

The following prompt was used to get a quick overview of what factors play into TIA design: “What are the main considerations when designing a transimpedance amplifier (TIA).” To this prompt ChatGPT answered with general information followed by brief descriptions, the answer provided, and a good range of considerations given the project. The overall information provided was for the most part correct and allowed for further research into some aspects that had not been considered previously. These answers could have some downsides however, first, the answers do not fully build off each other, for example, ChatGPT says “Higher R_f increases sensitivity.” Although technically correct, this could be misleading as a higher R_f also implies a higher tau ($\tau=RC$) and therefore lower bandwidth. Overall, this prompt yielded good results, however, further research is required on a user’s end to verify that the information provided is fully accurate.

A second prompt for part selection was used to get a quick overview of potential parts used for the TIA: “What are some common integrated circuits suited for TIA design based on photodiode currents in the range of μA ?” To this prompt ChatGPT answered only a list of potential ICs with no other context. From a research standpoint this was not too useful as every part had to be individually looked at to determine if it was viable. Additionally, some of the parts provided were not viable based on project requirements, highlighting the need for verification when using an LLM for research. However, this list of ICs ultimately was useful as all four of the options considered for the TIA selection came from the list, the lack of context provided by ChatGPT allowed for more than just superficial research and forced the team to consider all factors of the TIA design when selecting a part.

Overall, ChatGPT provided good information, although somewhat lacking in its answers, it was a good setup for further research and development. Regardless of issues with answers, the use of this LLM was overall beneficial to the project.

5.1.3.2 Google Gemini

Similarly to ChatGPT, Google Gemini was asked for a quick overview of what factors play into TIA design: “What are the main considerations when designing a transimpedance amplifier (TIA).” To this prompt Google Gemini answered with general information followed by a bullet list containing the factor and an in-depth overview of the factor and why it is applicable to the project. The overall information provided was correct and unlike ChatGPT it considered how one factor may affect another. Furthermore, the answers were able to provide specific guidelines, for example: “A larger R_f increases sensitivity for small currents but can limit the maximum measurable current before saturation” This information was quite useful when it came to testing the parts themselves as the team was aware of the implications of utilizing a higher R_f even if not everyone was fully aware of the TIA needs and requirements. However, this answer also

has some drawbacks. First, the answer provides almost too much detail, although this may be a good thing initially, even ChatGPT made mistakes with small answers, as such greater care to verify all the information that Google Gemini output had to be taken. Although this led to even further research it could be a negative if a user was to implicitly trust the LLM, leading to errors in the design process.

Like with ChatGPT, a second prompt was asked to Google Gemini for a quick overview of parts for the TIA: “What are some common integrated circuits suited for TIA design based on photodiode currents in the range of μA ?” To this prompt Google Gemini, again, answered similar IC’s to ChatGPT but this time described key specifications outlined in the datasheet of each IC. This was quite helpful when determining which part was worth researching. However, this answer had quite a few issues. First, some of the specifications were incorrect or misleading, rather than being obtained from the datasheet they seem to have been obtained from resources like Reddit, where a user may ask a question about their specific use case. This highlights the importance of researching and using the correct sources when looking at part selection.

Overall, Google Gemini provided lengthy and detailed answers that were good for initial understanding, however, much verifying was needed to trust these answers. Although there were issues with answers, the use of this LLM was beneficial in general.

5.1.4 Case Study 4

For this section we used 3 popular LLM’s (ChatGPT, Claude, and Google Gemini) to see what it would output as the best choice for MCU’s for this project. To keep the generated responses fair this is the following prompt given to each model: “Salutations [name of LLM] I would like to pick a Micro controller for the purpose of reading data from a transimpedance amplifier and sending the data to a computer for analysis. This microcontroller should also be able to control stepper motors as well”.

5.1.4.1 ChatGPT

After entering the prompt in ChatGPT these were the recommendations that the application suggested: Arduino, Raspberry Pi Pico, and ESP32. ChatGPT outline the important features mentioned in the prompt and recommended these three microcontrollers and guided the user to look at specifications like ADC resolution, GPIOs, Stepper Control, Data transfer, and then highlighting each pros and cons. Additionally, it states it best use case for the MCU, for example, the ESP32 is “Best For: A compact, Wi-Fi-enabled solution. Great general-purpose pick.” Compared to the Raspberry which is best for “Advanced real-time motor control or USB-native logging.”. ChatGPT seems to try to give the user a bunch of options trying to cover all possibilities that the user might need.

Upon a initial look at this prompt it does provide a lot of concise information about the microcontrollers mentioned. ChatGPT highlights key requirements for a microcontroller; ADC, GPIOs, Serial / USB communication, Real-time controll, etc. These requirements can narrow down a multitude of options but this can be a detriment if one doesn’t mention any other iterations of an MCU.

5.1.4.2 Claude

After entering the prompt in Claude these were the recommendations that the application suggested: ESP32-S3, STM32F4, Arduino Uno R4 WiFi. Claude lists these MCUs along with key features that goes with the prompt, highlighting features like ADC resolution and what edge the MCU provides. For the ESP32-S3 it states that it has a Dual Core Processor and its wifi capabilities. Comparing this to the other language model it does show a preference for one particular product and giving a simple bullet list of advantages. The concern with the LLM's seems to be that it simply gives a regurgitated description of the project with little elaboration.

This LLM is shorter compared to the other two mentioned in this section. This can be a benefit to those that want a simple and easy way to get a list of microcontrollers that can help. However this simple listing fails to provide any insight and further information about the product. Comparing it to ChatGPT, for example, the user wouldn't know how many available GPIO pins an ESP32 would have which can limit how many peripherals the user could add to their system.

5.1.4.3 Google Gemini

After entering the prompt in Gemini these were the recommendations that the application suggested: Arduino Uno, ESP32, STM32, PIC. This LLM provides a wider array of products with each a simple paragraph explaining the use what it best offers for the user. After the recommendation it does guide the user by pointing out important considerations when selecting a proper MCU as per the prompt given to it. Here are some of the considerations; ADC resolution, PWM Channels, Processing Power, Connectivity to PC, Development Ecosystem.

The other LLM's used in this section serves its information in a bulleted format which tends to be easier to digest information. As mentioned above the simple paragraphs that Google Gemini provides would necessarily point the user to specifics about the product only broad descriptions of the capabilities. The vague phrases like "more I/O pins" can leave questions for the user like what is considered "more" and "what is the standard". Although this does push the user to search for the information, comparing this model to ChatGPT and Claude it seems to lack any quantitative values that can assist being more specific.

6. Hardware Design

6.1 Power Delivery

6.1.1 Power Delivery System Schematic

To power the 5V (MP1584EN) regulator the Mean Well LRS-50-12 AC-DC converter will supply 12VDC. As per the data sheet, the recommended range for the inductor of the circuit is 0.7-13 μ H therefore an inductance of 4.7 μ H was selected. Similarly, capacitor selection is recommended to be within 4.7 μ F and 100 μ F as such a 22 μ F will be selected

for the output capacitor and other varying values for inputs. The 3.3V LDO regulator that will be used is an LM1085-3.3, it is a fixed 3.3V regulator that can handle inputs $> 4.8\text{V}$. Therefore, no voltage divider is required as shown in the datasheet and only capacitors need be selected. For the circuit two $10\mu\text{F}$ capacitors will be used. When integrated onto the PCB this will be individual modules that can be plugged in or unplugged for both simplicity and ease of repair/modification. It is worth noting that currently there is no -5V rail, however, depending on the needs for the transimpedance amplifier this could be added in the future and would require redesign of the system.

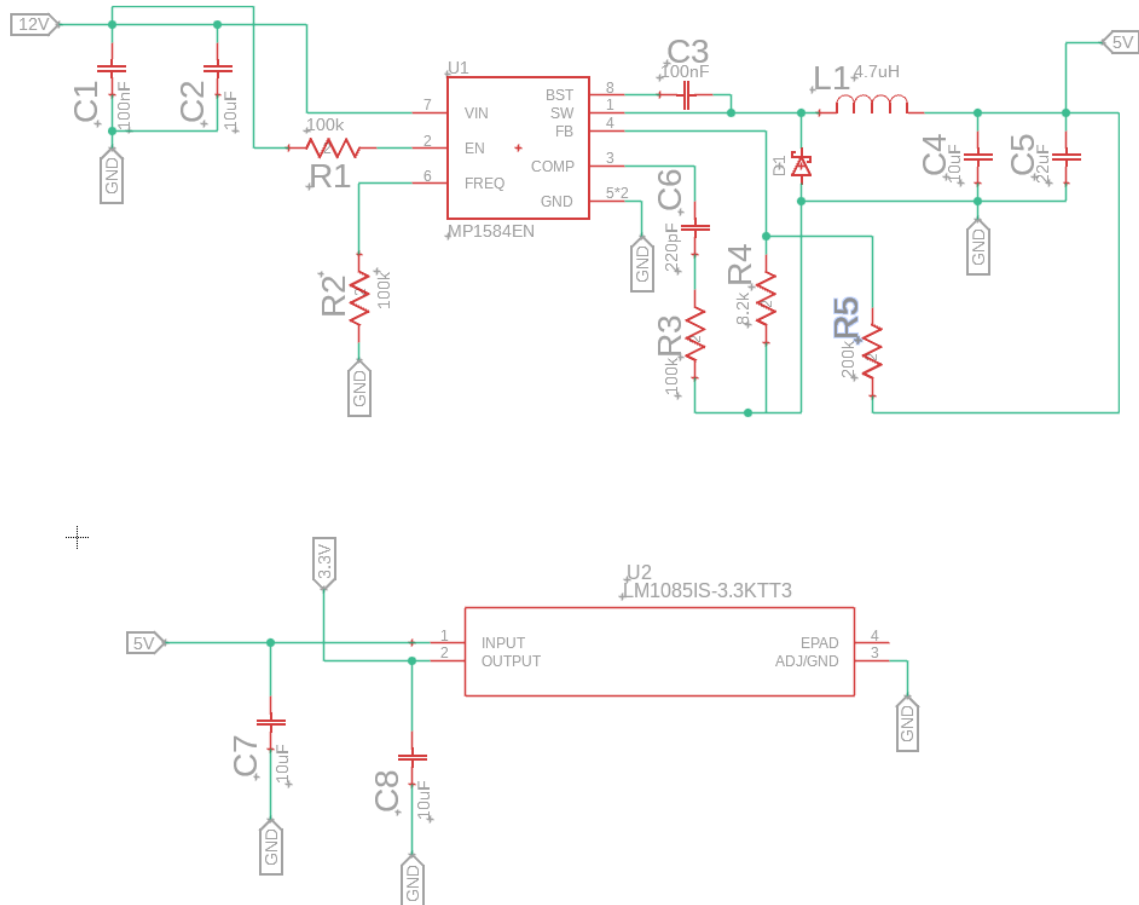
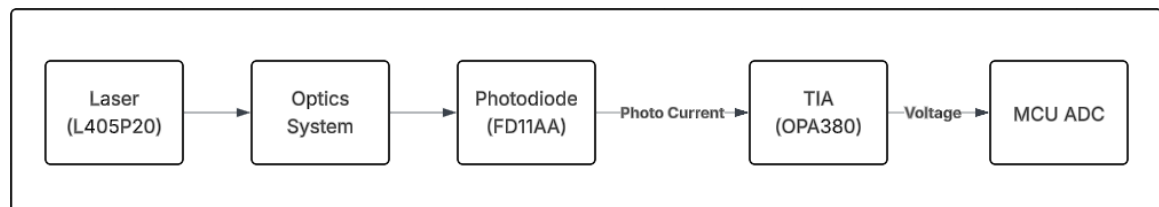


Figure 8: 5V and 3.3V Regulators Schematics

6.2 Transimpedance Amplifier

6.2.1 Low Level Block Diagram



6.2.2 Transimpedance Amplifier Schematic

The OPA380 TIA in the CLSM will be used to convert the photocurrent from the FD11A photodiode into a readable voltage signal to the ESP32. The photodiode will be reverse biased and connected as close as possible to the inverting input of the op-amp. A feedback resistor of $1\text{M}\Omega$ is used for the gain, and 2pF is used in parallel with R_f to account for parasitic capacitance, noise and filtering. The non-inverting input is grounded as well as V_- . V_+ is set at 5V in accordance with the datasheet provided by Texas Instruments (see appendix C). The output will be connected directly to the ESP32's internal ADC (pin 4) for signal processing. It is worth noting that the photodiode in the circuit will be placed at a minimal distance from the input. This will allow for less noise and avoid capacitance between the photodiode and TIA which would in turn limit bandwidth.

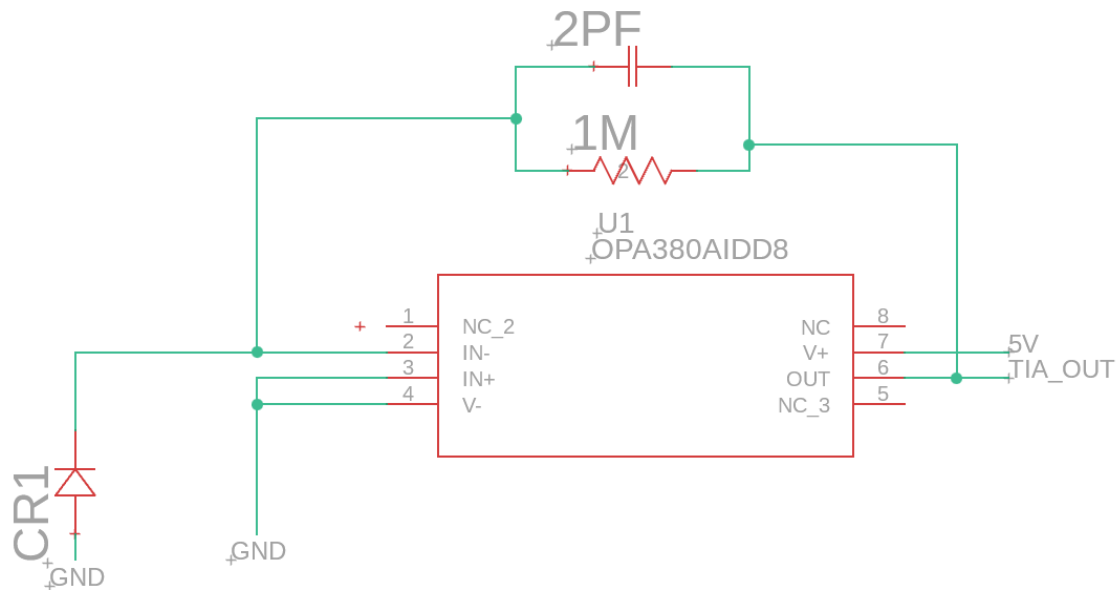


Figure 9: Transimpedance Amplifier Schematic

6.3 Motor Controllers

6.3.1 Low Level Block Diagram

6.3.2 Motor Controller Schematic

The schematics shows the motor control units for three unipolar stepper motors using three ULN2003 driver ICs connected to an ESP32. Each motor is driven by a separate ULN2003, with four GPIO pins from the ESP32 controlling the IN1–IN4 inputs of each driver (see 6.1.1 for MCU pinout). The outputs (OUT1–OUT4) connect to the motor coils in standard order (BLUE, PINK, YELLOW, ORANGE), and the COM pin is tied to $+5\text{V}$ to enable the internal flyback diodes for inductive protection. All GNDs are shared to ensure proper reference between the ESP32, drivers, and motor power supply. This setup

allows independent and reliable control of each motor. LEDs are in place for each output to verify functionality while in use. Note that a single unit is shown for better clarity.

Much like the regulators, the design of these controllers will be approached with modularity in mind, this is due to several factors. First, the modules will be more closely tied to the stage, the OpenFlexure stage has an integrated compartment to store these, which will be more space efficient. Additionally, ULN2003 can be damaged easily when there are even small electrical fluctuations, as such a modular approach is necessary for ease of repair.

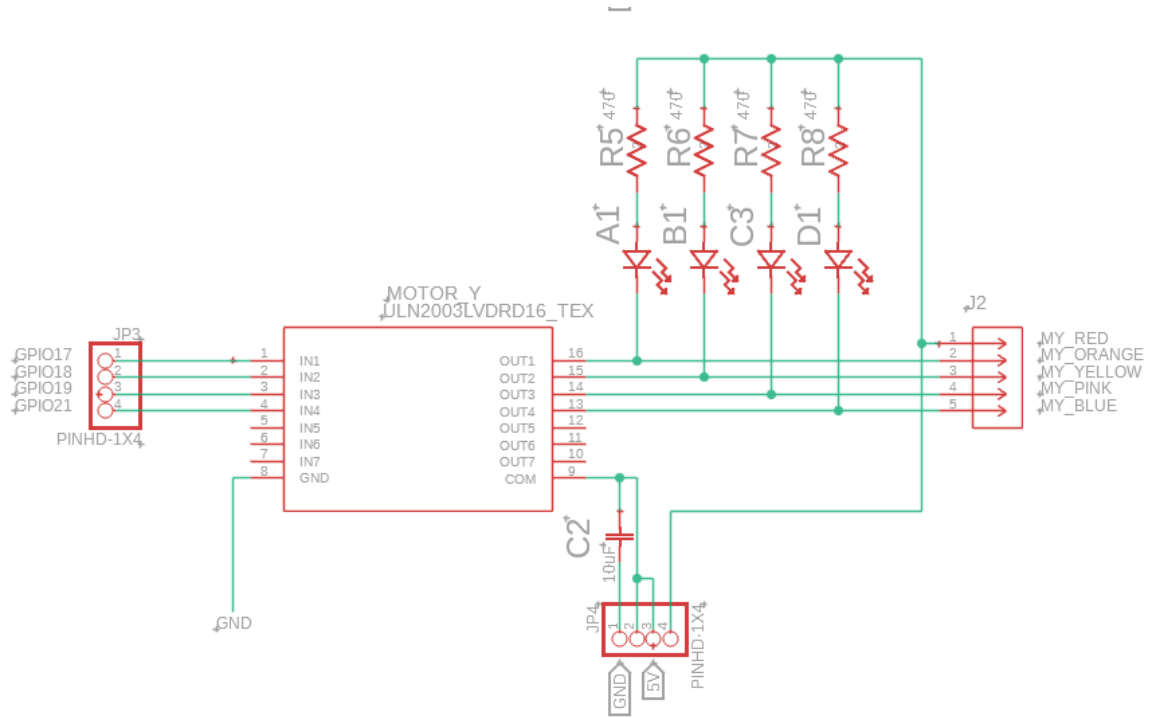


Figure 10: Single Motor controller unit schematic

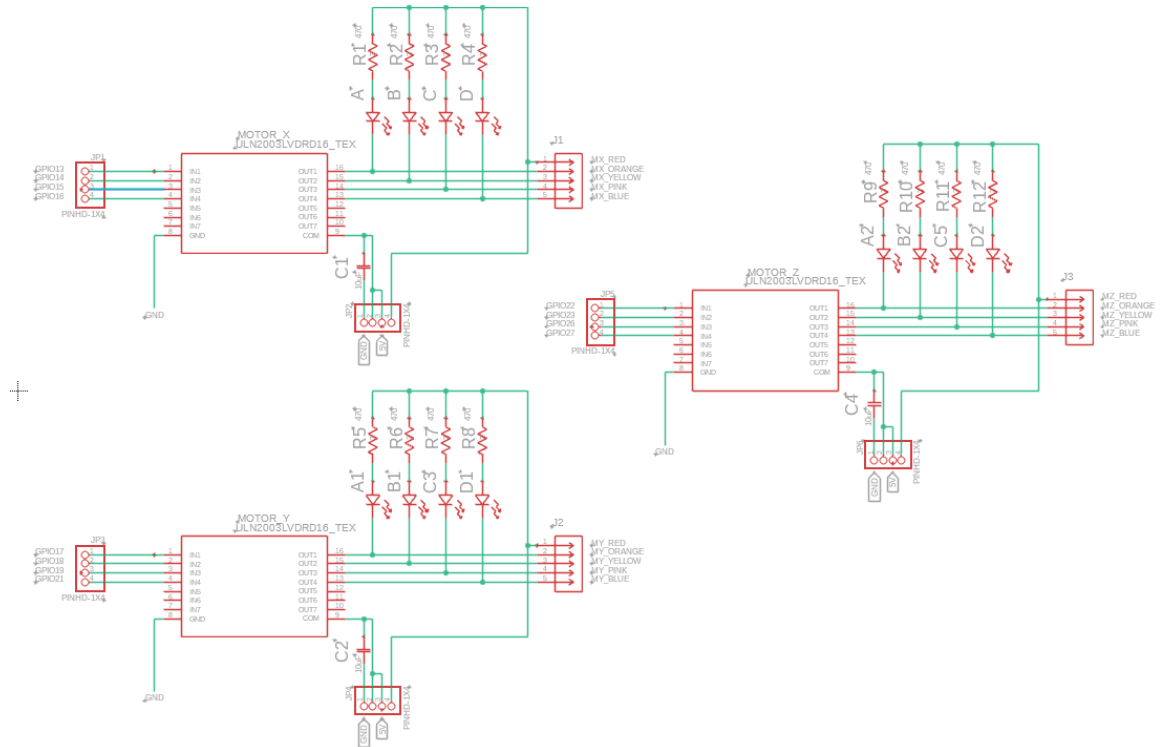
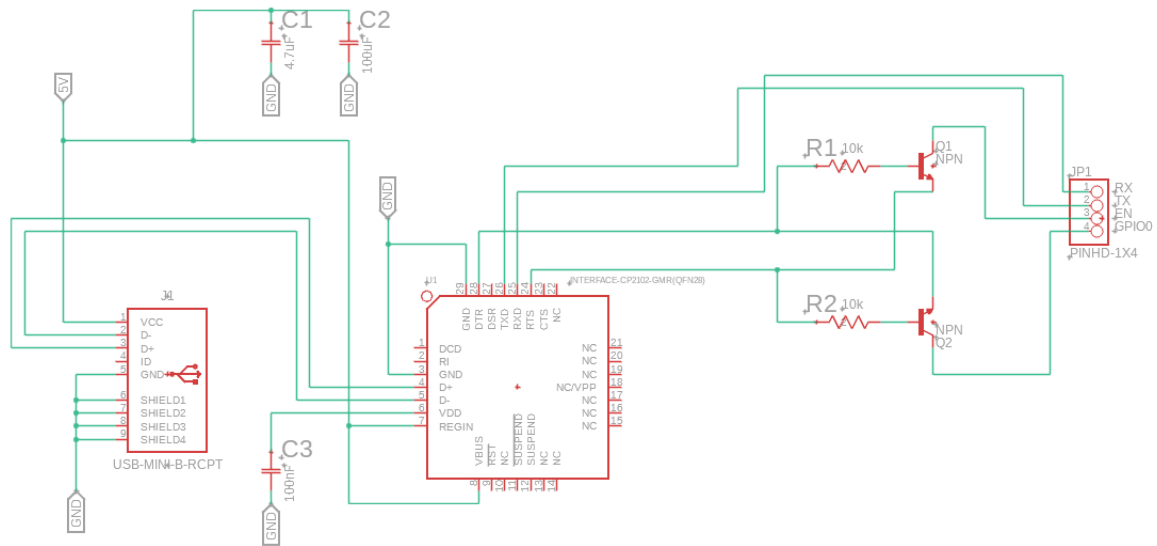


Figure 11: 3 Motor controller units as per project scope

6.4 UART-USB Converter

This schematic is a USB-to-UART interface based on the CP2102-GMR chip, designed to allow serial communication and programming of the ESP32. A Mini-USB connector (J4) brings in the 5V supply and USB data lines (D+ and D-), which are routed to the CP2102. The chip handles USB-to-serial conversion and outputs UART TX and RX signals. Power stabilization is provided by decoupling capacitors (C1, C2, and C3), and the CP2102's internal regulator outputs 3.3V to power its core logic. The header (JP1) provides UART TX/RX along with EN and GPIO0 lines, which are pulled low using two NPN transistors (Q1 and Q2) when triggered by the CP2102's GPIO pins. These transistors, driven through 10kΩ base resistors (R1 and R2), automate the reset and boot mode for devices like the ESP32, enabling one-click programming without manual button presses. Overall, the design follows standard recommendations from the CP2102 datasheet for reliable USB-UART interfacing with automatic control of boot and reset.



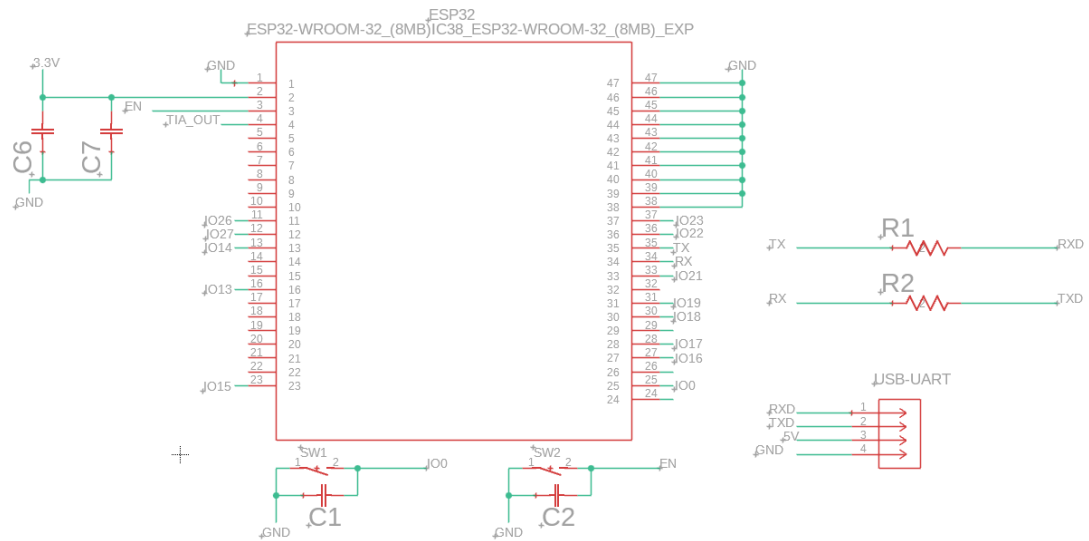


Figure 13: MCU Schematic

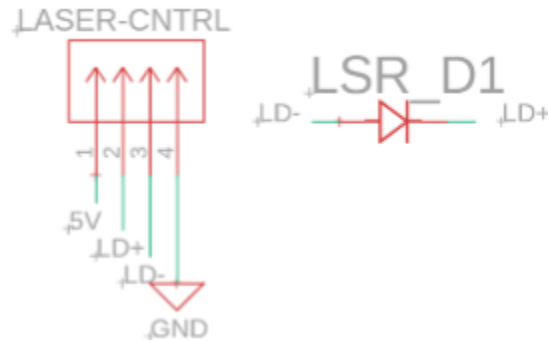


Figure 14: Laser Controller Connections

6.6 Overall Schematic Design

6.6.1 Low Level System Block Diagram

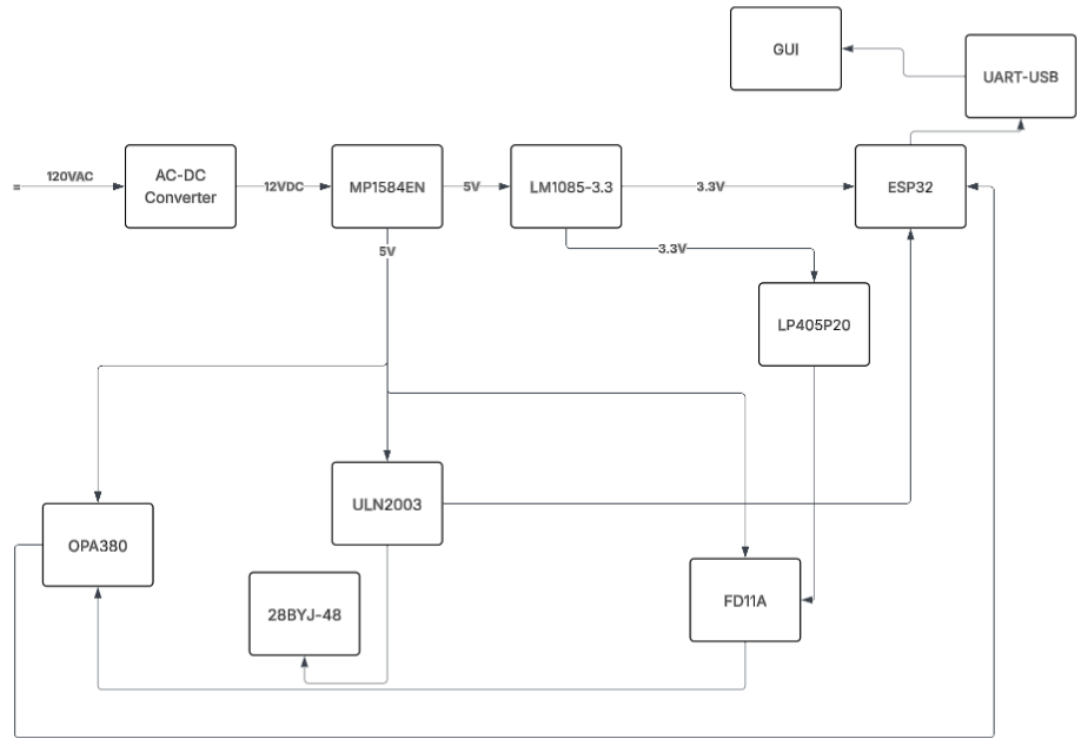


Figure 15: Low Level System Block Diagram

6.6.2 System Schematic

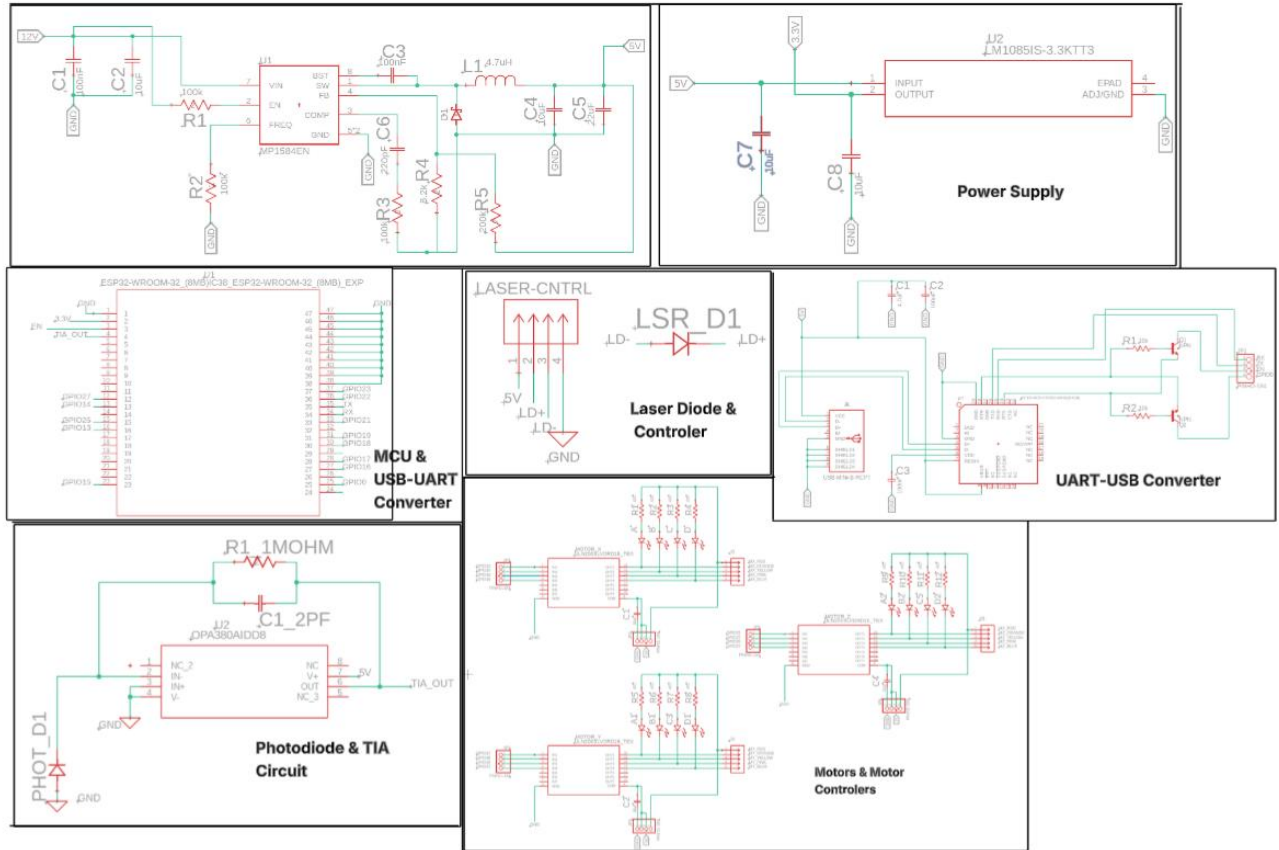


Figure 16: System Schematic

7. Software Design

When working with the software side of the project there are 3 general areas that we need to program. The first part is that the microscope requires that we move the stage accordingly on the three major axis. This movement is significant for capturing the height / roughness of one spot on the object. Moving the stage would then move the object to get a different point. The second part of the project would be gathering data from a transimpedance amplifier (TIA). The data that comes from the TIA is significant because the value that we get from this device would essentially define how high or low the surface of the new point of the object is. The final part of the project would be computer side where the user would interact with the microscope (UI / GUI) and the analysis of gathered data from the TIA.

7.1 MCU Programming

7.1.1 Delta Stage Movement

The OpenFlexure Delta Stage represents a compact and precise motion control platform commonly used in microscopy and micro-positioning applications. Unlike traditional Cartesian positioning systems that utilize orthogonally aligned linear actuators to move in the X, Y, and Z directions independently, a delta stage achieves three-dimensional motion through the coordinated actuation of three vertically mounted stepper motors. These motors, arranged in a triangular configuration, control the vertical displacement of flexure-based arms that, in turn, manipulate the central stage platform.

The defining characteristic of the delta stage is that it lacks a one-to-one correspondence between actuators and spatial axes. Instead, each of the three motors contributes partially to motion in all three spatial dimensions. Vertical motion along the Z-axis is achieved by simultaneously actuating all three motors in the same direction. Conversely, lateral displacements in the X and Y directions are the result of differential movement among the three motors. This geometric coupling necessitates a kinematic transformation to convert target spatial coordinates into specific motor commands. Therefore, controlling a delta stage requires the use of inverse kinematics algorithms to compute the individual actuator movements necessary to achieve a desired XYZ translation of the stage's platform.

To implement this control logic, the ESP32 microcontroller serves as an efficient and capable platform. The ESP32 features sufficient GPIO resources and computational power to simultaneously control three stepper motors, perform real-time kinematic calculations, and manage communication interfaces for external control or data reporting. The stepper motors commonly used in low-cost delta stages, such as the 28BYJ-48 in combination with ULN2003 driver boards, require four GPIO pins per motor to perform stepping operations. Thus, the ESP32 must manage a total of twelve GPIO outputs to independently control each of the three actuators.

$$\begin{bmatrix} x \\ y \\ z \end{bmatrix} = \begin{bmatrix} -\cos(30) & \cos(30) & 0 \\ \cos(60) & \cos(60) & -1 \\ 1 & 1 & 1 \end{bmatrix} \begin{bmatrix} a \\ b \\ c \end{bmatrix}$$

The equation above is the main matrix used for processing the movement for the stage to move. The firmware would receive XYZ values and translate them into coordinated abc motor movements.

The control process begins by receiving a target position, either hardcoded or provided via a communication interface (e.g., serial or Wi-Fi). Upon receiving a target position in the form of spatial coordinates (X, Y, Z), the ESP32 performs inverse kinematic calculations based on the physical geometry of the delta mechanism. These calculations yield the required displacement—expressed in motor steps—for each actuator. The controller then generates the appropriate sequence of coil energizations for each stepper motor, adhering to the selected stepping mode (full-step, half-step, or wave drive). The motors are stepped in a synchronized fashion to ensure smooth and coordinated motion of the stage.

To ensure precision and reliability, the system may be further enhanced with optional features such as acceleration profiles, homing routines using limit switches, or closed-loop feedback mechanisms.

The diagram below illustrates how the typical scanning process will be performed. The application would initialize the stage at the origin point. Here there will be calibrations at the Z axis trying to determine the height of the elevation (the roughness) by the TIA. Once this point is documented the X and Y axis will move accordingly to the next point to repeat the process of changing the Z axis.

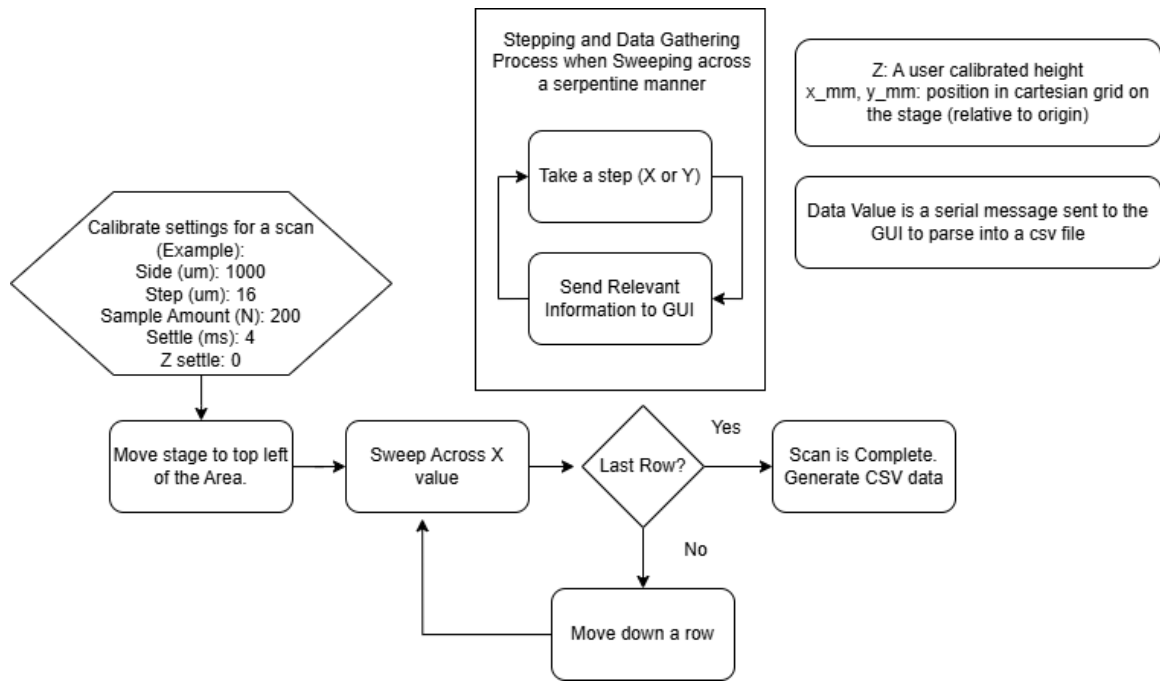


Figure 17: Object Scanning Process

7.1.2 ADC Data Gathering

The ESP32 microcontroller is responsible for collecting analog voltage data from the output of a transimpedance amplifier (TIA). The TIA is used in this project to convert the small current generated by a photodiode into a readable voltage signal. This voltage signal represents the amount of light the photodiode detects and is connected to one of the ESP32's analog input pins.

The ESP32 comes with built-in analog-to-digital converters (ADCs) that allow it to read voltages and convert them into digital values. These digital values range from 0 to 4095, corresponding to a voltage range from 0 volts to approximately 3.3 volts. In this setup, one of the input-only pins on the ESP32 is used to receive the voltage signal from the

TIA. This pin is ideal because it is designed for input and has good performance with the ADC system.

To collect data, the ESP32 regularly samples the voltage signal at a fixed time interval. For example, the ESP32 can be programmed to take a reading every 10 milliseconds. Each time it takes a reading, it stores or transmits the result, depending on the system's design. These readings are then converted into actual voltage values using a simple formula that relates the raw ADC number to the voltage scale.¹²

Since analog signals can be affected by electrical noise, especially when working with sensitive components like photodiodes and TIAs, it is common to apply basic filtering. One approach is to take the average of several readings to reduce random noise. Another is to apply a software-based filter to smooth out sudden changes. These techniques help make the collected data more accurate and reliable.

7.2 Computer Side

The software element on the computer side is quite different compared to the elements in the microcontroller. There are different languages and IDE that will be used to facilitate data collection and the creation of the graphical user interface.

7.2.1 Data Collection

Once the ESP32 gathers the voltage data from the transimpedance amplifier (TIA), the next step is to send this information to a computer for further analysis. This is done through a USB connection using the ESP32's built-in serial communication feature. The microcontroller transmits the data as a continuous stream of information, which is received by the computer using a terminal program or a custom data logging interface.

Each piece of data sent includes not just the voltage reading from the TIA, but also the corresponding X, Y, and Z coordinates of the location where the reading was taken. These coordinates are typically provided by the movement of a stepper motor system that positions either the sensor or the object being scanned. By combining the positional data with the voltage reading, each data point represents a specific location on the surface of the object.

As the ESP32 moves across the object's surface, it collects a series of voltage measurements, each tagged with its own position in space. This forms a complete set of three-dimensional data. The voltage values can be interpreted as either elevated or recessed areas, depending on how the TIA responds to the reflected or transmitted light. Higher or lower voltages suggest changes in surface characteristics, such as height differences, roughness, or slopes.

This continuous stream of voltage and coordinate data is stored on the computer and used to generate a visual representation of the object's surface. When plotted, the collection of data points forms a map that can be used to create a heat map or 3D surface image. Areas with higher voltage values may appear as peaks, while lower values may represent valleys or dips. This process provides insight into the topography and structure of the scanned surface, allowing for both qualitative and quantitative analysis.

x_mm	y_mm	z_mm	raw	mv	conv_us	v	idx	total	timestamp_ms
-0.5	0.5	0	2193	1921	45	1921	1	2601	5687
-0.48	0.5	0	2195	1920	41	1920	2	2601	5899
-0.46	0.5	0	2196	1919	42	1919	3	2601	6104
-0.44	0.5	0	2192	1921	42	1921	4	2601	6317
-0.42	0.5	0	2192	1922	42	1922	5	2601	6521
-0.4	0.5	0	2161	1923	41	1923	6	2601	6735
-0.38	0.5	0	2175	1929	42	1929	7	2601	6940
-0.36	0.5	0	2195	1920	41	1920	8	2601	7153
-0.34	0.5	0	2200	1925	42	1925	9	2601	7357
-0.32	0.5	0	2204	1925	41	1925	10	2601	7571
-0.3	0.5	0	2216	1932	42	1932	11	2601	7776
-0.28	0.5	0	2204	1920	41	1920	12	2601	7989
-0.26	0.5	0	2206	1930	42	1930	13	2601	8194
-0.24	0.5	0	2211	1933	41	1933	14	2601	8407
-0.22	0.5	0	2209	1932	42	1932	15	2601	8611
-0.2	0.5	0	2257	1921	41	1921	16	2601	8826
-0.18	0.5	0	2160	1892	42	1892	17	2601	9030
-0.16	0.5	0	2194	1916	42	1916	18	2601	9244
-0.14	0.5	0	2192	1916	42	1916	19	2601	9447
-0.12	0.5	0	2187	1913	41	1913	20	2601	9661
-0.1	0.5	0	2181	1911	42	1911	21	2601	9867
-0.08	0.5	0	2181	1918	42	1918	22	2601	10080
-0.06	0.5	0	2207	1933	42	1933	23	2601	10284
-0.04	0.5	0	2210	1933	41	1933	24	2601	10495
-0.02	0.5	0	2153	1883	41	1883	25	2601	10699

Figure 18: CSV Data Tabulation

The figure above is how the data is organized after collecting data. Once the ESP32 moves the stage to a new position (x_mm, y_mm, z_mm) it begins to collect N amount ADC values (raw, mv, conv_us, v) averaged across the amount. After collecting it would send the position values along with ADC and debugging values (x_mm, y_mm, z_mm, raw, mv, conv_us, v, idx, total, timestamp_ms) to the GUI through serial communication. The csv that gets produced from the scanning process is what makes the image.

7.2.2 Graphical User Interface (GUI)

The Graphical User Interface (GUI) for this project is developed using the Java programming language within the Eclipse IDE. Java was chosen because of its wide platform compatibility, strong support for graphical interfaces through libraries such as Swing and JavaFX, and its object-oriented structure, which makes it easier to manage complex behaviors like scanning, stage control, and data handling. Java is also known for its portability, allowing the GUI application to run on different operating systems such as Windows, macOS, or Linux without major changes to the codebase.

Eclipse was selected as the development environment because it provides powerful tools for building Java applications. These tools include project management features, built-in

debugging, and GUI design support. Eclipse also integrates well with version control systems, making it easier to manage updates and collaborate if needed. By using Eclipse, the development process is more streamlined, and any issues in the code can be identified and fixed more efficiently through features like syntax highlighting and step-by-step debugging.

The Graphical User Interface in this project is designed to manage and visualize the data collection process between the ESP32 and the computer. Its main role is to allow users to control the scanning sequence and observe the data in a structured and organized way.

One of the primary functions of the GUI is to perform calibration. Before scanning begins, the user can initiate a calibration step that moves the scanning stage to the top-left corner of the object. This position is treated as the origin, or starting point, for the scan. From this location, the stage follows a square-like scanning pattern, moving row by row across the surface of the object. This structured movement ensures that each reading corresponds to a specific position on the object, making the data easier to process and visualize.

The GUI also provides a setting to adjust the speed of the scanning process. If scanning the entire surface at full resolution takes too long, users can enable an option to skip certain points in the scan. This feature is useful for creating a quicker scan when full detail is not necessary or when the user is only interested in general surface trends. This approach creates a smoother, faster scanning experience while still generating a usable surface map.

To maintain user control, the GUI includes simple settings that allow the user to enable or disable fast scanning, adjust how many points are skipped, and begin or stop a scan. Once the scan is complete, the data is processed and can be displayed or exported for further analysis. While the full visual rendering of a heat map or 3D surface may be added in future improvements, the current GUI focuses on structured data collection and providing users with efficient ways to control the scanning process.

7.3 Diagrams

7.3.1 Flowchart

The flowchart diagram visually represents the operational sequence of the scanning system from start to finish. It outlines the step-by-step process executed by both the GUI and the ESP32 microcontroller, emphasizing the interaction between system components and the logical decisions that guide the scanning behavior.

The flow begins with the System Initialization stage, which represents the startup of both the computer interface (GUI) and the embedded ESP32 system. At this point, communication between the ESP32 and the GUI is established, and the system prepares to receive user commands. Once initialized, the flow proceeds to the Calibrate Stage block. This operation is initiated from the GUI and instructs the ESP32 to move the scanning stage to the top-left corner of the object. This position is set as the origin point (0,0) for the scan, ensuring consistency across all subsequent movements.

After calibration, the system reaches the first decision point: “Scan Object?” This block represents user input, typically in the form of a “Start Scan” button on the GUI. If the user chooses not to proceed, the flow exits to an End block, halting further activity. However, if scanning is approved, the flow continues to the next decision: “Fast Scan Mode?”

This second decision determines the resolution and speed of the scan. If the user has selected Fast Scan Mode, the ESP32 will follow a reduced scanning pattern by skipping designated coordinates to shorten scan duration. In this case, the system jumps directly to the Perform Fast Scan block. Here, the ESP32 moves in larger steps across the scanning grid and collects voltage readings at fewer points. Once completed, the scan data is sent to the computer, and the flow proceeds to the End block.

If Fast Scan Mode is not selected, the system follows the path to Perform Full Scan. In this mode, the ESP32 moves across the surface in smaller, evenly spaced increments—typically point-by-point—and takes a voltage reading at each position. These readings, along with their corresponding X, Y, and Z coordinates, are sent back to the computer. This results in a higher-resolution dataset that more accurately represents the topography of the scanned object.

In both scanning paths, after data is collected, the ESP32 performs a Data Transmission step, sending the collected information to the GUI over the serial connection. The computer processes this data for visualization or storage. Finally, the process reaches the End block, marking the completion of the scanning cycle.

This flowchart provides a clear overview of how the system behaves based on user inputs and scanning settings. It highlights the modular and decision-driven nature of the software design, making it easier to understand, test, and modify as the project evolves.

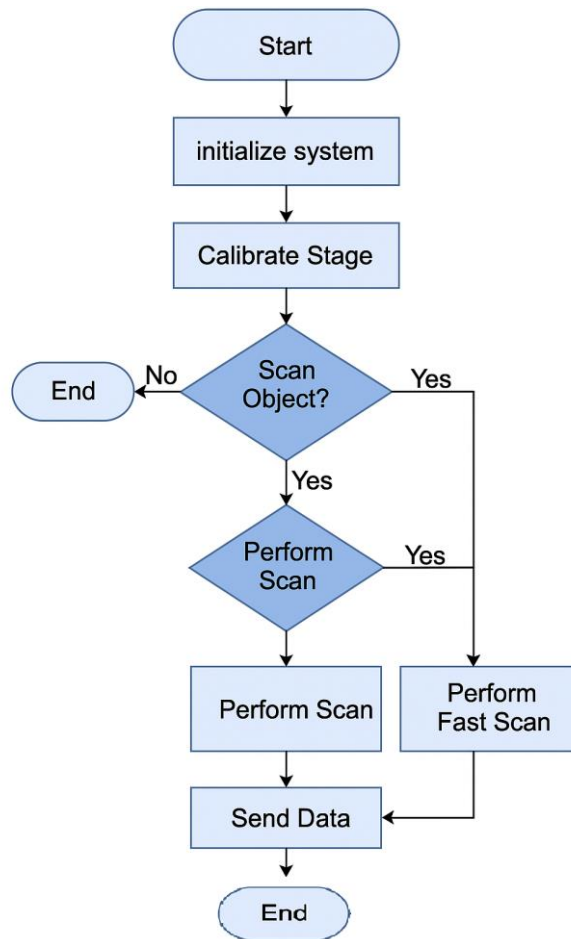


Figure 19: Flowchart Diagram

7.3.2 UI Mockup Drawing

The user interface (UI) mockup represents the visual and functional layout of the desktop application used to control and monitor the scanning process. It is designed with simplicity, clarity, and practicality in mind, ensuring that users can interact with the system efficiently while maintaining full awareness of the scanning status. The mockup demonstrates a balance between user control and data visualization.

At the center of the UI is a large display panel reserved for the heat map visualization. This panel dynamically renders the scanned data as it is received from the ESP32. Each data point is plotted based on its X and Y coordinates, with color representing the measured voltage value. The resulting image provides a visual map of the scanned object's surface, where different colors correspond to different elevations or surface intensities. This allows the user to easily detect raised or recessed features based on shading or color gradients.

Positioned to the side or bottom of the heatmap are a series of interactive buttons that control the system's functionality. These include:

Calibrate – Initiates the calibration sequence, commanding the ESP32 to move the scanning stage to the top-left origin of the object. This button must be pressed before any scanning can begin.

Start – Begins the scanning process using the current scan settings. Once pressed, the ESP32 will move across the scanning grid, collect voltage data, and transmit it to the GUI for display.

Speed: Normal / Fast – This toggle button allows users to switch between standard full-resolution scanning and Fast Scan Mode. When fast mode is selected, the system will skip points in the scan to reduce the total time, and the GUI will use interpolation to estimate the missing data.

Enable Interpolation – A dedicated toggle that allows users to turn interpolation on or off independently. When enabled, the GUI will fill in skipped areas using estimation techniques to maintain a continuous and readable map even when fewer data points are collected.

Each button is clearly labeled and spaced to prevent user confusion. The layout emphasizes ease of access, ensuring that important actions are always visible and ready to use. The mockup also assumes a neutral color palette (such as grays and whites) for the background, with more vibrant colors used in the heatmap to highlight data patterns and anomalies.

The overall design of the GUI mockup promotes a user-friendly experience by minimizing clutter and presenting controls in a logical sequence. The interface guides the user through a simple workflow: calibrate, configure, scan, and observe. Its modular structure also allows for future improvements, such as adding export options, scan history, or 3D rendering capabilities, without disrupting the main user experience.

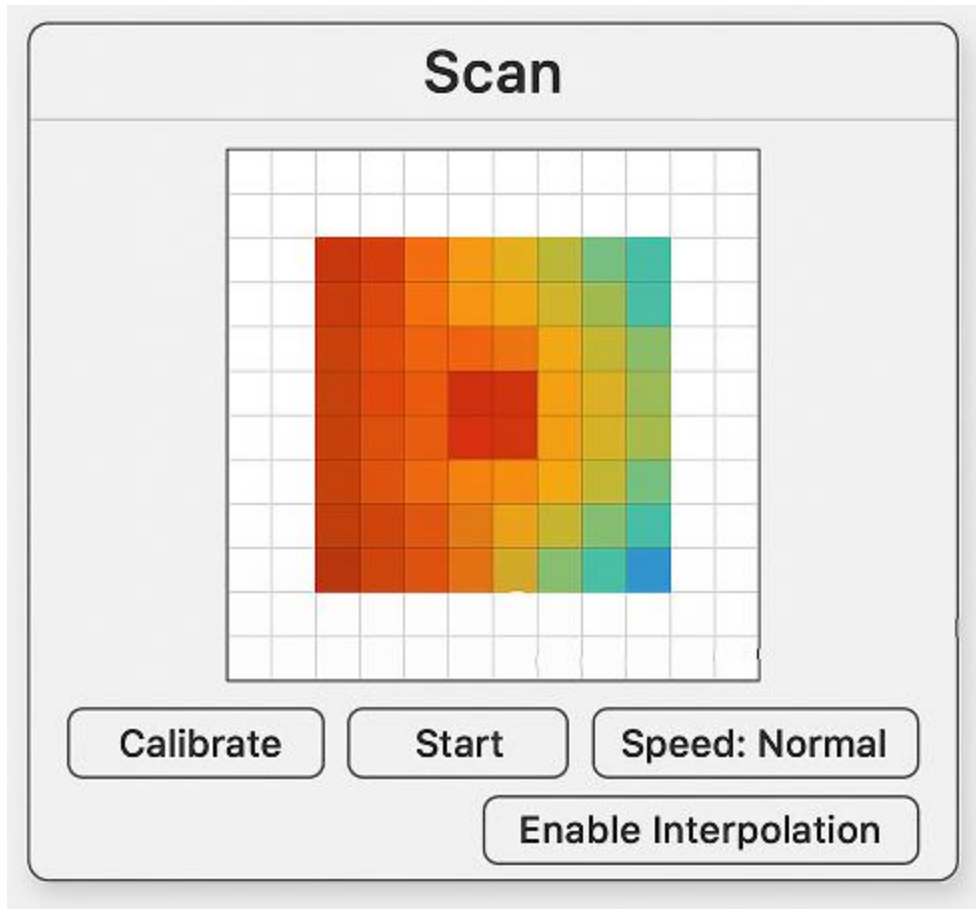
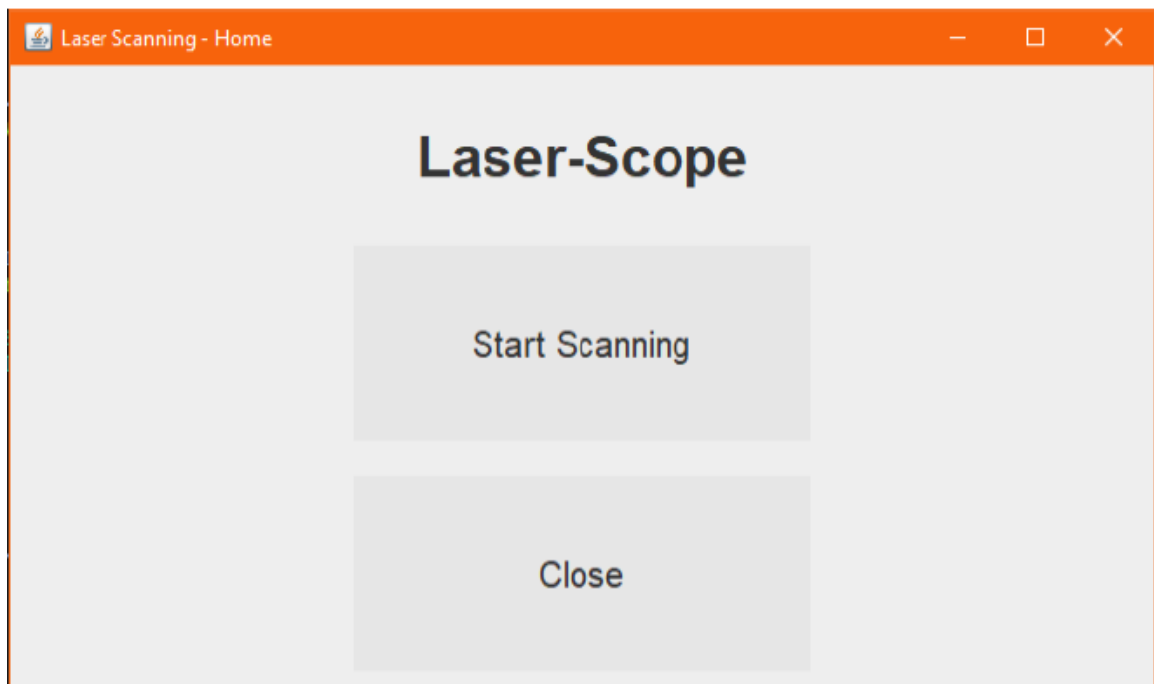


Figure 20: First Iteration Idea



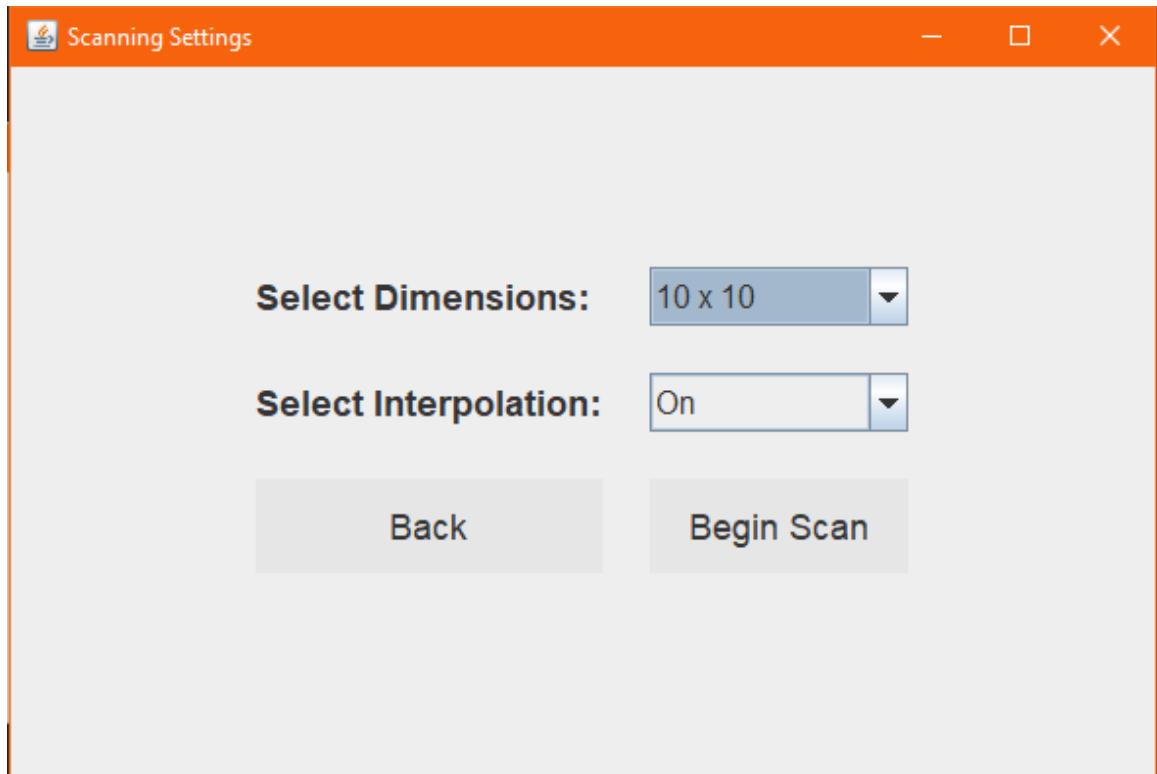


Figure 21: Home and Scanning Screen Mockup Second Iteration

The final iteration of the GUI had considerable changes. This is due to adding settings for the stage, image generation, and adding statistics for the user to see.

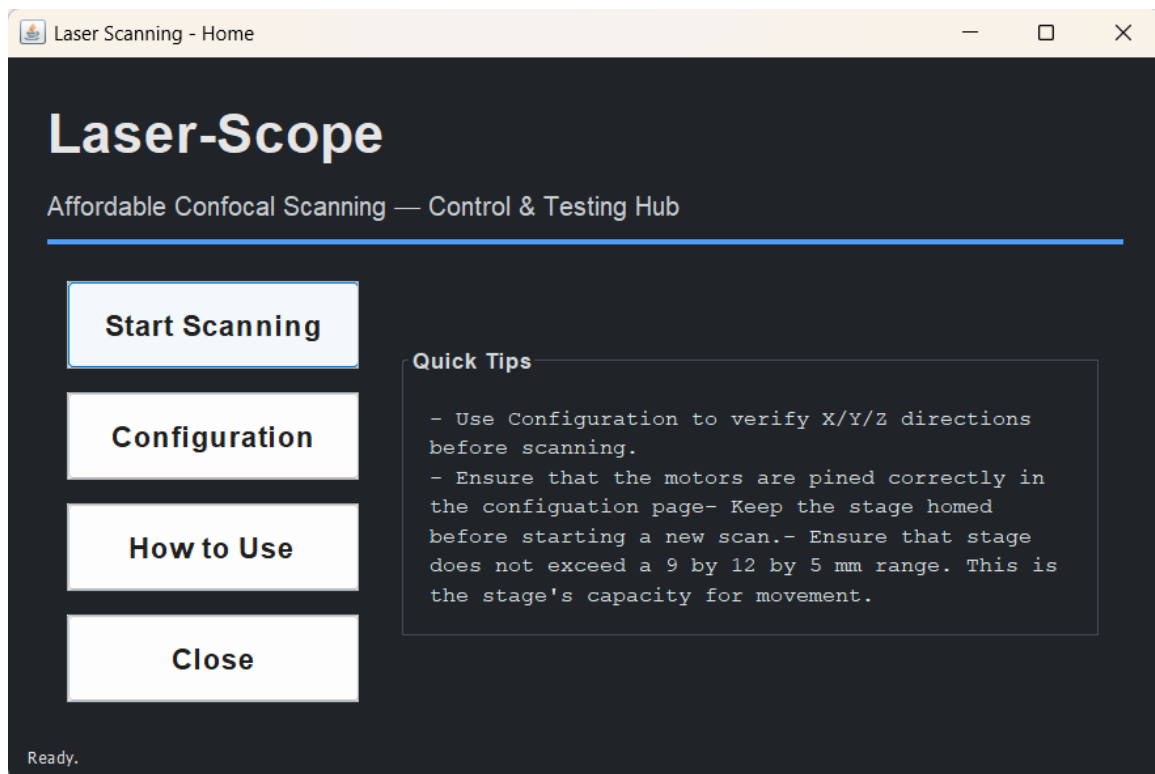


Figure 22: Home Page

The home page has various buttons (“Start Scanning”, “Configuration”, and “How to Use”) that take you to different parts of the application.

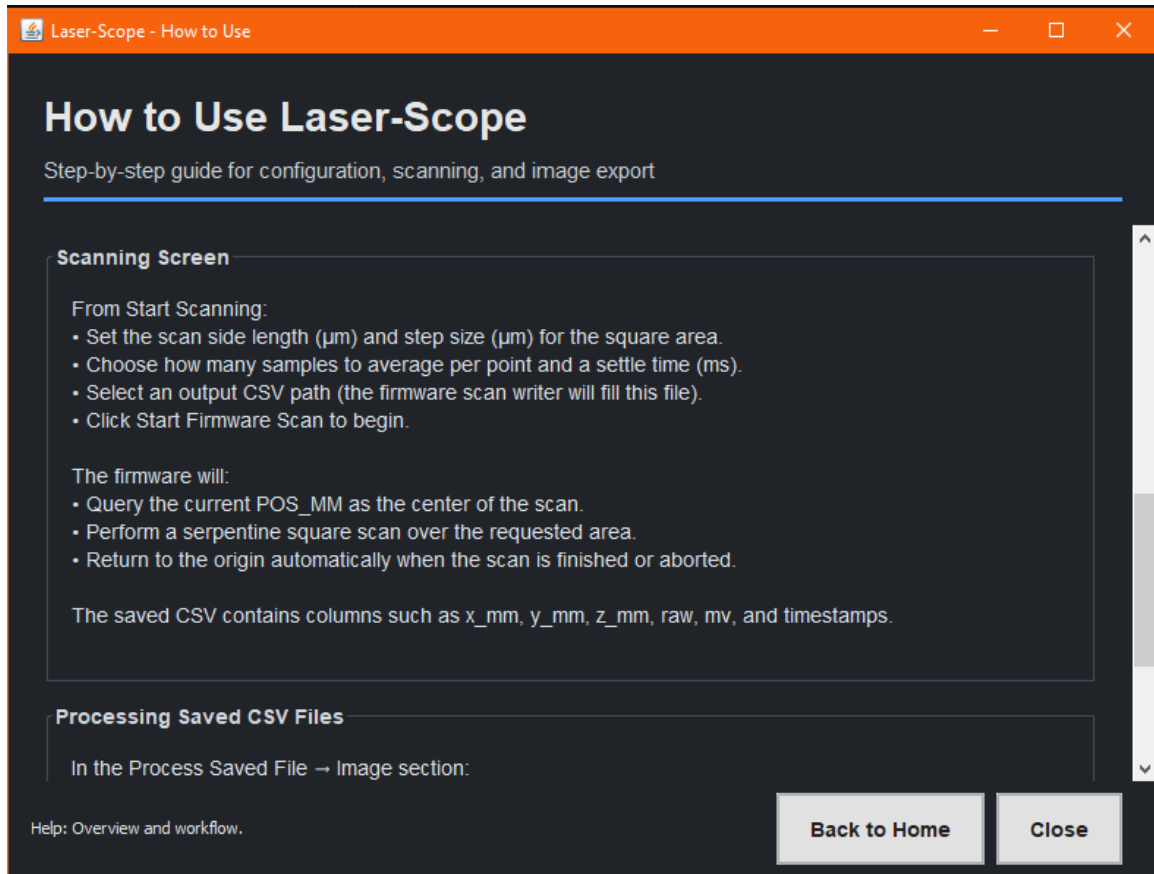


Figure 23: How to Use page

This is the “how to use” page, the user can navigate through this page to understand how to use this application.

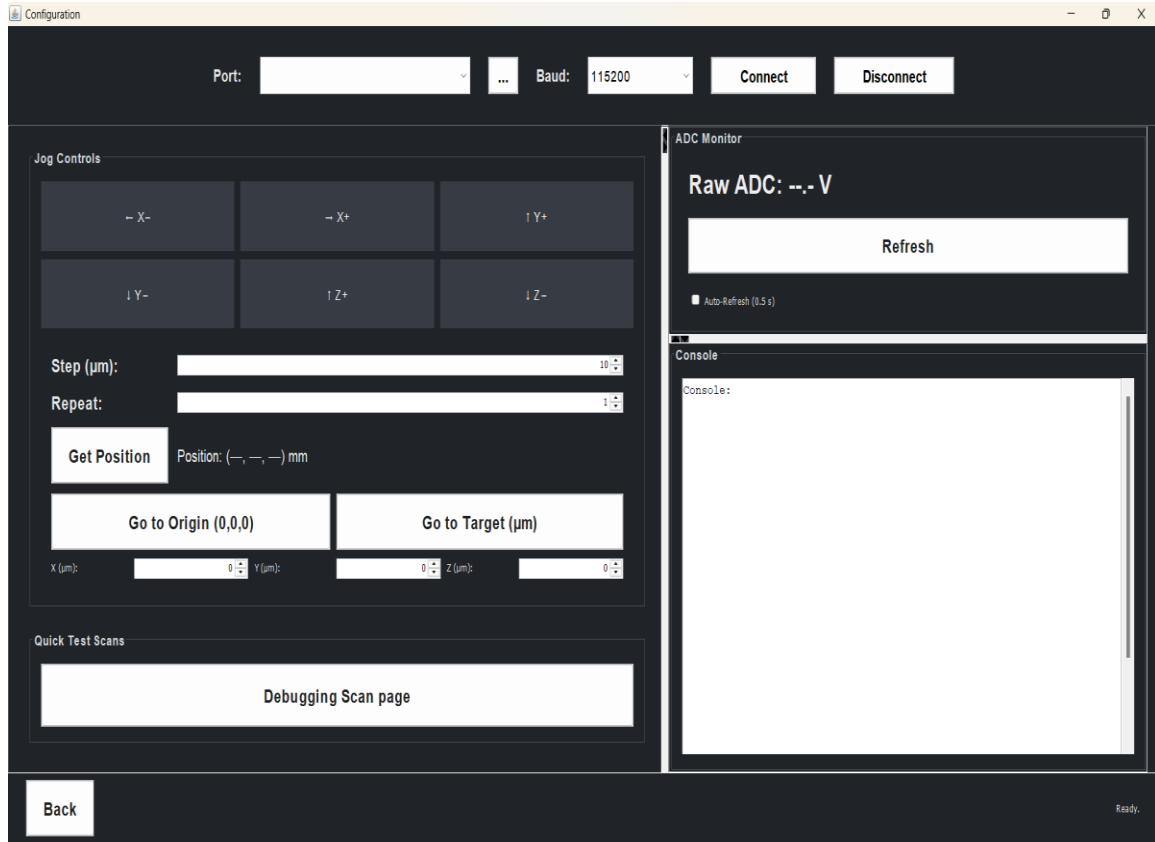


Figure 24: Configuration Page

This is the configuration page, this allow you to connect to the ESP32, configure the stage, see the serial output of MCU, read the ADC monitor , and have access to the debugging section. The first step upon landing on this page would be to connect to the ESP32 by selecting the proper com port and baud rate.

The user can control the stage using the jog controls. By inputting a step value and pressing a button in the cardinal direction it would move the stage in that direction. The other buttons in this card is as follows, “Get Position” which allows to user to see where the stage is relative to the start of the program. “Go to Origin” is a simple button that moves the stage to the original position of the stage upon boot up, essentially reversing any action the user has made. “Go to Target” is where the user can set up a cartesian value and it allows for the stage to move to that point.

ADC monitor and Console are features that the user can use to see what are the ADC values are and what serial prints the ESP32 has made to perform certain actions.

Scanning

[Back to Configuration](#) Scanning

Firmware Scan (Square Area)

Scan Area (square): Side (μm):

Step (μm): Samples/pt:

Settle (ms): Z-Safe (mm):

Output CSV: [Bro...](#)

[Start Firmware Scan](#) [Abort](#) ETA: — Per-point: —

Pseudo Scan (ADC \rightarrow CSV)

Output file: [Browse...](#)

Sample period (ms):

[Start](#) [Stop](#) Lines: 0

Ready.

Z-Line Calibration Scan (Z_LINE_SCAN)

Output CSV: [Browse...](#)

Samples per height:

[Run Z-Line Scan](#) [Generate Gradient Bar](#)

Runs the firmware Z_LINE_SCAN routine at (0,0).
 The stage moves from -200 μm to +200 μm in +5 μm Z steps.
 At each height it averages N ADC samples and writes CSV rows:
 0,0,z_um,avg_mv
 At the end the firmware returns to (0,0,0).

Process Saved File \rightarrow Image

Input CSV: [Browse...](#)

Colormap: Value column:

Ready.

Figure 25: Debugging Scan Page

The figures above are the features in the “Debugging Scan” page. Firmware scan card is where the user can change the setting of a scan to produce certain images. “Step size” is a value that tells the MCU how far the stage should move to get the next point. “Sample” is how many ADC values we are averaging (allows for the reduction of noise). “Settle ms” is the time it takes for the ESP32 to wait before collecting ADC values. “Z-safe” is the

distance value to allow for the sample to have clearance (to prevent bumping the sample with the objective). When the user is satisfied with the settings, clicking on the browse button will prompt the user to name and save the CSV file to a location. When the file is saved the user can start a scan.

The Pseudo Scan is a one-dimensional scan feature that gathers ADC values at one point. Changing the sample period to a lower number increases the speed at which we get points. This can be used for calculating the signal to noise ratio.

Z-line calibration card is a feature that performs a sweep of the sample in the Z direction. This would allow for finding the relative surface topography of the sample. Typically, this function would be used for different types of samples. The samples buttons allow for more values to be averaged across the scan to reduce noise. The user would save the CSV file to a location and perform a scan across a 400-micron range (-200 down to 200 above the origin) attributing a value of mV to each increment of 5 microns (81 entries would be on the CSV).

Process Saved File card is where the user can select a saved CSV file and produce an image. Clicking the browse button prompts the user to select any CSV file. The colormap setting lets the user switch the color style of the (purely a preferential feature). The value column allows the user to choose which column of the CSV to make the image.

The screenshot displays the 'Laser-Scope — Scanning Hub' application window. At the top, there are fields for 'Port' and 'Baud' (set to 115200), along with 'Connect' and 'Disconnect' buttons. Below this is a section titled '2) Configure & Run Scan'. It contains five sliders for 'Scan Size (µm)' (set to 1,000), 'Step (µm)' (set to 16), 'Samples/pt' (set to 200), 'Settle (ms)' (set to 4), and 'Z-Safe (mm)' (set to 0). Underneath these sliders is an 'Output CSV' field with a 'Browse...' button. Below that are 'Start Scan' and 'Abort' buttons, followed by a progress bar and labels for 'ETA: --' and 'Per-point: --'. The bottom section is titled 'Process Saved File → Image'. It includes an 'Input CSV:' field with a 'Browse...' button, a 'Colormap:' dropdown menu (currently set to 'grayscale'), and a 'Value:' dropdown menu (currently set to 'mv').

Figure 26: Scanning Page

From the “Home Page” to this “Scanning Page” is where the user can immediately perform a scan. This page assumes that the stage is perfectly calibrated to the user’s settings. The settings in this page are similar to “Debugging Scan” page.

7.3.3 UI Navigation Flow

The UI navigation flow diagram represents how the typical engagement with the application is suppose to go. Upon starting the application the user would have access to the home page. This page has a simple layout that would only have two options to close the application and to start a new scan. Upon clicking the button it would take us to the next page the Scan Page.

Before directing us to the scanning page, it would provide an important initialization steps before we make any scans. The first thing it accounts for is if there is an connection to our MCU, if this failed a prompt would tell the user that there isn't an ESP32 connected. If there is an ESP32 connected, it would initialize the motors to the starting point on the stage. Finally, it would check to see if we have readings with the TIA.

The Scan Page has a couple of selections and buttons to engage with. The first one is self explanatory which is the home button, this will direct you back to the home page. The next two are selections that the user can click on. The dimensions option allows you to customize the dimensions of the scanning area and the interpolation option would serve to speed up scanning by skipping certain points of the scanning process. This will drop the quality of the image.

The last button "Start Scan" begins the scan of the object. Once the required inputs of setting up the dimensions and interpolation are complete the scan will begin and move on to the scanning process. Once the process is complete the user will expect to receive a PNG of image.

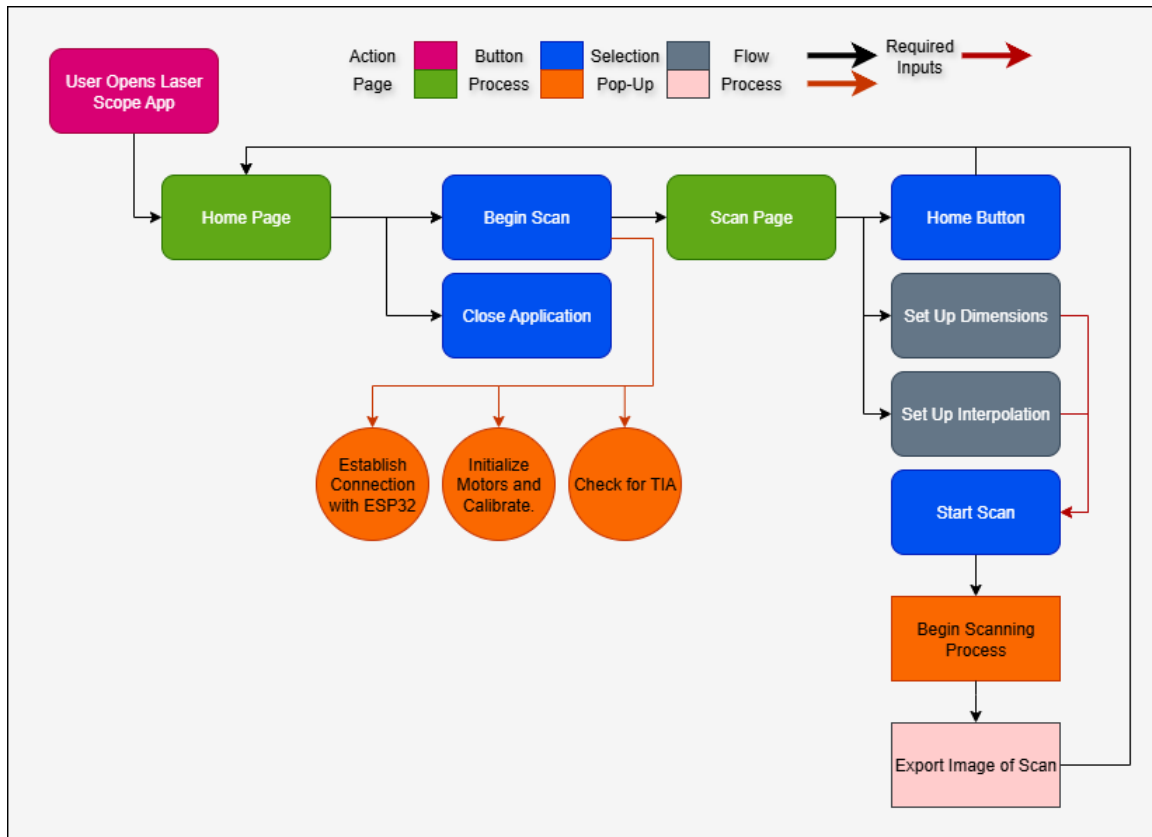


Figure 27: UI Navigation Flow

7.3.4 Use Case Diagram

The use case diagram outlines the interactions between the user and the scanning system, focusing on the functional requirements that the software must support. It serves as a high-level visual summary of the system's capabilities from the user's perspective, making it clear what actions the user can initiate and how the system responds. This diagram is especially useful for capturing the scope of the project and ensuring that the software design aligns with real-world usage scenarios.

In the diagram, the primary actor is the User, represented by a stick figure on the left-hand side. This actor interacts with the scanning system entirely through the Graphical User Interface (GUI), which communicates with the underlying ESP32 hardware. Each oval in the diagram represents a specific use case or functional feature that the user can trigger during a typical session.

The core use cases include:

- **Home Screen** – The home pages serves to allow the user to traverse through the different pages. This page goes to the scanning page and configuration page.
- **Scan Screen** – This page serves to setup and perform scans. This page utilizes various features to carry out the scanning function.

- **Configuration Screen** – This page serves to setup the stage and monitor the ESP32 stats like ADC values and serial prompts. This page utilizes various features to carry out the scanning function.
- **Scan Debugger** – This was originally made to test out the code for scanning and image generation.
- **ESP32** – Houses all the function to perform scans and stage movements. The ESP32 essentially receives its commands from the serial manager class.
- **Serial Manager** – The class that sends serial command to the ESP32 and parses data from the ESP32.
- **File System** – The manner in which the user can store and retrieve CSV files that the GUI can use to process images.

In summary, the use case diagram captures the full range of actions available to the user and maps them clearly to the system's core functionality. It confirms that the system is user-driven and highlights the flexibility and modularity built into the design. This diagram also serves as a guide for implementation and testing, helping developers ensure that all expected user interactions are properly supported.

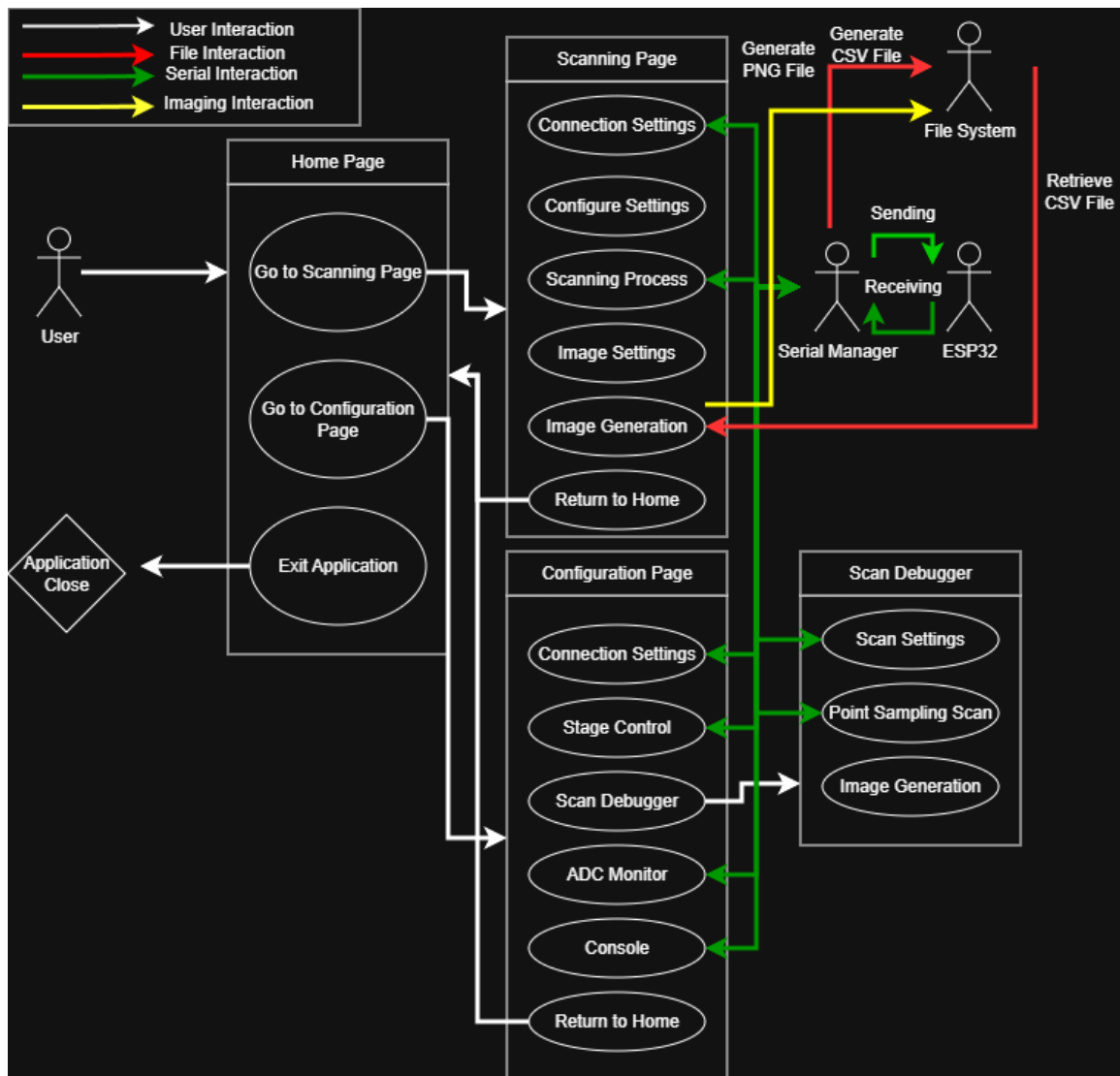


Figure 28: Use Case Diagram

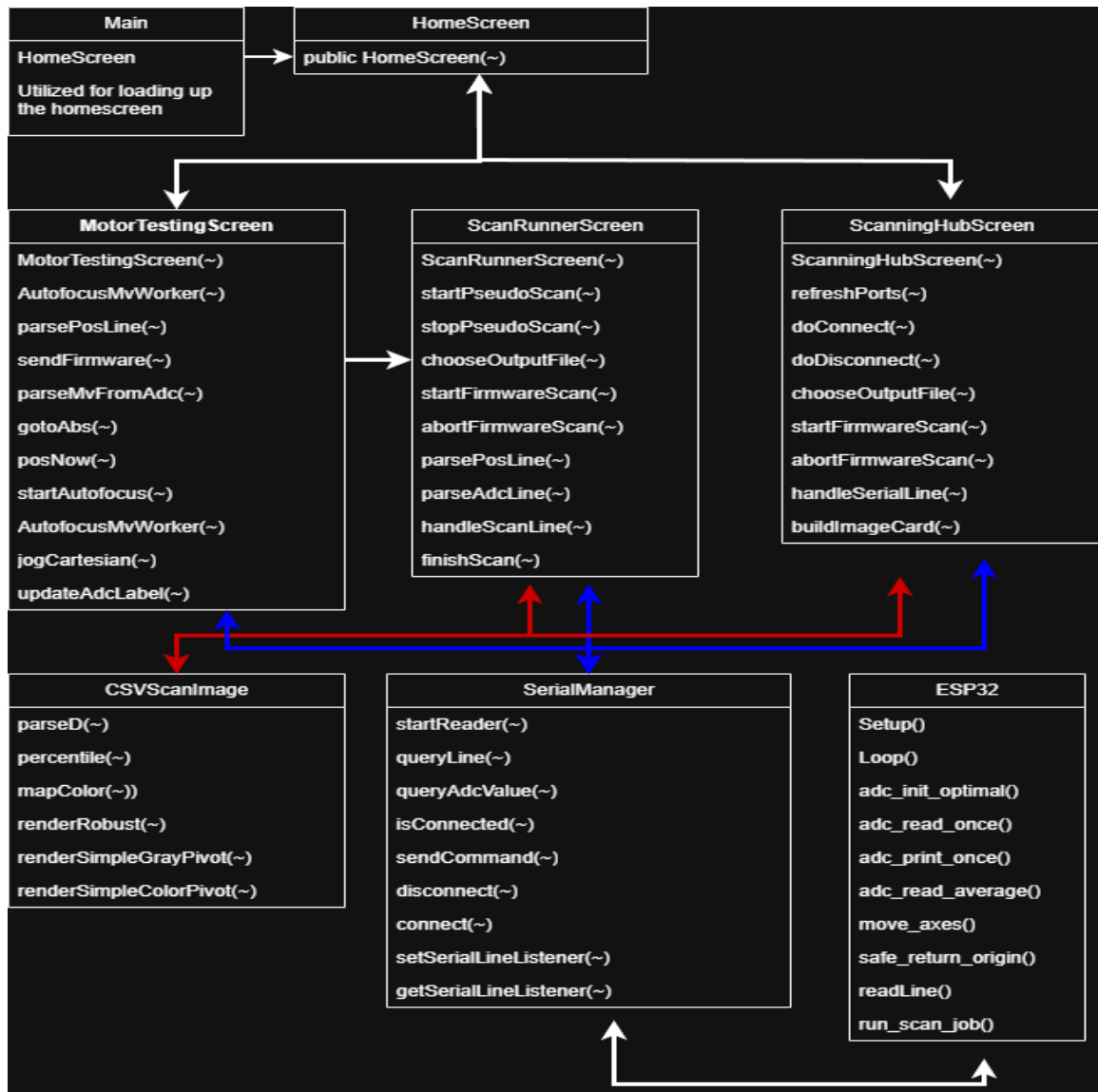


Figure 29: Class Diagram

8. System Fabrication

8.1 PCB Layout

8.1.1 5V and 3.3V Regulators

For the CLSM's PCB design it was decided to separate both regulators from the main ESP32 board. This was implemented mainly due to ease of testing, repairability but most importantly fault considerations. The trace sizes (40mil for 12V traces and 32 for 5V traces) were selected based on the expected amount of current flow. For the CLSM's input the Mean-Well LRS 50-12 will deliver ~4A at 12V (48W) wide traces are needed

for these conditions, especially the stepper motors, this is because each motor can draw 250mA per phase and up to 500mA (two phases active at a time at most at a time). Similarly, for our 3V regulator we implement the same logic, using 32mil traces for all 5V input and 24 for all outputs. This regulator will be dedicated to powering ESP32. The design of this regulator is minimal due to it being a set 3.3V regulator, therefore only bypass capacitors were added. For both regulator systems vias for thermal regulation are still being considered and will be added based on test results.

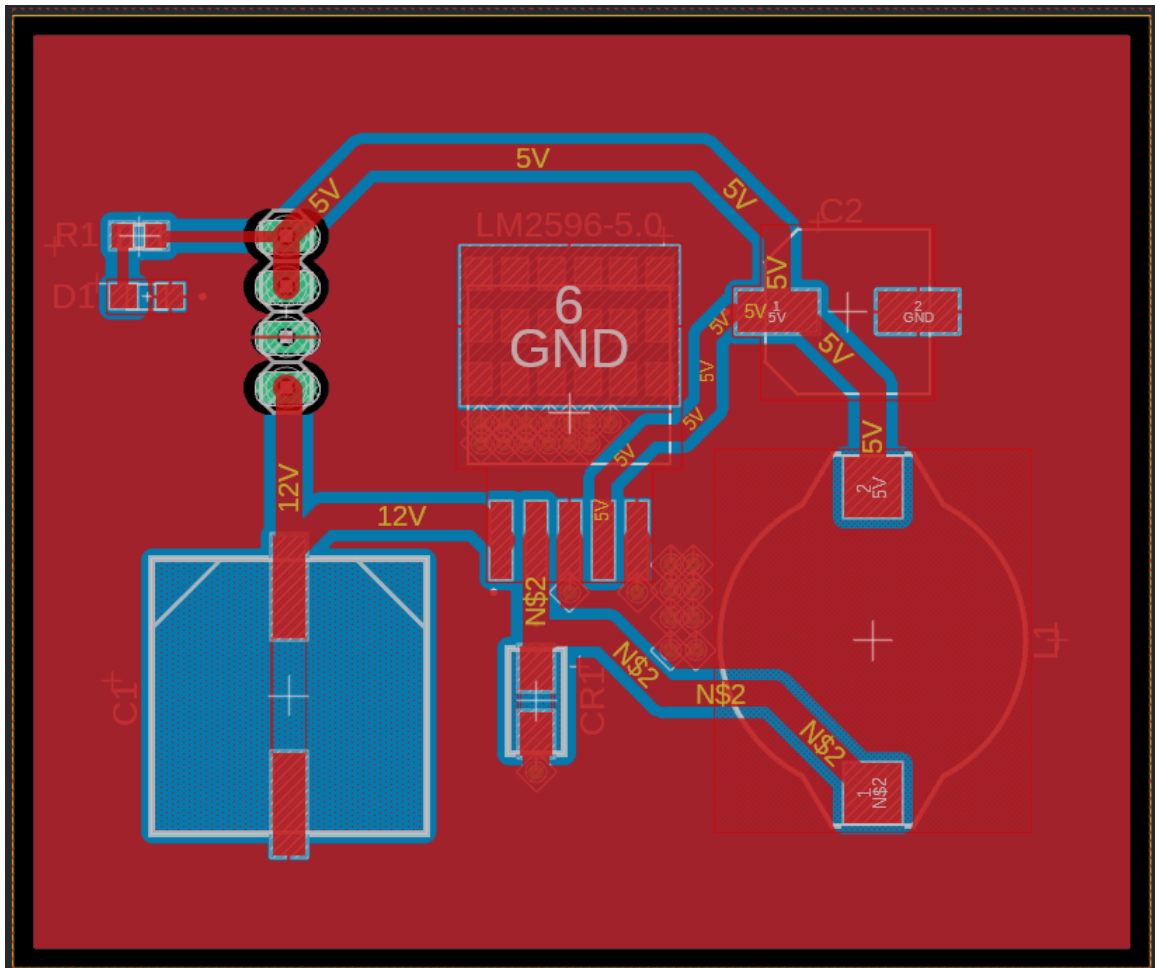
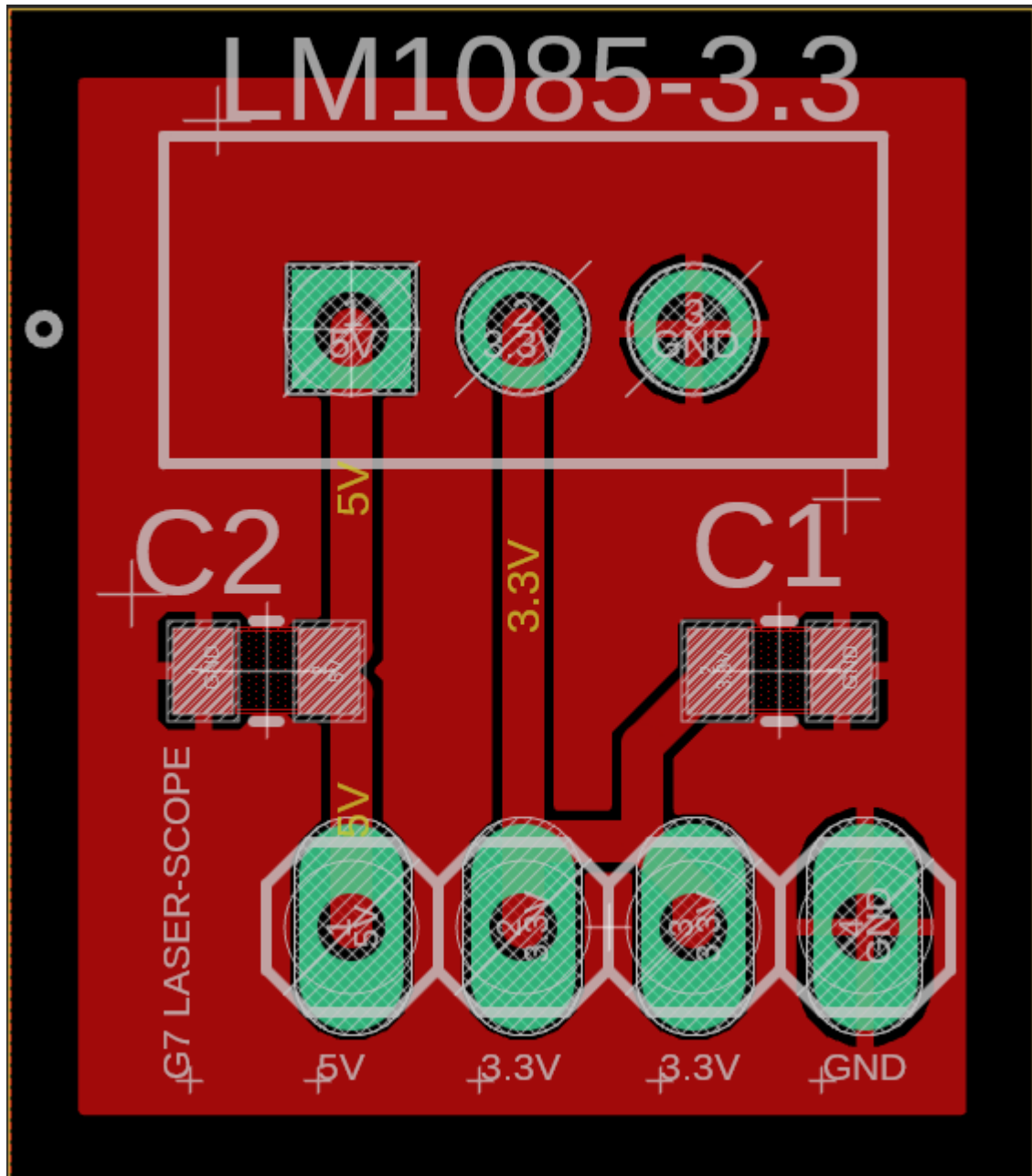


Figure 30: 5V Regulator



8.1.2 Motor Controller

For the motor controller design it was decided to separate the controller from the main board. This is due to restrictions on wiring within the selected stage. The motor controller is based off the ULN2003 driver, however, given its propensity to be damaged by minimal spikes it was decided to also keep this aspect modular, as such, a DIP-16 header was put in its place for ease of repair. Furthermore, the controller will receive its inputs from the main board onto the header pins labeled IN1-4 as well as a 5V and GND

connections via labeled pins. The inputs coming from a GPIO pin from the ESP32 board will send a high or low signal to the ULN2003 driver and it will in turn output high or low values for each phase of the motor, allowing for full control over the motor's movement. Additionally, LEDs are placed in line with each phase of the motor (labeled A,B.C and D), these are in place for ease of debugging as well as visualizing motor function.

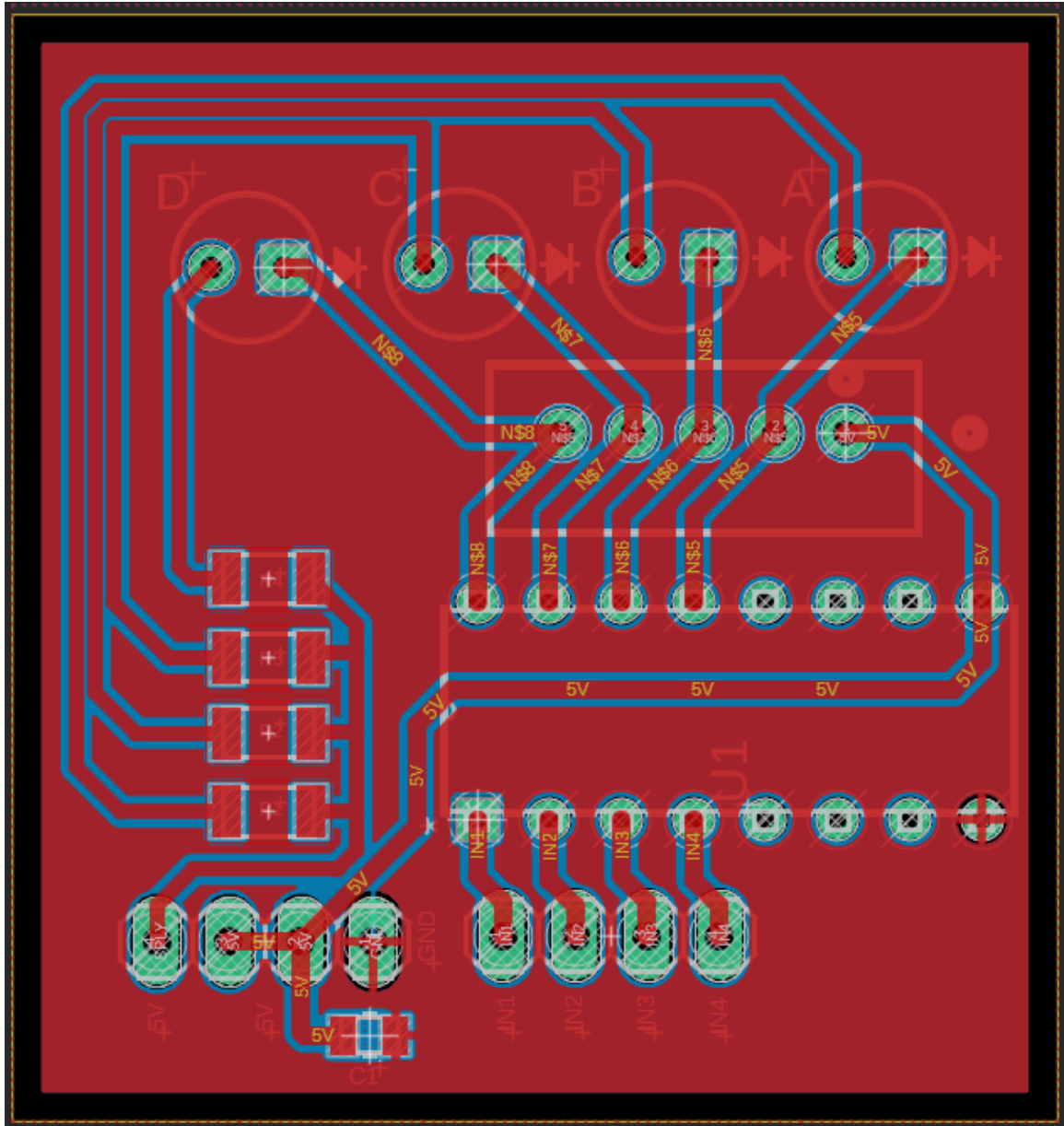


Figure 32: Motor Controller

8.1.3 CLSM Main Board

The main board for the CLSM is designed to serve as the central control and signal routing hub, integrating power regulation, microcontroller control, and analog signal processing. Power is supplied via a 12 V input terminal, which feeds the two regulators providing 5 V and 3.3 V rails. The 5 V line supports peripherals and off-board motor drivers, while the 3.3 V rail powers the ESP32 and analog circuitry, isolating sensitive components from higher-voltage noise.

At the core of the board is the ESP32-WROOM-32 microcontroller, positioned centrally to minimize routing complexity and keep GPIO traces short and direct. Control signals for three stepper motors are routed from the ESP32 to headers grouped by axis for organized wiring. A USB-UART interface is included for programming and serial communication, with routing kept short to reduce noise.

The photodiode and a transimpedance amplifier is placed near the bottom-left corner, physically close to reduce trace length and minimize interference/noise. Clean power and proper grounding are ensured through dedicated bypass capacitors and a full ground pour on the top layer.

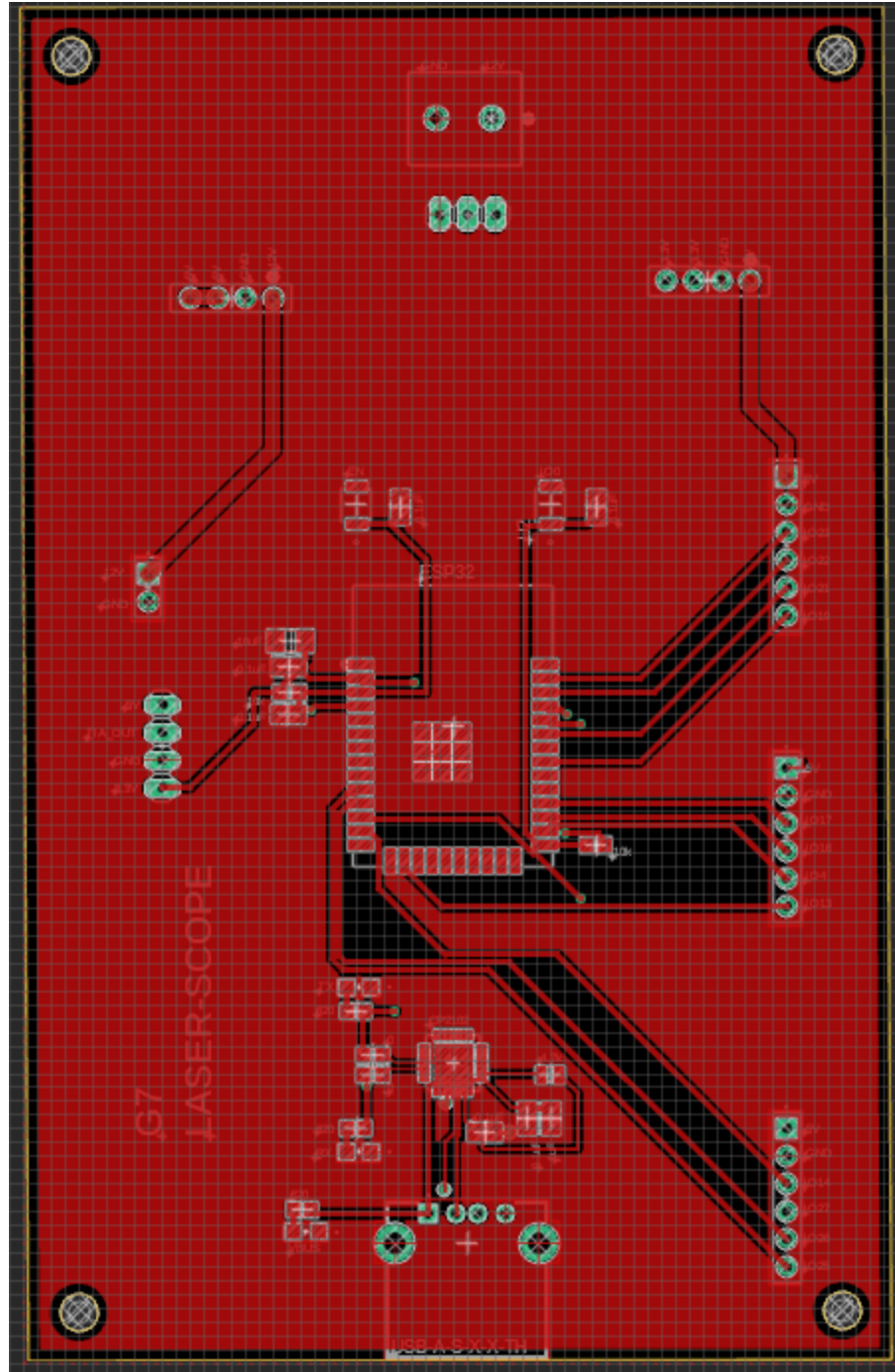


Figure 33: CLSM Main Board

8.1.4 UART-USB Converter

The UART-USB converter serves as the bridge between the ESP32 board and the GUI, here we utilize the CP2102 as our bridge, we use a USB-Mini. Currently it has been decided to keep this board separate from the main board for reparability, modification and testing, however, due to costs and other variables associated with the manufacture of this part of the board it is likely to be implemented in the main board in the future.

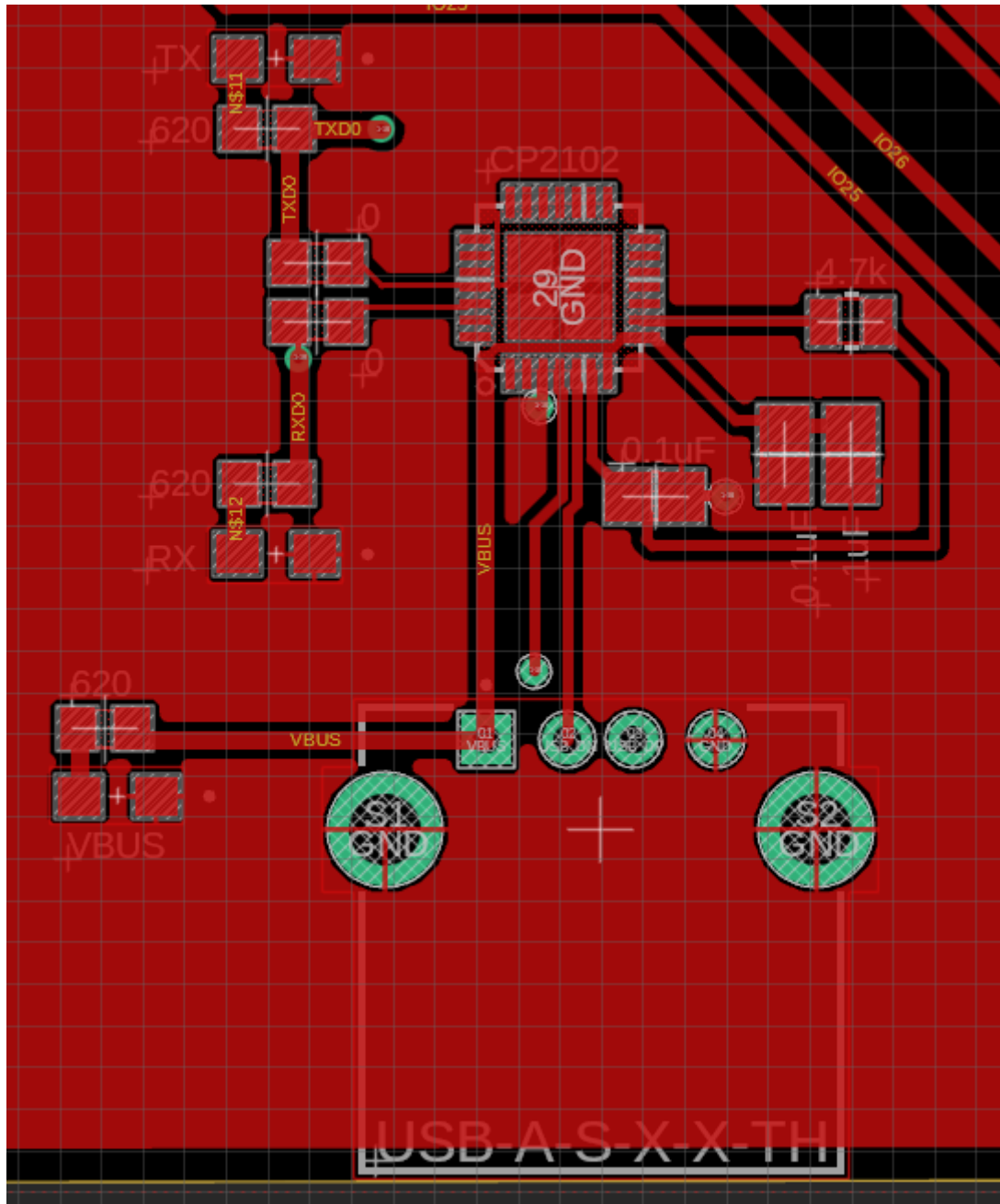


Figure 34: UART-USB Converter

Note that all PCB layouts are likely unfinished. Further development over the course of senior design II is required as well as a review by Dr. Weeks. The overall design of all boards is subject to change in order to meet requirements based on feedback from reviewers, Dr. Weeks and Dr. Chan.

8.2 Stage

For the CLSM, the OpenFlexure Delta Stage was selected due to its compact design, submicron resolution capabilities, and open-source aspect. The OpenFlexure stage uses a

monolithic flexure mechanism that is 3D printed using PLA, providing high-precision movement in X, Y, and Z directions using flexing rather than sliding components. For the stage construction, instructions and guidelines on the OpenFlexure website were followed with minor modifications made to accommodate the custom motor controller integration. The stage is set up with all three 28BYJ-48 stepper motors directly mounted. These motors are the driving factor to achieve all stage displacement. It is worth noting that the motor controller PCB will be designed around the storage allocation of the OpenFlexure Delta Stage.

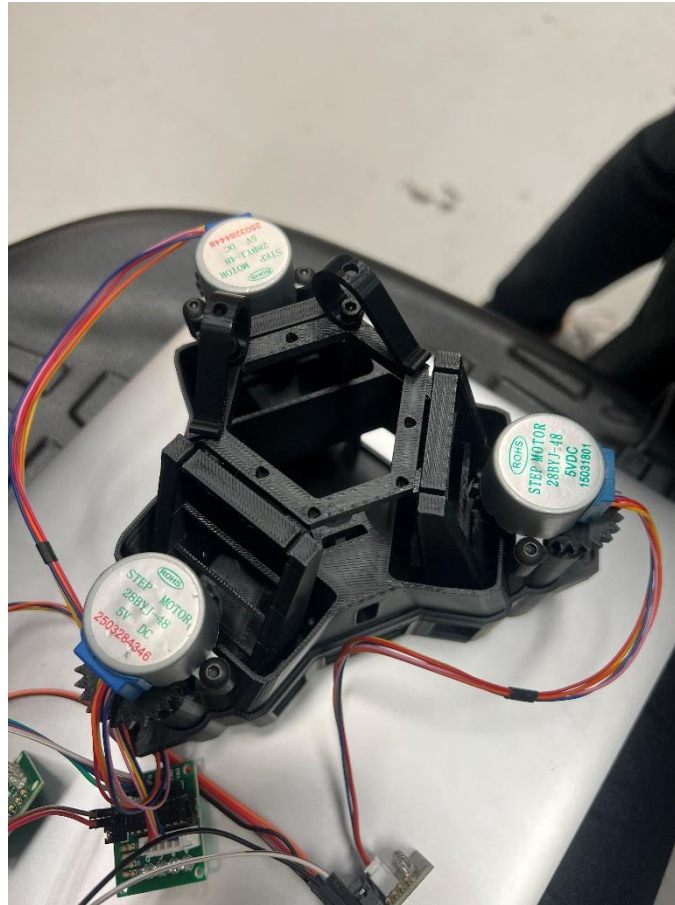


Figure 35: OpenFlexure Delta Stage

8.3 Microscope Head Design

To control proper beam alignment through the CLSM the way the optics elements are positioned and held while scanning can be seen with a 3D printed microscope head. The microscope head encloses all the optics elements as well as holding the photodiode and TIA in their respective spots during scanning. The layout of the microscope head will be very similar to Figure 2 in section 2.5.1. The laser diode and beam expander elements will be positioned 45 degrees from the rest of the beam path as this allows for the beam to

be directed into the microscope objective beneath it, as well as allowing the beam to pass back through the microscope objective and beam expander into the focusing lens and pinhole onto the photodiode.

8.4 System Stabilization

To ensure repeatability and precision in the CLSM system, steps must be taken to address one of the major limitations of using a 3D-printed PLA-based flexure stage: its sensitivity to environmental disturbances. The OpenFlexure Delta Stage, while highly effective in providing precise motion through stepper motors, is inherently lightweight and susceptible to external vibrations, table movement, and air currents. Even minor mechanical or acoustic disturbances can cause positional drift or introduce noise into imaging data, especially if sub-micron resolution is desired.

To mitigate these issues, we are constructing a custom stabilization platform made of concrete. This block will serve as a foundation and a vibration absorber for the entire CLSM system. Concrete was chosen for its damping characteristics, which allow it to effectively absorb low-frequency vibrations or impacts and mechanical shocks that might be caused by the lab bench or desk. By significantly increasing the mass of the system, we reduce the amplitude of any induced motion, creating a more stable base for precision imaging tasks.

The concrete block will be cast in a form-fitting mold to support the microscope stage and electronics uniformly, with embedded mounting points or rubber isolation pads to decouple it from the supporting surface. The leveling of the block is critical to ensure that the stage sits in a neutral, strain-free position, allowing the flexures to operate symmetrically in all directions. Bubble levels and adjustable feet may be integrated into the support frame to allow fine adjustment post-curing.

This approach enhances not only stability but also the thermal and mechanical consistency of the system. Unlike the lightweight PLA frame alone, the concrete base resists sudden thermal shifts and maintains alignment over longer periods. The result is a more robust platform for repeatable scanning and imaging, allowing for higher quality images and increased repeatability.

9. System Testing and Evaluation

All hardware had been acquired for the system and therefore preliminary testing and evaluation were able to be completed for every sub-system to some extent. All power supply components have been tested for input and output voltage and current as well as heat dissipation. The ESP32 in conjunction with a breadboarded motor controller was tested to ensure controller design accuracy and compatibility. Additionally, the ESP32's ADC was tested in conjunction with the photodiode-TIA circuit to get initial testing values for imaging as well as fixing any potential issues of noise, parasitic capacitances, and configuration. Furthermore, preliminary stage testing was done in order to verify micron to sub-micron resolution capabilities. All results will be presented and discussed in the following sections.

9.1 Hardware Testing

9.1.1 Power Supply Testing

First, to ensure initial reliability of power the Mean-Well LRS-50-12 was tested for voltage accuracy, current handling capability, heat dissipation, and general safety and stability. As discussed in chapter 3, the Mean Well LRS-50-12 is rated for 12V DC and can output up to 4.2A, allowing it to power all regulators, microcontroller, stepper motors and other peripherals in the CLSM. However, this test was conducted under no-load conditions first and then a load was applied.

To test voltage, a digital multimeter (DMM) was used. First, the Mean Well LRS-50-12 was wired, utilizing a wall outlet cable, with standard connections (Black – Line, White – Neutral, Green – Ground). Furthermore, to ensure current capabilities were not exceeded, both V+ and V- outputs on the supply were wired using 18 AWG wire, which is suitable for handling the 4.2A maximum.

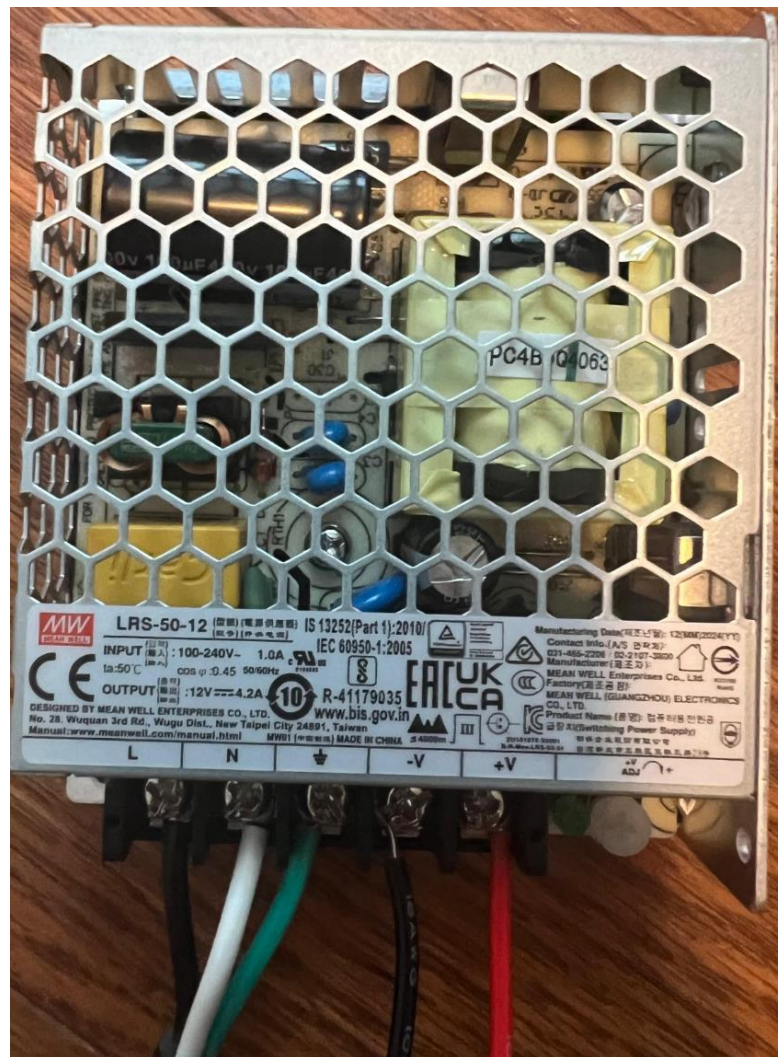


Figure 36: AC-DC Converter Setup

Once this was done the DMM was utilized to see voltage accuracy, the results proved that the supply could deliver 12V with $\sim \pm 1\%$ discrepancy. The supply was then connected to a resistor box capable of handling this current to simulate operational current draw. At full load, the voltage only dipped slightly, demonstrating effective internal voltage regulation.

To assess current capability, the power supply was connected to the same resistor box used for the voltage test. By creating an open circuit and placing the DMM probes in series, a total current of $\sim 4.2 \pm 2\%$ was seen, indicating the supply could deliver this amount of current without triggering any protection mechanisms, similarly to the previous test, no voltage drops, or instability was observed.

The final test was thermal performance, to do this the supply was left running near full load for around 20 minutes, the Mean-Well LRS-50-12 has an aluminum chassis which acts as its heat sink. When we measured its temperature by utilizing an IR thermometer, the temperature was around 50-55°C and showed no signs of overheating.

Following all these tests, the power supply was connected to an MPS1584 regulator board. This showed a proper 12-5V conversion and output about 2.8A to our test load, which is expected due to the MPS1584's max current output of 3A. Furthermore, when connected to LM1085-3.3, testing with another load and this circuit about 0.8A were seen coming out of the 3.3V regulator, which will be enough to power the ESP32. Both 3.3V and 5V regulators were tested using the same IR thermometer and showed no signs of overheating even after prolonged operation.

Table 9.1: Power Supply Test Results

Device	Input Voltage	Output Voltage	Input Current	Output Current
Mean Well LRS-50-12 MPS1584 Regulator Board Bread- boarded LM1085-3.3	120VAC	12VDC	$\sim 1.3\text{A}$	Up to 4A
	12VDC	5VDC	$\sim 3\text{A}$	2.8A
	5VDC	3.3VDC	2.8A (with another load connected)	$\sim 0.8\text{A}$ (With another load connected)

Finally, it is worth noting that all tests involving a direct 120VAC were conducted using line man's gloves and fire retardant/100% cotton clothing as personal protective equipment to ensure user safety.

9.1.2 ESP32 Testing

To verify the proper functionality of the ESP32 microcontroller, several fundamental tests can be performed. The first is the Power-On and Boot Test, which ensures that the device is receiving power and successfully entering its boot process. Upon connecting the ESP32 to a USB port or an external power source, users should observe an onboard

power LED turning on, followed by boot messages printed through the serial monitor. These messages typically appear at standard baud rates like 115200 or 74880 and confirm that the ESP32 has initialized successfully and is ready to run its application code or enter bootloader mode. This initial test is essential for identifying hardware faults or firmware loading issues.

The second stage of testing involves evaluating GPIO Pin Functionality, which is critical for interacting with external devices. This can be done by programming the ESP32 to blink an LED using the `digitalWrite()` function or by detecting input from a push-button using `digitalRead()`. These simple tests help verify that the digital input/output pins are functioning as expected and that the GPIO configuration in software is correctly mapped to the hardware. Visual confirmation, such as an LED toggling on and off or responding to a button press, provides immediate feedback on pin responsiveness and logic level integrity.

Another important diagnostic is the Serial Communication Test, which validates that the ESP32 can send and receive data over its UART interfaces. Using the USB-to-UART bridge built into most ESP32 development boards, users can open a serial monitor and use commands like `Serial.print()` to observe messages sent from the board. This test not only confirms that the UART hardware is operational but also ensures that the board can communicate effectively with a host computer or other serial devices. For more advanced testing, additional UART ports (such as `Serial1` or `Serial2`) can be used to communicate with external modules or microcontrollers.

Finally, the Analog-to-Digital Converter (ADC) Test allows users to verify that the ESP32 is accurately reading analog voltage levels. By connecting a variable voltage source, such as a potentiometer, to one of the ADC-capable pins and using the `analogRead()` function, users can observe how the digital value changes in response to varying input voltages. These readings can be monitored via the serial interface, allowing for real-time validation. This test is especially important in applications involving sensors or analog signal acquisition, as it confirms that the ESP32's ADC is calibrated and functioning within expected voltage ranges.

9.1.3 Motor Controller Testing

Based on the schematic design on chapter 6, the motor controller was fully breadboarded and tested to verify proper voltage regulation, current delivery, thermal behavior and stepping capability. The motor controller built around the ULN2003 can handle 250mA per phase with a maximum of two active phases. Input power to the motor controllers, supplied via a 5V rail from the MP1584, was used. This rail will power, the ULN2003, motor, and LEDs associated with each phase of the motor. The ESP32, powered via the 3.3V rail from the LM108 5-3.3, will send signals to this motor controller through GPIO pins.

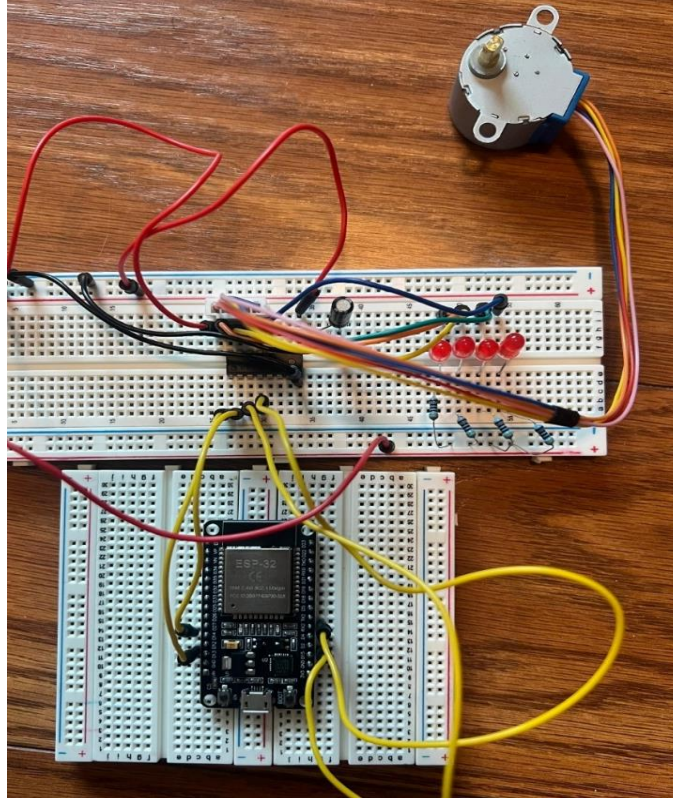


Figure 37: Motor Controller Prototype

In testing, input voltage of the motor was measured at 5.02V using a DMM, verifying that all circuitries held steady under load. Current draw was tested with both idle and active stepping patterns, showing that a single 28BYJ-48 motor pulled ~200-250mA during stepping, which is consistent with datasheet values. The ULN2003 driver is protected by onboard flyback diodes and the COM pin has a 10 μ F bypass capacitor to reduce noise and account for any voltage fluctuation. All LEDs light up properly based on motor movement, which was verified via both haptic feedback and the code utilized.

Finally, to test thermal dissipation the motor was left running at full stepping speed for ~15 minutes. All components were then tested using an IR thermometer and were well under operational heat maximums. This indicates the design is sufficient for sustained operation of the CLSM, however, further testing is required on the physical stage to verify that thermal results will hold at this level.

9.1.4 Stage Testing

Testing the OpenFlexure Delta Motor Stage is essential to ensure that all three motors are functioning correctly and that the mechanical system is capable of achieving precise and coordinated movement across the X, Y, and Z axes. The initial step involves verifying that each stepper motor is properly wired to its respective motor driver and that the ESP32 microcontroller is correctly sending control signals. This includes confirming that the power supply delivers consistent voltage and current levels appropriate for the stepper

motors in use, typically 28BYJ-48 motors driven by ULN2003 boards. Once the electrical connections are verified, each motor should be tested independently using simple step commands that rotate the motor a fixed number of steps in forward and reverse directions. This helps confirm that the motor windings are intact and that no mechanical obstructions are present in the stage. Following this, coordinated movement must be tested by issuing synchronized commands to all three motors. Since the delta configuration relies on the simultaneous motion of multiple arms to achieve translation along traditional Cartesian axes, it is vital to implement or use inverse kinematics algorithms that calculate the required steps for each motor to move the stage along X, Y, or Z. To evaluate positional accuracy, users can execute test patterns such as raster scanning or circular movements and visually inspect whether the stage returns to the origin consistently after each sequence. Additionally, measuring tools such as a dial gauge, laser pointer, or camera-based feedback can be used to quantify displacement and repeatability at the micron level. Software-level safeguards like endstop checks or step count limits should also be tested to prevent collisions and ensure safe operation. Finally, testing should be conducted under different load conditions to ensure the stage can maintain precision when holding or moving a sample. These comprehensive tests collectively verify that the OpenFlexure Delta Motor Stage operates with the precision and reliability required for high-resolution scanning applications.

9.2 Software Testing

9.2.1 GUI

The GUI for this project was developed in the Eclipse IDE using the Java programming language, with graphical components implemented using the `javax.swing` and `java.awt` libraries. Serial communication with the ESP32 is established through the use of a third-party serial communication library such as `jSerialComm`, enabling real-time data exchange over a USB connection. Testing the GUI involves ensuring both functional correctness and usability. One of the first areas of focus is the responsiveness of user interface components—buttons, sliders, and input fields must react immediately to user actions. Lambda expressions were heavily utilized in this application to simplify the implementation of action listeners and streamline the logic tied to user interaction events. These lambda-based listeners are ideal for assigning clear, concise behavior to GUI elements like button clicks, making it easier to isolate and test individual functions.

To verify functionality during development, console output played a critical role. System messages were printed to the console in response to specific user actions, such as initiating a scan, selecting a COM port, or sending commands to the ESP32. This allowed for rapid validation of whether button presses correctly triggered the expected operations and whether the internal state of the application (e.g., selected port, scan parameters) was updated as intended. Additionally, testing involved verifying that the GUI properly sends formatted serial commands based on user input and that it can receive and display responses from the ESP32 without corruption. The GUI also includes error handling routines that detect scenarios such as disconnected devices or failed serial port initialization; these events are captured and reported to the user through both popup

dialogs and console messages. File logging was tested to ensure that all scan data, including stage coordinates and voltage readings, is saved correctly and consistently. Overall, GUI testing ensured the interface was not only responsive and reliable but also provided helpful runtime feedback through the console during development and debugging.

9.2.2 ESP32

Testing the software running on the ESP32 microcontroller is crucial to ensuring that the device can reliably control the motor stage, acquire analog voltage data, and maintain stable communication with the GUI. The ESP32 firmware was developed using the Arduino framework, which provides high-level abstractions for serial communication, GPIO manipulation, and task scheduling. Initial testing began with basic validation of core functionalities, such as verifying that the ESP32 could initialize without errors and output boot messages via the serial console. From there, individual subsystems were tested incrementally. Motor control functions were evaluated by issuing manual commands through the serial monitor to trigger forward and reverse movements on each motor. Observing the physical response of the stage helped confirm the correctness of pin assignments, stepping sequences, and delay timing between steps. These tests ensured that all three motors responded independently and accurately before implementing more complex coordinated movement logic.

Analog voltage acquisition was another major focus of ESP32 testing. Using the built-in ADC channels, the ESP32 read voltage signals from a transimpedance amplifier that reflects laser intensity from the sample. To validate this functionality, known voltage sources and variable resistors were used to simulate input signals. Output readings were printed to the serial monitor in real-time to assess consistency, accuracy, and resolution. Additional safeguards, such as clamping voltage ranges or smoothing noisy signals, were tested to ensure robust performance under varying conditions.

Serial communication testing involved sending and receiving structured messages between the ESP32 and the GUI application. This required validating message integrity, timing, and responsiveness. The ESP32 was programmed to recognize specific serial commands, parse them correctly, and take corresponding actions (e.g., start scan, reset stage, or report status). During testing, dummy messages were sent manually to confirm the firmware's parsing logic and response generation. To avoid blocking operations and improve responsiveness, timing-sensitive tasks such as scanning and data acquisition were placed in non-blocking loops or FreeRTOS tasks, depending on system complexity. Console print statements played a critical role during this stage, offering insight into execution flow, sensor readings, and potential faults such as communication timeouts or ADC saturation. Together, these testing strategies ensured that the ESP32 software remained reliable, modular, and capable of supporting the real-time demands of the scanning process.

9.3 Optical Layout Testing

The testing done for the optical layout can be seen in figure 27. On the right side the OUI, or in this case a beam block used as the sample, can be seen farther away from the microscope objective when compared to the left side of the figure. Measuring the power of the reflection of the 1mW laser beam, it can be seen that the side that has the OUI out of focus (farther away from the objective). This beam being too far out of the working distance of the microscope objective lets us assume the base reflected power of the initial beam through the beam splitter is $4.02\mu W$. On the left side the OUI had been moved closer, or rather inside of the microscope objectives working distance. When measuring the power of the reflected beam back through the objective, there is a visible increase in power from $4.02\mu W$ to $4.73\mu W$.

While not shown in this section, more testing was done with the photodiode and TIA with the same setup shown in figure 27, where the power meter was substituted for the photodiode. Across the TIA there was a voltage difference across a feedback resistor of $1M\Omega$. With the OUI being out of focus and reading the voltage across the TIA, it was seen to be ~ 0.41 V. Once the OUI was moved into the working distance of the microscope objective, the voltage across the feedback resistor jumped up to ~ 0.56 V. This reading was a more substantial reading than was anticipated. While this testing was only done with the 1mW laser, more testing will need to be done once the 20mW laser diode is implemented.

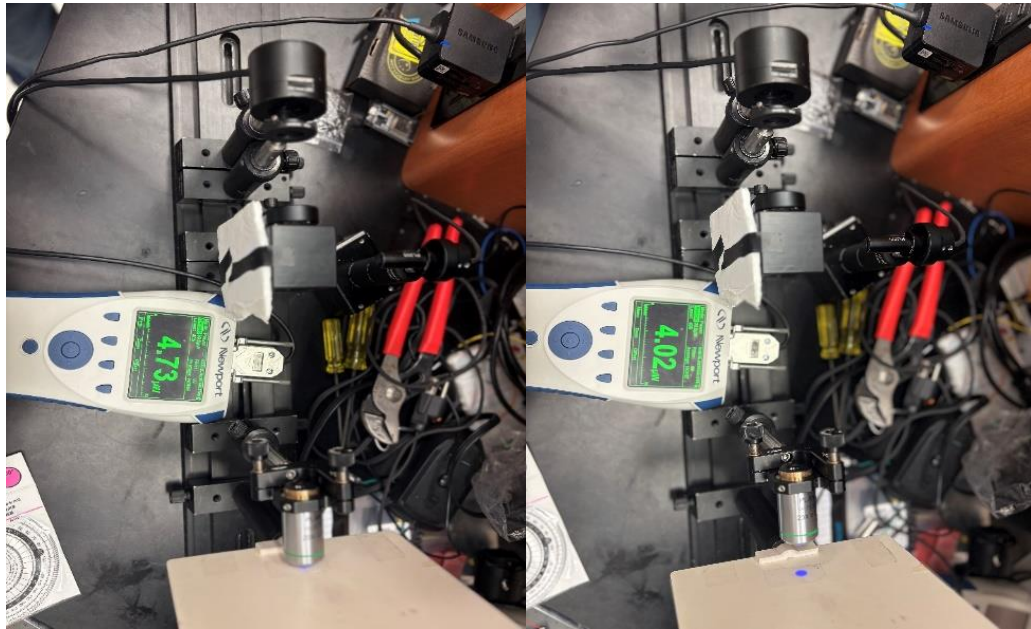


Figure 38: Optical Test Layout (left image is in focus, right image is out of focus)

9.4 Optoelectronics Feasibility Study

9.4.1 Photodiode

To characterize the photodiode and test its real parameters against those given on the spec sheet, measurements were taken of the photocurrent response to light stimulus on the device.

The photodiode was connected in series with a 100k Ω resistor and a DC power supply configured to supply 3V. The photodiode was configured so that the 3V biasing voltage put the diode in reverse bias. Then the lights in the room were turned off and an index card was used to cover the active area of the device in order to simulate total darkness. Using a DMM, the voltage across the resistor was measured and then converted to a photocurrent measurement value through calculation using Ohm's Law. Under these conditions in which there was no light stimulating the device, the resistor voltage was measured at 0.7mV and the dark current value was determined to be 7nA.

Next, a blue screen was illuminated on a cell phone in the dark room to provide ambient lighting and the index card was removed from covering the active area of the photodiode device. The blue screen was chosen to provide a similar wavelength to that of the selected photodiode. Using a power meter, the ambient lighting was determined to be approximately 1 μ W. A measurement was made of the voltage across the resistor and was used to calculate corresponding photocurrent value. The voltage was measured to be 14.5mV, corresponding to a 145nA photocurrent. Using the measurement of the ambient optical power and the magnitude of the photocurrent, the responsivity of the photodiode was determined to be 0.145A/W, which is a reasonable value and comparable to the 0.17A/W listed on the spec sheet for the photodiode.

Finally, a 405nm 120 degree divergence angle laser diode was positioned roughly 1 meter from the photodiode in the dark room and turned on. Using the power meter, the incident light at the position of the photodiode was approximately 47mW. Using the same methods previously described, the resistor voltage was measured to be 850mV which corresponds to 8.5mA of photocurrent. Using the incident optical power and photocurrent value, the responsivity of the photodiode to the laser diode under these circumstances was calculated to be 0.18A/W, which is reasonable and comparable to the value of 0.17A/W listed on the spec sheet.

Table 9.1: Photodiode Test Results

	Dark	Blue Light (1 μ W)	Laser (47mW)
Resistor Voltage	0.7V	14.5mV	850mV
Photocurrent	7nA	145nA	8.5mA
Responsivity	N/A	0.145A/W	0.18A/W

9.4.2 Transimpedance Amplifier

For the TIA circuit our expected input will come from the photodiode, from testing our output photodiode current can be expected to be $\sim 1\mu\text{A} \pm 8\text{-}12\%$ which should be able to be picked up by the OPA380 given its minimum pickup range of $\sim 1\text{nA}$, in testing we see this to be true, as the TIA is able to amplify this signal consistently to $\sim 0.8\text{-}1.2\text{V}$ which is suitable for the ADC that is built into the ESP32. The following was used to build the TIA circuit.

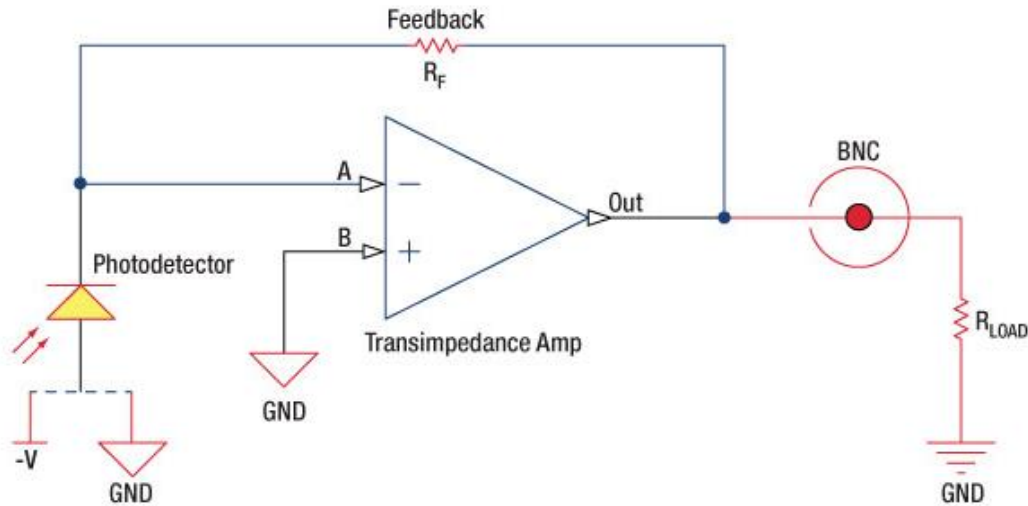


Figure 39: Amplified Detector Circuit by Thorlabs Inc.

Utilizing the sample circuit from Thorlabs an R_f of $1\text{M}\Omega$ was selected, this gives a gain of $1 \times 10^6 \text{ V/A}$, this was chosen as a signal of $0.8\mu\text{A} \times 1\text{M}\Omega$ would yield 0.8V . During testing it was concluded that this gain was enough as we saw a signal of $\sim 0.8\text{-}1.2\text{V}$. However, during connection to the ADC we saw a time delay between alterations of the accuracy of the laser diode and the ADC output. From this it was concluded that a capacitor needed to be added in parallel to R_f to compensate for parasitic capacitance/high frequency oscillation. A 2pF capacitor sufficed to remediate this. This could be influenced by multiple factors such as operating temperatures, ambient light in the room, and quality of the power supply to the op amp itself. To mitigate these issues the temperature itself was within the range that a final version of the CLSM would be utilized in. Additionally, the TIA-Photodiode circuit was tested in a room with no overhead lights turned on to replicate the final conditions that the circuit will operate under.

Table 9.2: TIA Test Results

Test	Result
Input Current	$\sim 0.8\text{-}1.2\mu\text{A}$
Output Voltage	$\sim 0.8\text{-}1.2\text{V}$
Photodiode Responsivity	$\sim 0.17\text{-}0.18\text{A/W}$

9.5 Senior Design II Test Plan

Given the above information, all parts of the system have undergone basic functionality test and show expected values based on datasheets/calculations. As such what remains to be testing is the full integration of every sub-system as set out by the following sections.

9.5.1 Power Supply Testing

Once all components of the CLSM project have been integrated into a single prototyped breadboard we will:

- Test that the Mean Well LRS-50-12 can provide enough power for the entirety of the load with no undervoltage issues, if any issues of undervoltage are found the power supply will be upgraded to the Mean Well LRS-75-12
- Testing for the MPS1584EN was done using a pre-built regulator board, for our final application a break-out board has been acquired for the SMD part, we will test the design from the schematic for the same tests and then implement it on the power supply system under full load.

9.5.2 Optics

From the data collected from the optical layout test, the CLSM design will not include a polarizing beam splitter as it does seem very feasible to collect the data needed from the TIA to create the images that is wanted. However, after these results there will need to be more testing in a few areas.

- Testing the 20mW laser diode order from Thorlabs to make sure it does not overpower the photodiode (power across the feedback resistor cannot be $> 3.3V$)
- Test the beam expander with the 20mW laser diode instead of the test 1mW laser used in the optics testing.
- Implementation of the optics components into the 3D printed microscope head, and testing of the alignment of such microscope head

9.5.3 Stage Control

Given the results from the motor tests, we have deemed that enough testing has been completed to begin full development of the stage controller algorithm. At this stage, this is the next key development towards obtaining the first image by the system, to test and develop this system the following will be required:

- Full implementation of the custom motor controller in regard to the OpenFlexure Delta stage.

- Development of the scanning algorithm in order to achieve micron resolution first and then begin development of a sub-micron algorithm

9.5.4 UI System

With the successful testing of both the GUI and the ESP32 firmware, the foundational components of the system have been validated, allowing the project to progress to the next critical phase: developing a robust testing environment for data collection. This stage is essential for translating raw sensor data into a meaningful and interpretable image produced by the scanning process. To achieve this, attention must now shift toward three interconnected aspects of the data workflow: formatting, collection, and processing.

- **Formatting:** The goal is to design an efficient and consistent structure for organizing the scan data captured by the ESP32. This includes determining how positional information (X, Y, Z coordinates) and corresponding analog voltage readings from the transimpedance amplifier will be combined into a unified format. The format must be compact enough for real-time transmission over a serial interface, yet rich enough to retain all relevant metadata, such as timestamps, scan resolution, and motor state. JSON, CSV, or binary representations may be evaluated depending on the trade-offs between readability and transmission efficiency.
- **Formatting:** The focus shifts to data collection, where the host computer (running the GUI) receives the incoming data stream and must reliably store it in a structured and accessible format. This involves designing file storage routines that organize the scan data by session, preserve the integrity of the transmitted packets, and prevent data loss during high-speed scans. It also includes adding features like automatic file naming, directory management, and optional redundancy mechanisms to safeguard important scan sessions.
- **Processing:** where the collected voltage values are translated into an image representing the scanned surface. This would involve interpreting the analog signals in the context of their spatial coordinates to reconstruct a pixel map or bitmap. Processing may include interpolation for missing points, filtering to remove noise, normalization to enhance contrast, and conversion of voltage levels into grayscale intensity values. These processed datasets will then be visualized using image rendering libraries or exported for further analysis. Collectively, these three stages form the backbone of the scanning pipeline and will be essential in demonstrating the capability of the system to transform physical surface profiles into digital representations.

9.6 Senior Design II Developments, Changes, and Implementations

Between the end of SD I and full development in SD II, there were a few changes made to the project as progressed. On top of this there were design challenges that forced us to

go about finding new solutions to make sure we could achieve our key specifications. All sections on this project have undergone some sort of changes and will be discussed in detail in the sections below.

9.6.1 Optics

The first main challenge experienced when implementing the optics was the misalignment of optical components in the microscope housing due to the way the 3D-model was printed. Initially the microscope housing had a semi-circular mounting mechanism to hold the optics in place. This did not hold the optics straight in line with the optical path but rather, all optics were tilted at different angles. This made alignment of the laser diode into the optical path, all the way to the photodiode very difficult. To account for this, changing the mounting solution to just be a rectangular hole not only increased the accuracy of the print but also kept all the rounded optics completely straight, making only movement of the laser diode and photodiode necessary for complete alignment.

One improvement made to the optical design was substituting a 3D printed pinhole for one that needed to be ordered from a manufacturer. Not only did this help reduce cost, but it allowed for some customizability; if a rough alignment was necessary for testing other components, a larger pinhole could quickly be printed and placed into the optical system so precise alignment was not as necessary, and it was also easier to make each pinhole fit in the optical housing. One issue that was encountered was that due to the layering of the filament of the 3D printer, these pinholes could not be printed vertically or they would be warped and lose their circular shape. This was accounted for by printing these components separately from the housing and at a horizontal orientation, where the precision of the printer was more than sufficient to create this shape.

Additionally, the optical array was improved by adjusting the position of the pinholes and photodiode relative to the beam. It was found that better optical filtering was achieved when the pinhole size was increased from 1mm to 2mm diameter and positioned where the beam had a larger diameter. With this change, it was also determined that the photodiode could be positioned closer to the previous optics to increase the beam waist incident on the device and more efficiently fill its active area.

9.6.2 Electronics

The first challenge that was experienced when implementing the electronics was the laser diode's driver not matching the selected diode's specs. The MicroFlexDrive V5 can drive a minimum of 65mA, which while in range for the laser diode, it would put it past the range of 10mW that was desired for the project. As such, the LM317 was selected as a driver in order to utilize its constant current mode, where a resistor that ties Vout and Adj sees 1.25V across, by selecting a 39 Ω resistor we were able to output 31mA, which is sufficient to drive the laser diode to output 10mW of optical power.

The second and main challenge was reaching an equilibrium point between settle time and noise for the TIA. Initially, the TIA had a feedback loop of 1M Ω and 68nF. This yielded a very good signal-noise ratio and little to no noise was captured by the system. However, this network yielded a settle time of 132ms which in practice would increase

scanning time for a 1x1mm area to up to an hour for a 64x64 pixel scan. Additionally, because this mismatched the settle time on the code and a 9% loss of contrast was seen on the images. Through testing and refining a network of $1\text{M}\Omega$ and 680pF was reached. With this, the TIA's signal-noise ratio remained consistent, and noise was minimal enough that it could be neglected by simply averaging more points during a scan. Additionally, this network yielded a settle time of 3.2ms, which allowed for a 1x1mm 64x64px scan in under 20 minutes.

9.6.3 Software

After the main hurdles of the optics and electronics were cleared ensuring many of the routines are working accordingly are important. Routines such as facilitating communication protocol between the computer and the MCU, coordinating stage movement, GUI layout, and image generation are what produce the important results for the project.

The main problem software side faced was coordinating the motors. Upon producing actual images with the microscope, we noticed that the area covered in the image is about a fifth of what was intended. To resolve this problem was to multiply the intended movement by five. Originally when the user put in a side length of 1mm it would produce a 0.2 mm movement so this multiplication by five was able to fix this problem. The main downside to this resolution is that the scanning process time is increased considerably since motor movement is five times longer. So our 12 minute "1 x 1mm" (0.2 x 0.2mm) became a 23-minute scan.

The GUI layout compared to the was conceptually sketched is vastly different. This is due to what we want to display for the user. Communicating with the optics with this process was important because it allowed for the development of console and ADC monitoring. Additionally, having metrics for per pixels scan speed and ETA of scan allows for us to debug the scanning process. The hurdle for this area of software is ensuring a serial connection at every page. Whenever the user interacts with an element that requires serial communication it can render other elements of serial communication of other pages useless. The rectification for this problem initially was to restart the program. However, software side coding the buttons that changes the page to reset the communication and having a page to set the communication was a better adjustment.

10. Administrative Content

10.1 Budgeting and Financing

The project has no formal sponsor, and as such all costs will be equally divided among group members. The following sections will demonstrate the cost of development and the responsibilities of each group member in regard to project construction/development. The sections will be broken down from photonics parts to electronics hardware. Overall, the project goal is to retain a cost of under \$1000 dollars, and so, a tight budget must be

maintained.

Table 10.1: Budget and Finances

Components	Quantity	Cost
405 nm Laser Diode	1	\$50
Photodiode	1	\$60
Negative Meniscus Lens	1	\$25
Plano-Convex Lens	1	\$60
Beamsplitter	1	\$50
20x microscope objective	1	\$60
Iris	1	\$50
Focusing Lens	1	\$60
PLA Filament	1	\$40
PCB	1 (Modules like regulators included)	\$60-\$200
Amplifiers	1	\$4.11
Regulator circuits	2	\$10-\$20
AC/DC converter	1	\$10-\$25
MCU	1	\$10-\$45
Stepper Motors	3	\$8-\$15
	Total:	\$900

10.2 Bills of Materials

Table 10.2: Bill of Materials

Components	Quantity	Cost
405 nm Laser Diode	1	\$50
Photodiode	1	\$60
Bi-Concave Lens	1	\$40

Plano-Convex Lens	2	\$120
Beamsplitter	1	\$50
20x microscope objective	1	\$60
Bi-Convex Collecting Lens	1	\$60
PLA Filament	1	\$40
PCBs	1 (Includes all sister boards)	\$200
Amplifiers	1	\$4.11
Regulator circuits	2	\$5
AC/DC converter	1	\$12.99
MCU	1	\$10
Stepper Motors	3	\$8-\$15
8"x12" Optical Breadboard	1	\$50
Optical Posts and holder	2	\$20
1.5" x 1.5" MDF	1	\$5
Inner tube	1	\$8
Brackets	4	\$5
(M3 and ¼")Screws	1	\$5
USB-A to USB-A Cable	1	\$6
6 mm Diam. Magnets	1 (includes 200 magnets)	\$6
	Total:	\$894.11

10.3 Project Milestones

Table 10.3: Senior Design 1 Documentation Dates

Senior Design 1: Documentation			
Task	Start Date	Completion Date	Length
Team Formation	5/13/2025	5/20/2025	7 Days
Divide and Conquer Writing and Research	5/20/2025	5/30/2025	10 Days
Page Milestone: 30-Pages	5/30/2025	6/13/2025	14 Days
Page Milestone: 60-Pages	6/13/2025	6/27/2025	14 Days
Page Milestone: 90-Pages	6/27/2025	7/11/2025	14 Days
Page Milestone: 120-Pages	7/11/2025	7/25/2025	14 Days

Table 10.4: Senior Design 1 Design Dates

Senior Design 1: Design			
Task	Start Date	Completion Date	Length
System Design: Hardware and Software	5/30/2025	6/27/2025	28 Days
System Testing: Hardware and Software	6/27/2025	7/11/2025	14 Days
3D Printed Housing Prototypes	7/11/2025	7/25/2025	14 Days
PCB Initial Design, Implementation, and Ordering	6/1/2025	7/29/2025	58 days

Table 10.4: Senior Design 2 Design Dates

Senior Design 2: Design			
Task	Start Date	Completion Date	Length
Fully prototyped breadboard with all functionalities implemented	7/30/2025	8/18/2025	19 Days
Finish and order PCB design	7/30/2025	8/30/2025	30 Days
3D Print 1st Microscope Head iteration	7/30/2025	8/30/2025	30 Days
Finish basic GUI	7/30/2025	8/30/2025	30 Days
Finish scanning algorithm	7/30/2025	8/18/2025	19 Days

10.4 Table of Work Distribution

Table 10.5: Senior Design Work Distributions

Photonics Sciences Engineering	Responsibilities
Collin Barber	<ul style="list-style-type: none"> • Optical component selection and implementation following reflection back through objective • Design for housing of post-objective optics • Photodiode circuit
Photonics Sciences Engineering	Responsibilities
Luc Therrien	<ul style="list-style-type: none"> • Optical Component selection and implementation up until reflection back through the objective • Microscope head • OpenFlexure Delta Stage • Laser power circuit
Computer Engineering	Responsibilities
Omar Castro	<ul style="list-style-type: none"> • MCU Selection and Implementation • Software Design and Implementation <ol style="list-style-type: none"> 1. Motor Control. 2. Data Collection 3. GUI
Electrical Engineering	Responsibilities
Karol Josef Woodhouse	<ul style="list-style-type: none"> • PCB Design <ol style="list-style-type: none"> 1. Regulators 2. Motor Controllers 3. Main board (MCU, PD-TIA, UART-USB, etc.) • TIA/Filter Design and Signal Cleanup • Stage Motor Implementation

11. Conclusion

The CLSM project is ultimately about creating a fully functional confocal laser scanning microscope with a cost of less than \$1000 USD, while achieving near equivalent functionality to other commercially available CLSM systems that are far more expensive. The goal is to create a precise, modular, and compact optical scanning platform capable of micron to sub-micron level imaging using a combination of mechanical, optical, and electrical systems. The system integrates custom electronics, motor control, optical

alignment, and embedded firmware to enable fine-grained control of a laser's scanning path and collection of reflected light from a sample. The key engineering goals of the project include the implementation of precise stepper motor control, efficient power regulation for multiple subsystems, precise optical alignment for consistent image creation and power transmission, minimized optical aberrations for better image quality, robust signal amplification for photodiode readout, and integration with an ESP32 microcontroller to allow synchronized control and data acquisition.

The CLSM will utilize the OpenFlexure Delta Stage, a 3D-printed flexure stage modified to integrate custom-designed motor controllers. These controllers, based on the ULN2003A Darlington driver, were prototyped and tested both on a breadboard and as integrated PCB modules. Each motor controller interfaces directly with a 28BYJ-48 stepper motor and uses a 5V supply rail sourced from a 12V Mean Well LRS-50-12 power supply, regulated down via an MP1584 buck converter. Indicator LEDs, bypass capacitors, and careful trace layout were included to support both signal clarity and current handling, especially under peak load conditions during rapid scanning.

To meet the optical signal processing requirements of the CLSM, a custom transimpedance amplifier (TIA) was constructed using the OPA380 op-amp. This amplifier converts the low-level current signal from the photodiode into a usable voltage, which is then digitized and processed by the ESP32. The noise of this is further reduced by introducing a 3.3V linear regulator (LM1085-3.3), used to supply the ESP32 and sensitive analog components. Careful consideration was taken in terms of decoupling capacitors, power isolation between digital and analog domains, and trace width to ensure clean operation and minimal noise.

From a control and data handling perspective, the ESP32 microcontroller serves as the central unit coordinating motor actuation and signal acquisition. Step sequences were tested extensively to verify both smooth motion and positional accuracy, and system responsiveness was validated using both haptic feedback from the stage and visual confirmation via onboard LEDs. UART and USB interfaces were integrated via the CP2102 converter to allow easy programming and debugging during development.

Sufficient optical performance is necessary to the function of this microscope system. Precise alignment throughout the system will minimize aberrations and maximize transmission of optical power, which is the fundamental method for achieving the goal of micron-level resolution. To ensure this level of high performance, careful calculations were made during the design process to inform the selection of optical components and to determine the proper positioning for alignment. Verification of the spot size and optical power transmission were conducted in a lab setting to validate the performance metrics of the system, and measurements were taken of the output optical and electrical signal to verify their usability. Overall, the optics integration into the system has performed as expected and laboratory testing has confirmed the necessary performance metrics have been met to continue with the construction of the microscope system.

Three key constraints were addressed in the project: mechanical stability of the stage, electrical power distribution integrity, and photodiode signal clarity under real-world conditions. To address the first constraint, the stage was physically mounted to a custom-poured concrete base, acting as a vibration-damping platform. This mitigates the issues of

mechanical resonance and environmental noise, which are critical for repeatable high-resolution imaging. The second constraint was handled through power supply testing, including under-load performance evaluation of the MP1584 and LM1085 regulators, as well as the Mean Well 12V supply. Adequate trace widths and thermal relief in the PCB layout helped ensure reliable current delivery across all active components. The third constraint—ensuring clarity in analog signal acquisition—was addressed through the selection of low-noise components, clean PCB layout around the TIA, and shielding strategies to avoid coupling between the motor currents and photodiode signals.

Overall, the CLSM system has been tested to verify all major electrical and mechanical subsystems independently and in integration. The prototypes demonstrate successful motion control of the scanning platform, stable and regulated power delivery across all devices, and initial signal acquisition capabilities from the TIA subsystem. The remaining work includes full integration with the laser diode and finalized enclosure design, but given the established foundation and successful prototyping, these additions are expected to follow within the project timeline without major technical risk.

In conclusion, the CLSM project represents a comprehensive engineering effort spanning analog design, embedded systems, motion control, and system integration. By addressing both the technical requirements and real-world constraints, this design lays a solid foundation for a fully functioning, cost-effective, and scalable confocal microscope platform, with potential applications in research labs, educational environments, and low-cost diagnostic tools.

Appendix A – References

- 1) OpenAI. (2025). *ChatGPT* (Apr 16 version) [Large language model]. <https://chat.openai.com/>
- 2) OpenAI. (2025). *ChatGPT* (June 27 version) [Large language model]. <https://chat.openai.com/>
- 3) Fellers, T. J., & Davidson, M. W. (n.d.). *Introduction to confocal microscopy*. Evident Scientific. <https://evidentscientific.com/en/microscope-resource/knowledge-hub/techniques/confocal/confocalintro>
- 4) R Mihalik, The Culmination of 25 Years of Carl Zeiss Laser Scanning Microscopy, *Microscopy and Microanalysis*, Volume 13, Issue S02, 1 August 2007, Pages 1558–1559, <https://doi.org/10.1017/S1431927607077677>
- 5) Paschotta, Dr. R. (2005, June 24). *Fluorescence microscopy*. RP Photonics Encyclopedia. https://www.rp-photonics.com/fluorescence_microscopy.html
- 6) Teng, X., Li, F., & Lu, C. (2020). Visualization of materials using the confocal laser scanning microscopy technique. *Chemical Society Reviews*, 49(8), 2408–2425. <https://doi.org/10.1039/c8cs00061a>
- 7) Breaking Taps. (2021, April 21). *DIY Scanning Laser Microscope* [Video]. YouTube. <https://www.youtube.com/watch?v=9TYlQ4urcg8>
- 8) ARM. (n.d.). Embedded Programming with C and C++. <https://developer.arm.com/documentation/dui0491/i/C-and-C---Implementation-Details/C-and-C---implementation-details?lang=en>
- 9) Arduino. (n.d.). Arduino IDE 2.0 Documentation. <https://docs.arduino.cc/software/ide-v2>
- 10) Espressif Systems. (2023). ESP32 Technical Reference Manual. <https://www.espressif.com/en/support/documents/technical-documents>
- 11) USB Implementers Forum. (n.d.). Universal Serial Bus Specification, Revision 2.0. <https://usb.org/document-library/usb-20-specification>
- 12) Texas Instruments. (2020). Understanding SAR ADCs. <https://www.ti.com/lit/an/sbaa240/sbaa240.pdf>
- 13) Microchip Technology. (n.d.). AN10369 - UART Communication with PIC Microcontrollers. <https://safecoredevices.com/do-254-ip-cores/uart-do-254-ip->

[core/](#)

- 14) National Instruments. (n.d.). Data Acquisition Timing Considerations. <https://www.ni.com/en-us/innovations/data-acquisition>
- 15) NXP Semiconductors. (2021). Stepper Motor Control Design Reference Manual. <https://www.nxp.com/docs/en/user-guide>
- 16) Graeme, J. (1996). Photodiode amplifiers: Op amp solutions. McGraw-Hill.
- 17) Thorlabs. (n.d.). *Photodiodes*. Retrieved July 7, 2025, Thorlabs website: https://www.thorlabs.com/newgrouppage9.cfm?objectgroup_id=285
- 18) Plexim GmbH. (n.d.). *Transimpedance amplifier*. In *Plexim Academy: Analog Electronics*. Retrieved July 7, 2025, <https://www.plexim.com/academy/analog-electronics/transimpedance-amplifier>
- 19) Ultimate Electronics Book. (n.d.). *Op-amp transimpedance amplifier*. Retrieved July 7, 2025, <https://ultimateelectronicsbook.com/op-amp-transimpedance-amplifier/>
- 20) Digi-Key Electronics. (n.d.). *Introduction to linear voltage regulators*. Retrieved July 7, 2025, <https://www.digikey.com/en/maker/tutorials/2016/introduction-to-linear-voltage-regulators>
- 21) All About Circuits. (n.d.). *What is a linear voltage regulator?* Retrieved July 7, 2025, <https://www.allaboutcircuits.com/technical-articles/what-is-a-linear-voltage-regulator/>
- 22) Analog Devices. (n.d.). *Basic concepts of linear regulators and switching mode power supplies (AN-140)* [Application note]. Retrieved July 7, 2025, <https://www.analog.com/en/resources/app-notes/an-140.html>
- 23) Techspray. (2020, July 31). *How to select the right power supply for your medical application*. TDK-Lambda USA. Retrieved July 7, 2025, <https://www.us.lambda.tdk.com/resources/blogs/20200731.html>
- 24) Monolithic Power Systems. (n.d.). *Buck–boost converters*. In *MPScholar: Power Electronics*. Retrieved July 7, 2025, <https://www.monolithicpower.com/en/learning/mpscholar/power-electronics/dc-dc-converters/buck-boost-converters>
- 25) Thorlabs. (n.d.). *Photodiode fundamentals and theory* [User guide]. Retrieved July 7, 2025, https://www.thorlabs.com/navigation.cfm?guide_id=2537

- 26) Analog Devices. (n.d.). *Op amp circuit collection: Op amp circuits tutorial MT-077* [PDF]. Retrieved July 7, 2025, <https://www.analog.com/media/en/training-seminars/tutorials/MT-077.pdf>
- 27) Hamamatsu Photonics. (n.d.). *Photomultiplier tubes (PMTs): About PMTs*. Retrieved July 7, 2025, https://www.hamamatsu.com/us/en/product/optical-sensors/pmt/about_pmts.html
- 28) Teknic Inc. (n.d.). *Teknic*. Retrieved July 7, 2025, <https://teknic.com/>
- 29) Phidgets Inc. (n.d.). *Stepper motor and controller guide*. Retrieved July 7, 2025, https://www.phidgets.com/docs/Stepper_Motor_and_Controller_Guide
- 30) University of Central Florida. (2023). *Laser safety manual* [PDF]. Retrieved July 7, 2025, <https://ehs.ucf.edu/wp-content/uploads/sites/3/2023/02/Laser-Safety-Manual.pdf>
- 31) Thorlabs. (n.d.). *Laser safety*. Retrieved July 7, 2025, https://www.thorlabs.us/newgrouppage9.cfm?objectgroup_id=14648
- 32) Nikon Instruments Inc. (n.d.). *Introduction to microscope objectives*. In *MicroscopyU: Microscopy basics*. Retrieved July 7, 2025, <https://www.microscopyu.com/microscopy-basics/introduction-to-microscope-objectives>
- 33) McDermott, S., Ayazi, F., Collins, J., Knapper, J., Stirling, J., Bowman, R., & Cicuta, P. (2022). *Multi-modal microscopy imaging with the OpenFlexure Delta Stage*. *Optics Express*, 30(15), 26377–26395. <https://doi.org/10.1364/OE.450211> opg.optica.org+2opg.optica.org+2
- 34) ISO 11146-2:2021(en) - Lasers and laser-related equipment — Test methods for laser beam widths, divergence angles and beam propagation ratios. Retrieved July 7, 2025, <https://www.iso.org/obp/ui/#iso:std:iso:11146:-2:ed-2:v1:en>

Appendix B – Copyright Permissions

1) OpenFlexure Delta Stage Platform



josef woodhouse <kjosefwoodhouse1@gmail.com>
to contact ▾

Wed, May 28, 2:12 PM ☆ ☺ ↶ ⋮

Hello my name is Josef Woodhouse, I am an undergraduate student at the University of Central Florida, A team of 4 (myself included) are working on a laser microscope project as our capstone project, As part of this we are required to write a 120 page paper, I am reaching out on behalf of my group to request permission to use the materials in from the OpenFlexure Microscope project <https://openflexure.org/projects/microscope/build> in our paper with proper citations.

Thank you for your time,
Josef Woodhouse



Julian Stirling <julian@julianstirling.co.uk>
to me, contact ▾

Thu, May 29, 6:17 AM ☆ ☺ ↶ ⋮

Dear Josef,

Yes, feel free to use them in any work. Everything in the OpenFlexure project is Open Source so as long as you provide attribution you don't need to ask our permission.

Best wishes

.Julian

2) Thorlabs TIA Circuit Example

DATE 7/24/2025

Name of Publication: "Laser-Scope: The Affordable Confocal Scanning Laser Microscope"(the "Work")

Author: Karol Josef Woodhouse Thomae, Colling Barber, Luc Therien, Omar Castro

Publisher: University of Central Florida (the "Publisher")

Description or sample of Material: Research paper outlining, project description, research and investigation, standards & design constraints, applications of AI, hardware design, software design, system fabrication, and system testing of the Confocal Scanning Laser Microscope (the "Material")

Thorlabs, Inc. hereby grants permission to Publisher under a Creative Commons Attribution License (CC BY) to include the Material in the Work, and in all future editions and revisions thereof, without restriction, and to create derivative and ancillary works therefrom for research and academic purposes only subject to making such derivative work generally available under the grant of a similar license, and to publish such derivative work in all media now known or hereafter discovered throughout the world and in all languages, whether published by Publisher or its licensees.

A credit line to acknowledge use of the material is required and shall reference "Thorlabs, Inc." and the product part number(s).

Agreed and Accepted:

THORLABS, INC.

By: 

Date: July 25, 2025

Name: Chris Russo

Title: Senior Corporate Counsel

Appendix C – Datasheets

- 1) Espressif Systems. ESP32-WROOM-32 Datasheet, Version 1.9, February 2023. [Online]. Retrieved from https://www.espressif.com/sites/default/files/documentation/esp32-wroom-32_datasheet_en.pdf
- 2) Raspberry Pi Foundation. RP2040 Datasheet, Revision 1.1, June 2021. [Online]. Retrieved from <https://datasheets.raspberrypi.com/rp2040/rp2040-datasheet.pdf>
- 3) Microchip Technology Inc. ATmega2560 Datasheet – 8-bit AVR Microcontroller with 256K Bytes In-System Programmable Flash, Revision 2549Q–AVR–02/2014. [Online]. Retrieved from https://ww1.microchip.com/downloads/en/DeviceDoc/Atmel-2549-8-bit-AVR-Microcontroller-ATmega640-1280-1281-2560-2561_datasheet.pdf
- 4) Texas Instruments. (2007, September 10). *OPA380: Precision, high-speed transimpedance amplifier* [Datasheet Rev. G]. Retrieved July 7, 2025, from

<https://www.ti.com/lit/ds/symlink/opa380.pdf>

- 5) Texas Instruments. (n.d.). *LM1085: Low drop-out regulator* [Datasheet]. Retrieved July 7, 2025, <https://www.ti.com/lit/ds/symlink/lm1085.pdf?ts=1751861856949>
- 6) Texas Instruments. (n.d.). *TPS54JA20* [Product datasheet]. Retrieved July 7, 2025, <https://www.ti.com/product/TPS54JA20>
- 7) Hadex Electronics. (n.d.). *M513: Switching regulator* [Datasheet]. Retrieved July 7, 2025, <https://www.hadex.cz/spec/m513.pdf>
- 8) STMicroelectronics. (n.d.). *STEPPER DRIVER – STPD01* [Datasheet]. Retrieved July 7, 2025, <https://www.mouser.com/datasheet/2/758/stepd-01-data-sheet-1143075.pdf>

Appendix D – Software Code

Appendix E – AI Prompts & Results

Case Study 1:

Question: “what are some safety standards of lasers”:

ChatGPT:

“Laser safety standards are critical for protecting users, bystanders, and optical components from hazardous laser radiation. These standards are defined by international and national regulatory bodies and vary depending on laser power, wavelength, and usage. Below are key laser safety standards and guidelines:

1. Laser Classification (per IEC and ANSI standards)

Lasers are categorized by their potential to cause biological damage:

- Class 1: Safe under all conditions of normal use.
- Class 1M: Safe for unaided viewing; hazardous if viewed with magnifying optics.
- Class 2: Emits visible light (400–700 nm); safe due to the blink reflex (<1 mW).
- Class 2M: Visible lasers; safe without magnifying optics.
- Class 3R: Potentially hazardous under direct viewing (1–5 mW).
- Class 3B: Hazardous for direct eye exposure (5–500 mW).
- Class 4: High-power lasers (>500 mW); hazardous for eyes, skin, and fire risk.

Refer to ANSI Z136.1 and IEC 60825-1 for detailed classification criteria.

2. Key Safety Standards

Standard	Organization	Title / Purpose
ANSI Z136.1	Laser Institute of America (LIA) / ANSI	Safe Use of Lasers – main U.S. standard for laser use in labs, industry, and research.
IEC 60825-1	International Electrotechnical Commission	Safety of Laser Products – international standard for classification and labeling.
OSHA 29 CFR 1926.54	U.S. Department of Labor	Safety standards for lasers used in construction.
21 CFR Part 1040	U.S. FDA/CDRH	Regulations for laser product performance (labeling, emissions, user info).
ANSI Z136.8	LIA / ANSI	Safe Use of Lasers in Research, Development, or Testing.

3. Common Laser Safety Requirements

- Labeling: Lasers must be labeled with class, output power, and wavelength.
- Eye Protection: Use of wavelength-specific laser safety goggles for Class 3B and 4 lasers.
- Beam Control: Enclose beams wherever possible; use beam stops.
- Warning Signs: Area postings for Class 3B and 4 lasers ("Laser in Use" signs).
- Training: Personnel must be trained on laser hazards and safe procedures.
- Interlocks and Enclosures: Class 4 lasers often require key switches and interlocks.
- Controlled Access Areas: Class 3B and 4 lasers should operate in restricted zones.

4. Laser Safety Officer (LSO)

For Class 3B and 4 systems, a Laser Safety Officer is typically required to oversee:

- Risk assessments
- Administrative controls
- Equipment inspections
- Incident response plans

Let me know if you'd like a tailored summary of safety requirements for a confocal laser scanning microscope (CLSM) or any other specific system.” (OpenAI, 2025)

As shown in the response from ChatGPT, it gives a very good overview of some basic laser safety standards that need to be addressed when handling lasers. This is great for trying to get a basic understanding of how these standards work. However, when trying to understand these safety standards without the use of ChatGPT, safety standards usually go into detail of the hazards themselves so the user can get a full understanding of what they are using and why these standards exist. In this case from ChatGPT, it seems to have missed the more specific hazards when talking about laser safety such as electrical safety and less common hazards such as chemical or gaseous hazards.

Google Gemini:

Laser safety standards are crucial for protecting people from the potential hazards of laser radiation, which can cause severe eye damage, skin burns, and even fire hazards. These standards vary by country and region, but generally align around similar principles of classification and control measures.

Here are some of the key safety standards and concepts:

1. Laser Classification Systems:

Both international and national standards classify lasers into different hazard classes based on their potential for causing biological damage. This classification helps determine the necessary safety precautions. The most common classes are:

- Class 1: Safe under all conditions of normal use. The laser is either low power or fully enclosed, preventing access to hazardous radiation. (e.g., CD/DVD players, laser printers).
- Class 1M: Safe for viewing directly with the naked eye, but may be hazardous if viewed with optical instruments (e.g., binoculars, telescopes). Applies to large diameter or highly divergent beams.
- Class 2: Emits visible light (400-700 nm) and is safe because the human blink reflex (aversion response) will limit exposure to less than 0.25 seconds, which is typically insufficient to cause injury. (e.g., some laser pointers).
- Class 2M: Similar to Class 2 but hazardous if viewed with optical instruments.
- Class 3R: Considered low risk but potentially hazardous. The Accessible Emission Limit (AEL) can be exceeded, but with a low risk of injury. (e.g., some laser pointers above 1 mW).
- Class 3B: Hazardous if the eye is exposed directly to the beam, but diffuse reflections (e.g., from a matte surface) are generally not harmful. Requires protective eyewear where direct viewing is possible.
- Class 4: Hazardous under both direct beam and diffuse reflection viewing conditions. Can cause severe eye and skin damage, and may also be a fire hazard. Requires strict control measures and often dedicated laser safety officers.

2. Key International and National Standards:

- International Electrotechnical Commission (IEC) 60825 Series: This is the primary international standard for laser product safety.
 - IEC 60825-1: Safety of laser products - Part 1: Equipment classification and requirements. This is the fundamental document, defining laser classes, maximum permissible exposures (MPEs), labeling, and engineering controls. Many countries have adopted or based their national standards on IEC 60825-1.
 - Other parts of the IEC 60825 series cover specific applications, such as optical fiber communication systems (Part 2), laser displays (Part 3), and laser guards (Part 4).
- American National Standards Institute (ANSI) Z136 Series: In the United States, the ANSI Z136 series is the key set of voluntary consensus standards for the safe use of lasers. The Occupational Safety & Health Administration (OSHA) often references these standards in their regulatory framework for workplace laser safety.
 - ANSI Z136.1: American National Standard for Safe Use of Lasers. This is the parent document, providing comprehensive guidance on laser hazard evaluation, classification, and control measures for various laser applications.
 - Other ANSI Z136 standards address specific uses, such as lasers in healthcare (Z136.3), educational institutions (Z136.5), and manufacturing (Z136.9).
- Center for Devices and Radiological Health (CDRH) 21 CFR Part 1040: In the U.S., the FDA's CDRH regulates the performance safety of manufactured laser products. All laser products manufactured and sold in the U.S. must comply with these regulations.

3. Control Measures:

Regardless of the specific standard, laser safety programs generally incorporate a hierarchy of controls to minimize hazards:

- Engineering Controls (Most Effective):
 - Protective Housings/Enclosures: Fully enclosing the laser beam to prevent accidental exposure.
 - Interlocks: Safety devices that automatically shut off or reduce laser power if a protective housing or access panel is opened.
 - Key Switches: To prevent unauthorized operation of higher-class lasers.
 - Beam Stops/Dumps: Devices to absorb the laser beam at the end of its path.

- Warning Systems: Lights or audible alarms indicating when a laser is in operation.
- Administrative Controls:
 - Standard Operating Procedures (SOPs): Detailed written procedures for safe laser operation, maintenance, and emergency response.
 - Restricted Access: Limiting access to laser areas to authorized and trained personnel.
 - Warning Signs and Labels: Clear signage indicating laser hazards, class, and necessary precautions.
 - Designation of a Laser Safety Officer (LSO): A trained individual responsible for overseeing the laser safety program.
 - Training: Comprehensive training for all personnel who work with or around lasers, covering hazards, control measures, and emergency procedures.
- Personal Protective Equipment (PPE) (Least Effective as primary control):
 - Laser Safety Eyewear: Specifically designed to block or attenuate laser radiation at the relevant wavelengths and power levels. Selection of appropriate eyewear is crucial.
 - Protective Clothing/Gloves: For lasers that pose a skin hazard or fire risk.

By adhering to these standards and implementing a robust laser safety program, the risks associated with laser use can be significantly mitigated.

Case Study 2:

Question 1: “What are some key considerations in the selection of a photodiode for an imaging system?”

“When selecting a photodiode for an imaging system, several key considerations must be taken into account to ensure optimal performance for the intended application. These factors influence sensitivity, speed, resolution, and signal quality:

1. Spectral Response

- Choose a photodiode with peak sensitivity that matches the wavelength range of the light source or scene (e.g., visible, near-infrared, UV).
- Materials like Si, InGaAs, or Ge offer different spectral sensitivities.

2. Responsivity

This refers to the output current per unit of incident optical power, usually in A/W. Higher responsivity means better conversion efficiency, especially important for low-light imaging.

3. Dark Current

The leakage current in the absence of light affects the signal-to-noise ratio.

For low-light or high-precision systems, a photodiode with low dark current is crucial.

4. Response Time / Bandwidth

Determines how quickly the photodiode reacts to changes in light—important for high-speed or time-resolved imaging.

A small junction capacitance and reverse bias operation improve speed.

5. Active Area Size

Larger active areas capture more light but may reduce response speed due to higher capacitance.

Small-area photodiodes offer faster response but may require focusing optics.

6. Noise Characteristics

Consider both shot noise (proportional to signal and dark current) and thermal noise.

Low-noise designs are essential for detecting weak signals.

7. Linearity and Dynamic Range

The photodiode should respond linearly to a wide range of light intensities to maintain accurate image contrast and detail.

8. Packaging and Integration

The photodiode should be compatible with the imaging system's mechanical, thermal, and electrical interfaces.

Options include bare die, surface-mount, or hermetically sealed packages.

9. Temperature Stability

- Temperature affects dark current and responsivity.
- For outdoor or industrial imaging, photodiodes with low temperature dependence or temperature compensation may be necessary.
- By carefully balancing these parameters, you can select a photodiode that delivers optimal performance for your imaging system's sensitivity, speed, resolution, and environmental requirements.

Question 2: “How can a scanning laser microscope be tailored to perform scanning laser microscopy?”

“A **scanning laser microscope (SLM)** can be tailored to perform **surface topography**—i.e., mapping the 3D shape of a surface—by modifying its optical and detection systems to measure height variations with high precision. Here's how it can be done:

Key Modifications to Tailor an SLM for Surface Topography:

Incorporate Confocal Optics

Confocal laser scanning microscopy (CLSM) uses a pinhole to eliminate out-of-focus light.

By scanning at different focal planes (z-axis), the microscope can reconstruct a 3D surface map.

The height at which the signal is maximized corresponds to the surface height at that (x, y) position.

Use a Height-Sensitive Detection Method

Several detection schemes allow the microscope to measure surface height:

Focus Variation / Autofocus Scanning

Move the objective or sample in the z-direction while scanning with the laser. Measure the sharpness or brightness of the reflected light—peak sharpness indicates surface height.
Common in laser scanning confocal profilometers.

Interferometry Integration

Integrate white-light or laser interferometry with the scanning laser beam. Interference fringes correlate with surface height (nanometer-scale precision). Useful for smooth or reflective surfaces.

Triangulation (Angle-Based Measurement)

Use an off-axis detector to sense the position of the laser spot reflection. The lateral displacement of the reflected beam varies with surface height. Common in laser triangulation sensors.

Implement High-Precision Z-Scanning

Accurate z-stage or piezo actuators are required to vary focus in the vertical direction.
Enables depth resolution needed for topography.

Data Processing for 3D Reconstruction

Software reconstructs a 3D map from the intensity or focus measurements at each (x, y).
Often involves surface fitting, point-cloud processing, or height map creation.

If you're building or modifying an SLM for this purpose, you'd start by determining the desired **resolution, field of view, and surface type**, and then choose between **confocal, interferometric, or triangulation** approaches accordingly. Want help deciding between those methods?"

Case Study 3:

ChatGPT

Question 1:

“Main considerations when designing a transimpedance amplifier (TIA):

1. Feedback Resistor (R_f):
sets the gain: $V_{out} = -I_{in} \cdot R_f$. Higher R_f increases sensitivity.
2. Photodiode Capacitance (C_p):
Combines with op-amp input capacitance and feedback capacitor to affect stability and bandwidth.
3. Feedback Capacitor (C_f): Added in parallel with R_f to stabilize the op-amp and prevent oscillations. Typical value: $C_f = \frac{1}{2\pi R_f f_{3dB}}$
4. Op-Amp Bandwidth and Input Bias Current:
Choose a high-speed, low-input bias current op-amp (e.g., OPA381, OPA657). The gain-bandwidth product must support the expected signal frequency at the chosen gain.
5. Noise:
Dominated by thermal noise from R_f and op-amp current/voltage noise. Tradeoff between gain and noise.
6. Input offset and Bias Current:
Affects accuracy at low input currents- chose op-amps with low offset and bias current for high sensitivity.
7. Power Supply Range:
Ensure op-amp output swing accommodates expected signal range. Use split supply if necessary for negative output swing
8. PCB Layout:
Minimize stray capacitance and trace inductance. Keep photodiode close to the op-amp input. Use ground plane carefully to reduce noise.
9. Photodiode Biasing:
Typically reverse-biased to improve speed and linearity. Bias must be isolated from op-amp input unless current is injected directly.” (OpenAI, 2025)

In this case ChatGPT outputs multiple factors to be considered, all of which are good and mostly accurate for the CLSM’s TIA. Most notably it outputs why each consideration is important in detail.

Question 2: “What are some common integrated circuits suited for TIA design based on photodiode currents in the range of μA ”

“Here are some common ICs suitable for TIA design in the μA range:

- OPA381
- OPA380
- OPA657
- ADA4530-1
- ADA4627-1
- AD8627
- LT6230
- LTC6230
- LTC6268” (OpenAI, 2025)

In this case ChatGPT outputs only ICs, which unlike the previous prompt it does not specify any characteristics or considerations, further prompting would be necessary to get more information for each IC, but the output is serviceable enough to begin part research.

5.1.3.2 Google Gemini

Question 1: Main considerations when designing a transimpedance amplifier (TIA):

“Designing a Transimpedance Amplifier (TIA) involves a careful balance of several critical factors to achieve the desired performance in terms of gain, bandwidth, noise, and stability. Here are the main considerations:

1. Transimpedance Gain (R_f):
 - a. Purpose: The primary function of a TIA is to convert voltage to current. The feedback resistor (R_f) determines the transimpedance gain ($V_{out} = I_{in} * R_f$).
 - b. Considerations:
 - i. Desired Output Voltage: Choose R_f to provide a suitable output voltage range for the subsequent stages, considering the maximum input current.
 - ii. Dynamic Range: A larger R_f increases sensitivity for small currents but can limit the maximum measurable current before saturation (hitting the supply rails).
 - iii. Practicality: Extremely large resistors can introduce more noise and parasitic capacitance.
2. Bandwidth and Speed:
 - a. Factors influencing bandwidth:
 - i. Total Input Capacitance (C_{tot}): This is a critical parameter and includes the photodiode capacitance (C_d), op-amp input

capacitances (common-mode and differential), and parasitic PCB capacitance. Higher input capacitance generally leads to lower bandwidth.

- ii. Op-Amp Gain-Bandwidth Product (GBP): A higher GBP generally allows for higher closed-loop transimpedance bandwidth.

3. Noise Performance:

a. Dominant Noise Sources:

- i. Feedback Resistor Thermal Noise (Johnson-Nyquist Noise): This is proportional to R_f . Larger R_f means more noise.
- ii. Op-Amp Voltage Noise (e_n): This noise is gained up at higher frequencies due to the increasing noise gain caused by input capacitance.
- iii. Op-Amp Current Noise (i_n): This noise flows through the feedback resistor.” (Google Gemini, 2025)

Question 2: What are some common integrated circuits suited for TIA design based on photodiode currents in the range of μA

“Here are some common types of ICs that are well suited for μA currents:

- 1. JFET Input Op-Amps: JFET (Junction Field-Effect Transistor) input op-amps are known for their extremely low input bias currents, which is crucial when dealing with very small photodiode currents. High input bias current can introduce significant DC offset errors, especially when using large feedback resistors (which are common for μA -level currents to achieve reasonable output voltages).
 - a. Examples:
 - i. OPA380: This is a high-speed precision TIA op-amp. It offers a good combination of low input bias current (e.g., 50pA), low offset voltage, and decent bandwidth (90MHz GBW), making it suitable for applications requiring both precision and speed.
 - ii. ADA4625-1/2: These are 36V , 18MHz , low-noise, fast-settling JFET input op-amps with very low input bias current, making them excellent choices for precision TIA applications.
 - iii. LTC6268: These are extremely low input bias current (fA range at 25°C), high-speed (500MHz GBW) FET input op-amps, designed for wide dynamic range TIA applications. While their bias current is often overkill for just μA range, they provide exceptional performance if very low noise and high speed are also critical.
- 2. Dedicated TIA ICs (with integrated photodiode or optimized for TIA): Some manufacturers offer integrated TIA solutions, sometimes even with the

photodiode built into the same package. These are often optimized for specific performance characteristics (e.g., high speed for fiber optic communication) but can sometimes be adapted for general-purpose photodiode sensing.

a. Examples:

- LTC6560 (Analog Devices/Linear Technology): A low-noise TIA with 220MHz bandwidth, often used in LIDAR receivers. While designed for higher speeds, its low noise and transimpedance gain capabilities might make it suitable for fast μA applications.
- Koheron PD10TIA: This is a specialized TIA module with high gain (80 kV/A) and low input-referred current noise, designed for photodetectors with input currents up to 45 μA and bandwidths up to 1 MHz. (Note: This is a module, not just a standalone op-amp IC).” (Google Gemini, 2025)

Case Study 4:

Question 1: “Salutations ChatGPT I would like to pick a Micro controller for the purpose of reading data from a transimpedance amplifier and sending the data to a computer for analysis. This microcontroller should also be able to control stepper motor as well”

“Salutations! You're looking for a microcontroller that can:

Read data from a Transimpedance Amplifier (TIA) – typically via analog inputs (ADC).

Control a stepper motor – requiring GPIO pins and timing control (e.g., PWM).

Send data to a computer – via USB, UART, or Serial over USB.

Key Requirements Recap

Feature	Explanation
ADC (Analog-to-Digital Converter)	Needed to read the analog voltage from the TIA output
GPIOs / Timers / PWM	For stepper motor control (via driver modules like A4988, ULN2003, or DRV8825)
Serial/USB communication	To send the data to a computer (USB serial is easiest)
Processing power	Enough to sample ADC, control motor, and handle communication
Real-time control	For precise timing of motor steps and ADC sampling

Microcontroller Recommendations

1. ESP32

ADC: 12-bit (some noise, but usable with filtering)

GPIOs: Plenty, includes PWM and hardware timers

Stepper control: Yes, supports step/direction outputs via GPIO

Data transfer: USB via UART-to-USB (via onboard CP210x chip or direct UART)

Pros: Fast (dual-core), built-in Wi-Fi (optional remote logging), good ADC sampling

Cons: Slight ADC non-linearity without calibration

Best For: A compact, Wi-Fi-enabled solution. Great general-purpose pick.

2. Arduino Mega 2560

ADC: 10-bit, stable and reliable

GPIOs: 54 digital I/O, 16 analog inputs

Stepper control: Many libraries available (e.g., AccelStepper)

Data transfer: USB serial

Pros: Easy to use, massive community, very stable

Cons: Slower CPU (16 MHz), no native Wi-Fi or multithreading

Best For: Beginners or multi-stepper control with lots of I/O pins.

3. Raspberry Pi Pico / Pico W

ADC: 12-bit, fast and clean

GPIOs: 26 multifunctional pins

Stepper control: Excellent via PIO (Programmable I/O)

Data transfer: USB serial natively supported

Pros: Dual-core, USB host/device, fast ADC

Cons: Slightly more complex to program with PIOs, limited RAM

Best For: Advanced real-time motor control or USB-native logging.

Comparison Table

Feature	ESP32	Arduino Mega	Raspberry Pi Pico
ADC Resolution	12-bit	10-bit	12-bit
GPIO Count	~34	70+	~26
USB Support	UART-to-USB	Native USB	Native USB
Stepper Support	Yes	Yes	Yes (PIO or PWM)
Clock Speed	240 MHz (dual)	16 MHz	133 MHz (dual-core)
Programming Lang.	C++, MicroPython	C++	C++, MicroPython
Wi-Fi / BT	Yes (ESP32)	No	Only with external module (Pico W has Wi-Fi)

My Recommendation

Go with the ESP32 if:

You want Wi-Fi logging or a powerful, real-time capable MCU

You're comfortable with slightly noisy ADC (filtering helps)

Choose Arduino Mega if:

You need many GPIO pins and simple USB communication

You're okay with slower sampling/motor control

Try Raspberry Pi Pico if:

You want clean ADC data, native USB, and advanced real-time control

Would you like help writing example code for one of these platforms (e.g., reading from a TIA and controlling a stepper motor)?" (OpenAI, 2025)